

University of Windsor

Scholarship at UWindor

Electronic Theses and Dissertations

Theses, Dissertations, and Major Papers

2010

ER stress mediated effects on plasma membrane cholesterol and nitric oxide bioavailability

Ruchi Chaube
University of Windsor

Follow this and additional works at: <https://scholar.uwindsor.ca/etd>

Recommended Citation

Chaube, Ruchi, "ER stress mediated effects on plasma membrane cholesterol and nitric oxide bioavailability" (2010). *Electronic Theses and Dissertations*. 7934.
<https://scholar.uwindsor.ca/etd/7934>

This online database contains the full-text of PhD dissertations and Masters' theses of University of Windsor students from 1954 forward. These documents are made available for personal study and research purposes only, in accordance with the Canadian Copyright Act and the Creative Commons license—CC BY-NC-ND (Attribution, Non-Commercial, No Derivative Works). Under this license, works must always be attributed to the copyright holder (original author), cannot be used for any commercial purposes, and may not be altered. Any other use would require the permission of the copyright holder. Students may inquire about withdrawing their dissertation and/or thesis from this database. For additional inquiries, please contact the repository administrator via email (scholarship@uwindsor.ca) or by telephone at 519-253-3000ext. 3208.

ER Stress Mediated Effects on Plasma Membrane Cholesterol and Nitric Oxide Bioavailability

by

Ruchi Chaube

**A Dissertation
Submitted to the Faculty of Graduate Studies and Research
Through the Department of Chemistry and Biochemistry
in Partial Fullfillment of the Requirements for the
Doctor of Philosophy at the
University of Windsor**

Windsor, Ontario, Canada

2010

© 2010 Ruchi Chaube



Library and Archives
Canada

Published Heritage
Branch

395 Wellington Street
Ottawa ON K1A 0N4
Canada

Bibliothèque et
Archives Canada

Direction du
Patrimoine de l'édition

395, rue Wellington
Ottawa ON K1A 0N4
Canada

Your file *Votre référence*
ISBN: 978-0-494-62758-7
Our file *Notre référence*
ISBN: 978-0-494-62758-7

NOTICE:

The author has granted a non-exclusive license allowing Library and Archives Canada to reproduce, publish, archive, preserve, conserve, communicate to the public by telecommunication or on the Internet, loan, distribute and sell theses worldwide, for commercial or non-commercial purposes, in microform, paper, electronic and/or any other formats.

The author retains copyright ownership and moral rights in this thesis. Neither the thesis nor substantial extracts from it may be printed or otherwise reproduced without the author's permission.

AVIS:

L'auteur a accordé une licence non exclusive permettant à la Bibliothèque et Archives Canada de reproduire, publier, archiver, sauvegarder, conserver, transmettre au public par télécommunication ou par l'Internet, prêter, distribuer et vendre des thèses partout dans le monde, à des fins commerciales ou autres, sur support microforme, papier, électronique et/ou autres formats.

L'auteur conserve la propriété du droit d'auteur et des droits moraux qui protègent cette thèse. Ni la thèse ni des extraits substantiels de celle-ci ne doivent être imprimés ou autrement reproduits sans son autorisation.

In compliance with the Canadian Privacy Act some supporting forms may have been removed from this thesis.

While these forms may be included in the document page count, their removal does not represent any loss of content from the thesis.

Conformément à la loi canadienne sur la protection de la vie privée, quelques formulaires secondaires ont été enlevés de cette thèse.

Bien que ces formulaires aient inclus dans la pagination, il n'y aura aucun contenu manquant.

■+■
Canada

Co-Authorship Declaration

I hereby declare that this thesis also incorporates the outcome of a joint research undertaken in collaboration with Dr. Shane Miersch under the supervision of professor Bulent Mutus. The collaboration is covered in Chapter 3 of the thesis. My contribution in the work was in experiment design, conductance, data analysis and data interpretation.

I am aware of the University of Windsor Senate Policy on Authorship and I certify that I have properly acknowledged the contribution of other researchers to my thesis, and have obtained written permission from each of the co-author(s) to include the above material(s) in my thesis.

I certify that, with the above qualification, this thesis, and the research to which it refers, is the product of my own work.

Ruchi Chaube

08.02.2010

Abstract

Endothelial dysfunction is due in part to the decrease in the biosynthesis and the bioavailability of nitric oxide (NO) in the endothelial cell layer. The chronic exposure of blood vessels to cardiovascular risk factors such as LDL-cholesterol, free fatty acids, homocysteine and conditions of hyperglycemia can give rise to endothelial dysfunction. Many of these same risk factors have also been shown to induce endoplasmic reticulum (ER) stress, in endothelial cells. However, the potential links between endothelial dysfunction and ER-stress have not been clearly established.

The present study was undertaken with two objectives. Objective 1 was to determine how increased plasma membrane cholesterol content can affect NO diffusion, dynamics and signalling. Objective 2 was to determine whether the unfolded protein response mediated by ER stress can lead to increase in plasma membrane cholesterol in endothelial cells, how ER stress leads to increase in plasma membrane cholesterol and whether increase in plasma membrane cholesterol can influence eNOS activity and localization in the endothelial cells.

Objective 1 was carried out by taking Normal Human Fibroblasts (NHF1) and sterol transport-defective Niemann Pick type C1(NPC1) fibroblasts which exhibit

increase plasma membrane cholesterol content. NPC1 fibroblasts showed decreased activation of both intracellular sGC and VASP (Ser239) phosphorylation induced by exposure to exogenous NO exposure relative to their normal human fibroblasts (NHF) counterparts.

Objective 2 was to understand the underlying Unfolded Protein Response (UPR)/ER stress-mediated mechanisms responsible for the induction of endothelial dysfunction. We observed that ER stress and oxidative stress collectively cause elevations in plasma membrane cholesterol in endothelial cells and aortic cross-sections of ER stressed C57BL6 mice. The rise in plasma membrane cholesterol was associated with decreased eNOS activity, eNOS phosphorylation and increased eNOS localization to the Golgi. Interestingly, we observed that neutral sphingomyelinase 2 (NSMase2) becomes dysfunctional during ER stress and by *S*-nitrosation of cysteine and nitration of tyrosine residues.

This study is the first in its kind which links the attenuation of endothelial NO production to ER stress-mediated increases in plasma membrane cholesterol and implicates a key role for NSMase2 in this process.

**Dedication to my father who inspired me to pursue something
original**

Acknowledgements

I would to take the opportunity to express my gratitude to my advisor, Dr. Bulent Mutus for his constant inspiration, perseverance and invaluable guidance during the course of my Ph.D. I feel his excellent mentorship in grooming me as a researcher and his unwavering dedication to science has brought me to this verge of completing my Ph.D. with a mind of an inquiring researcher.

I would to further thank my co-advisor Dr. Sirinart Ananvoranich, who was always ready to impart her help whenever I needed. The time I spent under her guidance taught me how to approach a problem scientifically. Then I would thank Dr. Panayiotis O. Vacratsis, for being in my committee and giving me useful insights in matters related to my research. I would also thank my department outside reader, Dr. Lisa Porter for thoroughly reading my thesis and raising important points which improved the structure of the thesis. I addition, I would thank my external examiner, Dr. Dana M. Spence, from Michigan State University for giving his time and critically reading my thesis.

My gratitude is further extended to our collaborators- Drs. Geoff H. Werstuck: McMaster University and Thrombosis and Atherosclerosis Research Institute, Michael G. Espey: NIDDK, National Institute of Health and Rodney Tweten: University of Oklahoma. Dr. Werstuck and Dr. Espey helped me in giving valuable suggestions in study regarding cholesterol and nitric oxide respectively. Dr. Tweten provided me with the clone for cholesterol binding protein, which actually paved my way to start my research work.

I am thankful to Dr. Barbara Zielinsky: Dept. of Biology and her lab members for assisting me and letting me do all the tissue cross-sectioning work in her lab. I am also thankful for Drs. S. Pandey, M. Boffa and L. Lee for letting me to use their lab equipment.

I would like to acknowledge Mutus lab members who worked with me at the same time and made my overall experience in the lab memorable- Shane, Arun, Inga, Arzu, Adam, Harman, Suzie, Rebecca, Vasantha and Arthur. I am also thankful to some of the wonderful undergrads who worked for me like Natasha, Corina and Bei. My special thanks goes to my friend Mallika, who stood with me from the first day, helped and encouraged me throughout my stay here.

My thankfulness and appreciation also goes to Marlene and Michelle in the Chemistry office for their constant support and help whenever and wherever I needed.

Finally, I would thank my parents Dr. Ramesh Chaube and Dr. Usha Chaube who always encouraged me to be a researcher and inspired me to be someone useful to the society. I also express my gratefulness to my husband Dr. Yogesh Katare for staying with me, we had many invigorating discussions on important scientific matters together. Lastly I cannot wind this up without mentioning my darling son, Raman who has been such a wonderful kid throughout my Ph.D. period.

TABLE OF CONTENTS

DECLARATION	iii
ABSTRACT	iv
DEDICATION	vi
ACKNOWLEDGEMENTS	vii
LIST OF FIGURES	xiv
LIST OF SCHEMES	xv
LIST OF ABBREVIATIONS	xvi

Part I

Chapter 1- General Introduction

1.1 Endothelial dysfunction	2
1.1.2 Physiological function of the endothelial cells	2
1.1.3 Endothelial dysfunction and its relationship to endothelial cell injury	6
1.1.3.1 Oxidative stress	7
1.1.3.2 Endoplasmic reticulum stress	10
1.1.3.3 Metabolic stress	10
1.1.4.1 Indicators of endothelial dysfunction	12
1.1.5 Endothelial dysfunction in atherosclerosis	13
1.2 Cholesterol	15
1.2.1 Cholesterol and sphingomyelin interaction	16
1.2.2 Cholesterol and sphingomyelin homeostasis	16
1.2.3 Biosynthesis of cholesterol	17
1.2.3.1 Synthesis of mevalonate from acetate	17
1.2.3.2 Conversion of mevalonate to two activated isoprenes	17
1.2.3.3 Condensation of six activated isoprenes units to form squalene	18
1.2.3.4 Conversion of squalene to the four-ring steroid nucleus	19
1.2.4 Cholesterol transport to plasma lipoproteins	19
1.2.5 Influx of exogenous cholesterol	21
1.2.6 Cholesterol efflux from cells	23
1.2.7 Regulation of cellular cholesterol	23
1.3 Nitric oxide	26
1.3.1 Post-translational modification to the eNOS	28
1.3.1.1 Acylation	28
1.3.1.2 Intracellular Ca ²⁺ levels and calmodulin binding	29
1.3.1.3 Phosphorylation	30
1.3.1.4 S-Nitrosylation	31
1.3.2 Protein partners of eNOS in the caveolae	32
1.3.2.1 Caveolin	32

1.3.2.2 Endoglin	32
1.3.3 Signalling protein partners of eNOS	33
1.3.3.1 PI3K/Akt	33
1.3.3.2 hsp90	33
1.3.3.3 Phosphatases	34
1.3.4 eNOS sub-cellular localization and trafficking	37
1.3.4.1 NOSIP	37
1.3.4.2 NOSTRIN	37
1.4 Endoplasmic reticulum stress (ER stress)	39
1.4.1 Attenuation of translation	41
1.4.2 Induction of ER chaperones	42
1.4.3 Degradation of unfolded/misfolded proteins by ubiquitin-proteasome system	43
1.4.4 Apoptosis	43
1.4.5 NO-induced ER stress	46
1.4.6 ER stress and oxidative stress in diseases	48
1.4.6.1 Diabetes	48
1.4.6.2 Neurodegenerative diseases	48
1.4.6.3 Hyperhomocysteinemia and atherosclerosis	49
1.5 Sphingomyelinase	50
1.5.1 Sphingomyelin	50
1.5.2 Acid sphingomyelinase	52
1.5.2.1 Lysosomal Acid sphingomyelinase	52
1.5.2.2 Secretory Acid sphingomyelinase	52
1.5.3 Lysosomal Acid sphingomyelinase and vascular tone	53
1.5.4 Secretory Acid sphingomyelinase in atherosclerosis	53
1.5.5 Secretory Acid sphingomyelinase in heart failure	54
1.5.6 Neutral sphingomyelinase	55
1.5.6.1 Neutral, Mg^{2+} -dependent sphingomyelinase	55
1.5.6.2 Neutral, Mg^{2+} -independent sphingomyelinase	55
1.5.7 Neutral sphingomyelinase signalling pathways and cardiovascular Dysfunction	55
Objectives of the study	57

Part II

Chapter 2- Cloning, characterization and binding specificity of Perfringolysin O-Domain 4 (PFO-D4) with cholesterol on Bilayer Lipid Membrane (BLM)

2.1	Introduction	61
2.2	Materials and equipment	64
2.2.1	Materials	64
2.2.2	Equipment	64
2.3	Methods	66
2.3.1	Cloning of truncated PFO	66
2.3.2	Cloning of PFO-D4 in pTrcHisB vector	66
2.3.3	Cloning of PFO-D4-pTrcHisB plasmid with GFP in XL-1 Blue supercompetent cells	67
2.3.4	Transformation and protein expression of PFO-D4-GFP in XL-1 Blue supercompetent cells	67
2.3.5	Purification and quantification of PFO-D4-GFP protein	68
2.3.6	Bilayer Lipid membrane (BLM) setup	69
2.3.7	Cholesterol specificity of PFO-D4-GFP on BLM	69
2.3.8	Cholesterol specificity of PFO-D4-GFP with Methyl- β -cyclodextrin Treatment on the BLM	70
2.4	Results	71
2.5	Discussion	74

Part III

Chapter 3- Plasma membrane cholesterol content affects nitric oxide diffusion, dynamics and signalling

3.1	Introduction	80
3.2	Materials and Equipment	82
3.2.1	Materials	82
3.2.2	Equipment	82
3.3	Methods	84
3.3.1	Cell culture	84
3.3.2	Cloning of PFO-D4 with pTrchisB vector and purification	84
3.3.3	Preparation of cholesterol-loaded cyclodextrin	84
3.3.4	Cholesterol analysis	85
3.3.5	Modulation of cellular plasma membrane cholesterol	85
3.3.6	cGMP production and VASP phosphorylation as measure for intracellular NO signalling	86
3.4	Results	87
3.4.1	Cellular plasma membrane cholesterol content shifts the threshold for NO activation of cytoplasmic soluble guanylyl cyclase and the Downstream cGMP-dependent phosphorylation of VASP	87
3.5	Discussion	90

Part IV

Chapter 4- Endothelial dysfunction can be induced by endoplasmic reticulum stress mediated inhibition of neutral sphingomyelinase 2.

4.1	Introduction	97
4.2	Materials and equipment	102
4.2.1	Materials	103
4.2.2	Equipment	103
4.3	Methods	105
4.3.1	Cell culture and treatment condition	105
4.3.2	Animal care and treatment	106
4.3.3	Plasma membrane cholesterol estimation by cholesterol specific probe (PFO-D4-GFP) and cholesterol oxidase assay	107
4.3.4	Nitric oxide release	108
4.3.5	Endothelial nitric oxide synthase localization by double immune-fluorescence assay and by differential sucrose density gradient fractionation	109
4.3.6	Assay for neutral sphingomyelinase 2 activity	110
4.3.7	S-nitrosation, denitrosation and nitration of NSMase2	112
4.3.8	Oxidative stress	115
4.3.9	Western Blot analysis	115
4.3.10	Statistics	116
4.4	Results	117
4.4.1	ER stress induces the increase of cholesterol in the plasma membranes of BAEC and mouse aortas	117
4.4.2	ER stressed cells are less responsive to extracellular NO mediated signalling	118
4.4.3	Neutral sphingomyelinase 2 activity in BAEC is inhibited by Nitration and S-nitrosation by ER stressors	119
4.4.4	NSMase2 overexpression or inhibition affects NO production and plasma membrane cholesterol levels in BAEC	122
4.4.5	ER stress-mediated inhibition of NSMase2 leads to decreased eNOS phosphorylation, NO production but increased localization of eNOS in the Golgi	124
4.4.6	ER stress upregulates protein expression for GRP78 and SREBP-2 With no change in caveolin-1 protein expression	125

4.5	Discussion	128
5.1	Conclusion	155
	References	158
	VITA AUCTORIS	173

LIST OF FIGURES

1.1	Platelet aggregation cascade	4
1.2	Structure of cholesterol	15
1.3	Nitric oxide synthesis by nitric oxide synthase (NOS)	27
1.4	Post translational activation of eNOS	36
1.5	Structure of sphingomyelin	50
2.1.1	Pictures displaying the titration of cholesterol in bilayer lipid membrane (BLM) with PFO-D4-GFP	76
2.1.2	Titration of cholesterol in bilayer lipid membrane (BLM) with PFO-D4-GFP	77
2.2	Cholesterol specificity of PFO-D4-GFP on BLM cholesterol after extraction from methyl- β -cyclodextrin	78
3.1	PM cholesterol of NHF versus NPC1 fibroblasts by fluorescence imaging of Alexa 532 labelled D4	93
3.2	Differential cGMP response of NHF and NPC1 fibroblasts to exogenous NO	94
3.3	Differential VASP Ser ²³⁹ phosphorylation response of NHF and NPC1 Fibroblasts to exogenous NO	95
4.1(A)	Cholesterol analysis on PM isolates from BAECs and titration of PFO-D4-GFP on aortic wall cross-sections from C57BL6 mice	139
4.1(B)	Visualizing cholesterol by staining with PFO-D4-GFP on BAECs	140
4.1(C)	Titration of aortic cross-sections with PFO-D4-GFP	141
4.1(D)	Titration curve	141
4.1(E)	Aortic cross-sections stained with PFO-D4-GFP	142
4.2	Differential VASP Ser ²³⁹ phosphorylation response of BAECs to exogenous NO	143
4.3(A)	Activity of NSMase2 IP-isolated from BAECs	144
4.3(B)	Reactive Oxygen Species generation from from BAECs	144
4.3(C)	Western immunoblot for nitration of NSMase2 on IP-isolated from BAECs	144
4.3(D)	Double immunofluorescence assay to determine nitration on aortas	145
4.4	S-nitrosation and denitrosation of immunoprecipitated NSMase2 From BAECs determined by biotin switch assay and reductive tri-iodide chemiluminescent assay	146
4.5	Nitric oxide production by BAECs measured in the form of total Nitrite by Sievers Nitric Oxide Analyzer (NOA)	147
4.6	eNOS localization determined by differential sucrose density fractionation	148-149
4.7	eNOS Ser ¹¹⁷⁹ phosphorylation and total eNOS from isolated PM from BAECs	150
4.8	Western Immunoblot for GRP78/BiP	151
4.9	Western Immunoblot for SREBP-2	152

LIST OF SCHEMES

Scheme 1

154

LIST OF ABBREVIATIONS

ACAT	Acyl-CoA cholesterol acyl transferase
ADP	Adenosine diphosphate
ATP	Adenosine triphosphate
BAEC	Bovine Aortic Endothelial Cell
cGMP	Cyclic guanosine monophosphate
DMEM	Dulbeccos Modified Eagles Medium
DEA/NO	Diethylamine NONOate
ECs	Endothelial cells
EDTA	ethylenediaminetetraacetic acid
eNOS	endothelial nitric oxide synthase
GRP78	Glucose regulated protein mol wt. 78
GSNO	S-nitrosoglutathione
L-NMMA	N ^G -monomethyl-L-arginine
M β CD	Methyl- β -cyclodextrin
NADH	Nicotinamide adenine dinucleotide
NADPH	Nicotinamide adenine dinucleotide phosphate
NEM	N-Ethylmaleimide
NO	Nitric oxide
NSMase2	Neutral sphingomyelinase 2
Pm	Palmitate
PM	Plasma membrane
PMSF	phenylmethanesulphonylfluoride
POPC	1- palmitoyl 2- oleyl phosphatidylcholine
PVDF	Polyvinylidene fluoride
RNOS	Reactive nitrogen oxide species
ROS	Reactive oxygen species
sGC	soluble guanylyl cyclase
SDS-PAGE	sodium dodecyl sulfate polyacrylamide gel electrophoresis
SREBP 2	Sterol regulatory element binding protein 2
UPR	Unfolded protein response
VASP	Vasodilator stimulated phosphoprotein

Part I

Chapter 1

General Introduction

1.1 Endothelial Dysfunction

Endothelial dysfunction is characterized by an imbalance between relaxing and contracting factors, between anticoagulant and procoagulant substances, between anti-inflammatory and proinflammatory mediators or between growth inhibiting and promoting factors. Such dysfunction can result from the mechanical and biochemical injury to the endothelium. Physical damage of the endothelium is mostly caused by hypertension; several other risk factors such as hypercholesterolemia, diabetes and smoking probably cause injury to the endothelium through biochemical mechanisms. Therefore, vessel wall damage may result in endothelial dysfunction and can be clinically manifested as thrombosis and atherosclerosis [Rubanyi, *et al.*, 1993].

1.1.2 Physiological functions of the endothelial cells

A defining feature of endothelium is its capacity to keep blood in a fluid state [Arnout, *et al.*, 2006]. The coagulation cascade is initiated by the generation of an enzyme complex consisting of factor VIIa, an active protease and a catalytic accelerator termed tissue factor (TF), which catalyzes the conversion of inactive clotting factors IX and/or X to active proteases, factors IXa and Xa respectively. Factor Xa uses factor Va as a cofactor and converts prothrombin to thrombin, an active protease that cleaves plasma fibrinogen to fibrin. Fibrin then self-assembles

into a blood clot and the process is called thrombosis (Figure 1.1). The various active protease complexes of coagulation assemble on the platelet membrane surface which has exposed negatively charged phospholipids (phosphatidylserine) headgroups. In these activated platelets an enzyme called scramblase mediates transport of phosphatidylserine from inner leaflet of plasma membrane to outer leaflet. Endothelial cells (ECs) help in inhibiting coagulation by sequestering phosphatidylserine on the inner leaflet of their plasma membrane, depriving clotting factors of access to a suitable phospholipid surface. Degranulation of platelets provides another important source of a phosphatidylserine-rich surface. ECs prevent platelet degranulation by acting upon the three principle signals that activate platelets: They (a) express ectoenzyme such as endothelial-ADPase that degrade the activating that degrade the platelet activator, ADP (b) inhibit thrombin, in endothelial cells thrombomodulin, an integral membrane protein is bound to thrombin which activates protein C, an inhibitor of coagulation cascade. This activated protein C then inactivates factors Va and VIIIa of the coagulation cascade, and (c) prevent exposure of subendothelial collagen. Endothelial cells produce a protein called von Willebrand factor (vWF), a cell adhesion ligand, which helps endothelial cells adhere to collagen in the basement membrane. Under physiological conditions, collagen is not exposed to the bloodstream. vWF is

secreted constitutively into the plasma by endothelial cells and is stored in granules within the endothelial cells and platelets. When the endothelial layer is injured, collagen and vWF from the subendothelium is exposed to the bloodstream and when platelets contact collagen or vWF they are activated.

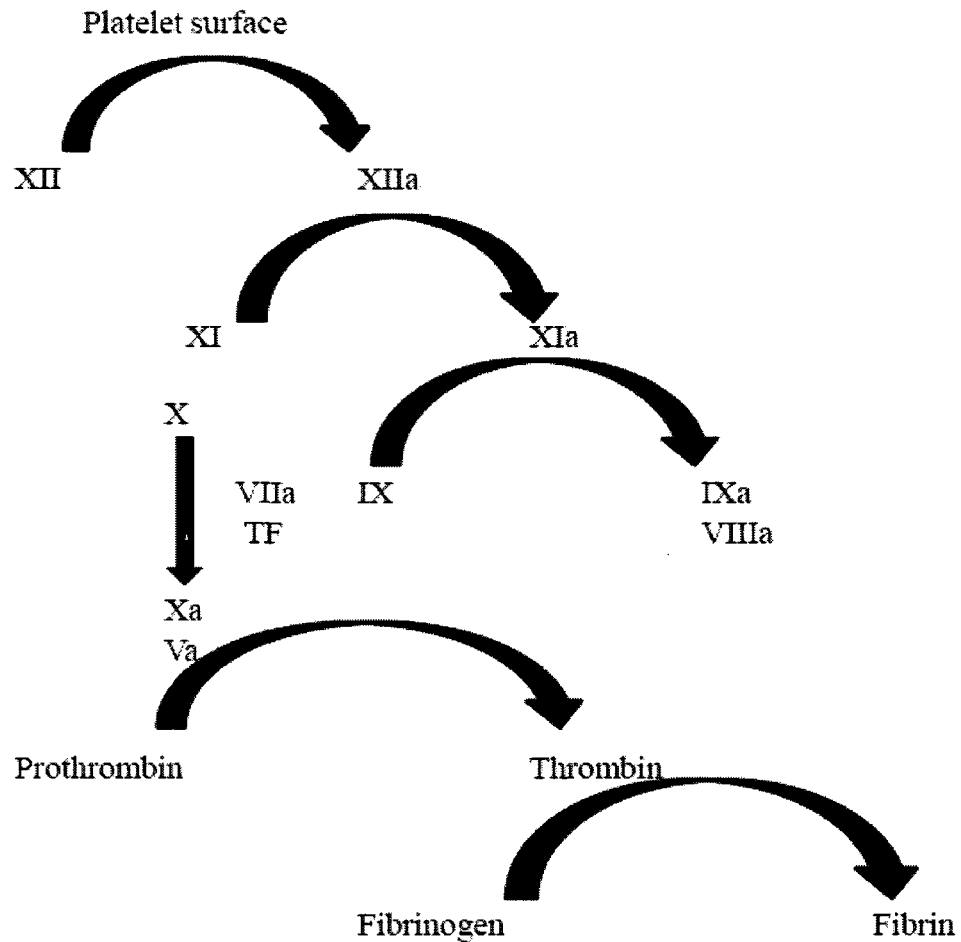


Figure 1.1 Platelet aggregation cascade

A second important function of ECs is the control of blood flow in the arterial circulation [Busse, *et al.*, 2006]. Tissue perfusion depends on cardiac output and on vascular resistance and this resistance is maintained by the tone of smooth muscle cells (SMCs) in conduit arteries. ECs are electrically coupled with these SMCs via gap junctions, permitting regulation of membrane potential and intracellular Ca^{2+} levels, but they also release diffusible regulators of SMC tone. Two of the most important of these are the vasodilators NO and arachidonic acid metabolites known as endothelium-derived relaxing factors, which regulates SMC membrane potential. NO is generated by endothelial nitric oxide synthase (eNOS) that converts arginine to citrulline, releasing NO [Sessa, *et al.*, 2004] NO relaxes SMCs principally by activating soluble guanylate cyclase, which generates cGMP and activates protein kinase G. ECs also causes vasoconstriction by producing vasoconstrictors, peptides such as endothelin I and angiotension II thus, the precise balance of vasodilators and vasoconstrictors is regulated in part by ECs.

A third important physiological function of ECs is quiescence of the inflammatory response by failing to express adhesion molecules that promote capture and transmigration of blood leukocytes into tissues. ECs and platelets express selectins shortly after cytokine activation by tissue macrophages. Activated ECs initially express P-selectins molecules, but within few hours after

P-selectins activation E-selectins expression occurs. Endothelial selectins bind to carbohydrates on macrophage transmembrane glycoproteins such as sialyl-Lewis^X. In unactivated endothelial cells P-selectins is stored in granules Weibel-Palade bodies and α -granules in unactivated platelets. [Ley, *et al.*, 2006].

1.1.3 Endothelial dysfunction and its relationship to endothelial cell injury and death

The endothelial cell death mostly occurs by apoptosis, a kind of programmed cell death [Kerr, *et al.*, 1972]. The features of apoptosis include plasma membrane vesiculation, nuclear condensation and nuclear fragmentation. An early biochemical indicator of apoptosis is the exposure of phosphatidylserine head groups on the outer leaflet of the plasma membrane-lipid bilayer, a change that can be detected experimentally by binding of exogenously added annexin V. Apoptotic cells cleave genomic DNA into histone-covered segments of approximately 200 bps known as nucleosomes [Compton, *et al.*, 1992]. Apoptotic death is caused by the cleavage of critical cellular proteins by a family of structurally related intracellular proteases known as active cysteinyl, aspartyl-directed proteases (caspases) [Logue, *et al.*, 2008]. Caspase cleavage of inhibitor of caspase-activated DNase (iCAD) releases active endonucleases, known as CAD, from inactive complex. CAD then cleaves genomic double-stranded DNA

at the segments separating histone-bound nucleosomes, releasing free nucleosomes. When the endothelial cells detach from their basement membrane a caspase dependent apoptosis is triggered and the phenomenon is referred to as anoikis [Gilmore, *et al.*, 2005]. However, certain other forms of endothelial cell death depend on intracellular pathways other than caspases, but they share with apoptosis the characteristic of being programmed. For example endothelial cells may respond to certain signals by the activation of cathepsin B in their cytosol, leading to mitochondrial release of apoptosis-inducing factor (AIF) [Li, *et al.*, 2005]. This protein (AIF) causes DNA degradation and endothelial cell death independently of caspases, with dying cells displaying nuclear condensation but not fragmentation.

However, having described about endothelial cell death, it is important to know how injurious stimuli trigger endothelial cell death. Several environmental stresses play a part in this including oxidative stress, endoplasmic reticulum (ER) stress and metabolic stress.

1.1.3.1 **Oxidative stress**

Reactive Oxygen Species (ROS) includes highly reactive molecules that are generated from the partial reduction of molecular oxygen, including superoxide and its dismutated product H_2O_2 . The most potent pathway for

generating ROS is catalyzed by the phagocyte oxidase (Phox) complex, which is expressed by neutrophils and macrophages. In addition to Phox, endothelial cells also express nonphagocyte NADPH dependent oxidase (Nox) complexes. Rodent, but not human, endothelial cells express xanthine oxidase (XO), an alternative mechanism for generating H₂O₂ but human endothelial cells (EC) may take up XO from plasma. The endogenous ROS generating systems in endothelial cells contribute more in generating second messengers that regulate EC growth, proliferation, EC barrier function, vasorelaxation and vascular remodelling [Rhee *et al.*, 2000] rather than producing oxidative stress. However, the endogenous Nox enzymes have also been considered to cause EC dysfunction in the pathogenesis of hypertension, atherosclerosis, cardiac hypertrophy and heart failure [Keaney, *et al.*, 2005]. Increasing evidence supports the idea that ROS generated from mitochondria significantly contribute to EC dysfunction and the progression of atherosclerosis [Nishikawa, *et al.*, 2003].

Mitochondrial electron transport chains consume oxygen by oxidative phosphorylation to form ATP. During this process, between 0.4 and 4% of the consumed oxygen is released in the mitochondria as ROS, resulting from the univalent reduction of molecular oxygen to superoxide anion (O²⁻) by electrons that leak from complex I and III of the mitochondrial electron transport chain. O²⁻

is in turn converted to H_2O_2 by mitochondria-specific manganese-dependent superoxide dismutase. H_2O_2 is a mild oxidant and is readily converted to the powerful hydroxyl radical ($\cdot\text{OH}$) via the Fenton reaction. O^{2-} , H_2O_2 and $\cdot\text{OH}$ cause multiple cellular actions if they are not appropriately regulated [Balaban, *et al.*, 2005]. In ECs, NO appears to be one of the major targets of ROS and its consumption results in EC dysfunction. Not only does O^{2-} alter endothelium-dependent vascular relaxation through interaction with NO, but the resultant formation of peroxynitrite can also oxidize the essential eNOS cofactor tetrahydrobiopterin (BH_4) and promote *eNOS uncoupling* [Landmesser, *et al.*, 2003]. For proper function of eNOS, BH_4 is essential in many ways including stabilizing the eNOS dimer and increasing the affinity of eNOS for L-arginine. In ECs native LDL [Pritchard, *et al.* 1995], oxidized LDL [Vergnani, *et al.*, 2000] can stimulate the O^{2-} production and hypercholesterolemia can also increase vascular O^{2-} production via NADPH oxidase [Warnholtz, *et al.* 1999] and/or xanthine oxidase [Ohara, *et al.*, 1993]. O^{2-} produced reacts with NO to form peroxynitrite [White, *et al.*, 1994] which in turn oxidizes the active eNOS cofactor BH_4 to cofactor-inactive molecules such as BH_2 [Laursen, *et al.*, 2001], thus limited availability of BH_4 would result in *uncoupling of eNOS*.

The biochemical responses that couple oxidative stress to apoptosis are increasingly well understood. Many of these responses are mediated by p38 mitogen-activated protein kinase (p38 MAPK) and/or by c-Jun N-terminal kinase (JNK), both of which may be activated by kinase cascades initiated by apoptosis-signalling kinase I (ASKI) and ASK I may be a common target of multiple types of stress leading to apoptosis.

1.1.3.2 Endoplasmic Reticulum Stress (ER stress)

Endoplasmic reticulum is an important site in the cell where the protein folding and modification takes place. ER also marks unfolded or misfolded proteins for their degradation. However, when a cell meets any adverse condition and is not able to function normally and unfolded protein response (UPR) is triggered in the ER and this phenomenon is termed as ER stress. ER stress is described in detail in section 1.4.

1.1.3.3 Metabolic Stress

ECs supply nutrition and oxygen to tissues, and may themselves experience stresses from abnormal metabolism (e.g., high glucose and high lipid levels), energy depletion or hypoxia. Insulin resistance, defined as decreased sensitivity and responsiveness to metabolic actions of insulin that promote glucose disposal, is an important consequence of metabolic stress to ECs. Insulin

resistance is observed in diabetes, glucose intolerance and dyslipidemias as well as in oxidative stress and inflammation. Normal insulin receptor/IGF1 receptor signal transduction is well characterized [Saltiel, *et al.*, 2001]. These receptors have intrinsic protein tyrosine kinase activity that is activated by ligand binding. The activated receptors phosphorylate several substrates, including insulin receptor substrate 1 (IRS 1), which leads to activation of phosphatidylinositol-3-kinase (PI3K)-Akt which leads to activation of the Ras-Raf-ERK signalling cascades. The PI3K-Akt pathway is the major branch of insulin signalling that regulates metabolic function, triggering glucose transporter 4 (GLUT4) translocation to the plasma membrane, where it mediates glucose uptake in skeletal muscle and adipocytes. Thus, IRS1/Akt activation underlies the molecular mechanism for insulin resistance and diabetes.

Hyperglycemia may induce expression of extracellular matrix and procoagulant proteins, increase EC apoptosis, decrease EC proliferation and inhibit fibrinolysis. Similarly, free fatty acids (FFAs) also inhibit EC proliferation and increase EC apoptosis.

Hypoxia is another source of metabolic stress that has not been extensively studied in ECs. ECs constitutively synthesize NO, which can regulate cellular oxygen consumption and the mitochondrial redox state. Recently it has been

proposed that in ECs, inhibition of mitochondrial oxygen consumption by NO may lead to metabolic hypoxia, a condition in which cells are unable to use available oxygen and are directed to apoptosis [Moncada, *et al.*, 2002].

1.1.4.1 Indicators of Endothelial dysfunction

Endothelial injury may result in the release of various factors that can be detected in the circulation and can be potentially used as markers of endothelial dysfunction.

Endothelin-1

Endothelin-1 is an endothelium derived peptide that has powerful vasoconstrictor properties. Increased levels of endothelin-1 have been demonstrated in conditions associated with endothelial dysfunction such as atherosclerosis, hypercholesterolemia and cigarette smoking [Lerman, *et al.*, 1991]. Furthermore, oxidized low-density lipoprotein has been shown to stimulate endothelin-1 production and secretion [Boulanger, *et al.*, 1992]. Injury to vascular endothelial cells probably triggers the release of endothelin-1 and therefore it has been suggested that the levels of circulating endothelin in plasma may represent a marker of endothelial dysfunction. Because endothelin-1 also has mitogenic properties, it may also play a role in the development of premature atherosclerosis.

von Willebrand factor

The von Willebrand factor (vWF) is a glycoprotein synthesized mainly by vascular endothelial cells. It has important functions in hemostasis, participating in the coagulation and in the formation of platelet plugs at the sites in patients with hypercholesterolemia. Its levels are elevated in situations characterized by vascular damage with injury of the endothelium and it has been suggested that the injured endothelial cells leak vWF leading to increased plasma levels.

Tissue plasminogen activator and plasminogen activator inhibitor-1

Tissue plasminogen activator is a protein released by endothelial cells. It activates the reaction in which plasminogen activator regulates the fibrinolytic activity of blood in balance with plasminogen activator inhibitor-1, another product of endothelial cells serving as the primary inhibitor of tissue plasminogen activator. These circulating vascular endothelial markers are elevated in hypercholesterolemia [Geppert, *et al.*, 1998].

1.1.5 Endothelial dysfunction in atherosclerosis

Endothelial injury is regarded as an important early event in atherogenesis [Ross *et al.*, 1990]. The consequence of endothelial damage that initiate fatty streak and plaque formation include increased adherence of monocytes, increased permeability to monocytes/macrophages and lipoproteins that accumulate in the

vessel wall, increased platelet adherence and increased smooth muscle cell migration and proliferation [Henderson *et al.*, 1991]. Endothelial dysfunction may also be accompanied by decreased availability of local NO. This may be due to decreased endothelial production of NO or to excess production of superoxide anions or both with consequent degradation of NO before it can reach its target tissues. Because NO is a local vasodilator that also inhibits platelet adherence and aggregation, smooth muscle proliferation and endothelial cell leucocyte interactions, reduced NO activity may also contribute to the initiation and progression of atherosclerosis [Cooke, *et al.*, 1994]. In hypercholesterolemia, superoxide production is enhanced with consequently decreased bioavailability of NO [Ohara, *et al.* 1993].

1.2 Cholesterol

Cholesterol is an alicyclic lipid molecule, the structure of which contains four fused rings (all *trans-anti*), a single hydroxyl group at carbon 3, a double bond between carbons 5 and 6, and an iso-octyl side chain at carbon 17 (Figure 1.2). The 3 β -OH function of cholesterol is important, since a fatty acid can be esterified to this position. Cholesterol is an essential component of cellular plasma membranes in higher organisms. The plasma membranes have been reported to contain from about half to as much as 90% of the total cellular unesterified cholesterol [Lange, *et al.*, 2000]. Since membrane cholesterol is unesterified, the free 3 β -OH group of cholesterol may engage in hydrogen bonding with water and possibly with co-lipids in the membrane. It is suggested that the capacity of plasma membranes to solubilise cholesterol is largely a function of its sphingomyelin content.

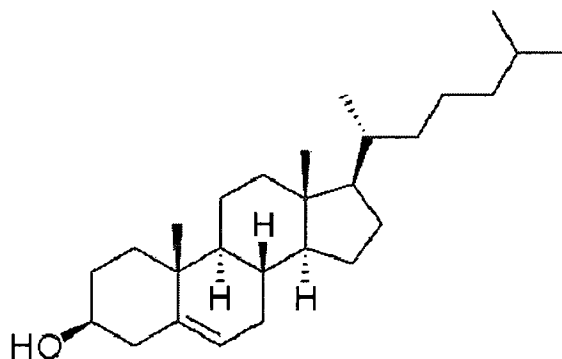


Figure 1.2 Structure of cholesterol

1.2.1 Cholesterol and sphingomyelin interaction

In cell membranes sphingolipids (sphingomyelin and glycosphingolipids) and cholesterol act as platforms for different cellular processes. There occurs a lateral interaction among sphingolipids and cholesterol to induce the formation of microdomains or rafts which helps in the recruitments of certain proteins to these domains as well as in the association of GPI-anchored proteins to plasma membrane invaginations, the caveolae. Cholesterol is assumed to associate with the rafts either by functioning as a spacer within the sphingolipid domains or by associating specifically with proteins (e.g. caveolin) in certain membrane domains (caveolae) [Murata, *et al.*, 2002]. There occurs specific cholesterol–sphingomyelin interaction in membranes which is stabilized by hydrogen bonds between the 3 β -OH group of cholesterol and the amide-linkage in sphingomyelin.

1.2.2 Cholesterol and sphingomyelin homeostasis

Cholesterol and sphingomyelin in biological membranes affect each other's homeostasis. The incorporation of sphingomyelin mass from liposomes into membranes results in the net flow of cholesterol from intracellular sites where it is stored as cholesteryl esters to the plasma membrane compartments. This is also accompanied by reduced acyl CoA: cholesterol acyltransferase (ACAT)-

catalyzed esterification of cell cholesterol and an increased formation of newly synthesized cholesterol. Also the degradation of sphingomyelin mass (with the aid of exogenous sphingomyelinase) leads to a dramatic activation of the endogenous ACAT-catalyzed esterification of cholesterol in endoplasmic reticulum [Slotte, *et al.*, 1988].

1.2.3 Biosynthesis of cholesterol

Cholesterol is made from acetyl-CoA. The process occurs in four steps, step 1. the three acetate units condense to form a 6-carbon intermediate mevalonate, step 2. mevalonate is converted into activated isoprene units, step 3. six 5-carbon isoprene units polymerize to form the 30-carbon linear structure of squalene, step 4. the cyclization of squalene forms the four ring steroid nucleus and further series of changes such as oxidation, removal or migration of methyl groups leads to the formation of final product- cholesterol.

1.2.3.1 Synthesis of mevalonate from acetate

The first step in cholesterol biosynthesis leads to the intermediate mevalonate. Two molecules of acetyl-CoA condense, forming acetoacetyl-CoA, catalyzed by thiolase. Acetoacetyl-CoA condenses with a third molecule of acetyl-CoA to yield the 6-carbon compound β -hydroxy-acetyl- β -methylglutaryl-CoA (HMG-CoA), catalyzed by HMG-CoA synthase. In the third reaction, HMG-CoA

is reduced to mevalonate by HMG-CoA reductase, an integral membrane protein of smooth endoplasmic reticulum.

1.2.3.2 Conversion of mevalonate to two activated isoprenes

The phosphate groups from 3 ATP molecules are transferred to mevalonate. In the next step, the phosphate attached to the C-3 hydroxy group of mevalonate in the intermediate 3-phospho-5-pyrophomevalonate and the nearby carboxyl group both leave, producing a double bond in the 5-carbon product Δ^3 -isopentanyl pyrophosphate the first of the activated isoprenes. Isomerization of Δ^3 -isopentanyl pyrophosphate yields an activated isoprene dimethylallyl pyrophosphate.

1.2.3.3 Condensation of six activated isoprene units to form squalene

Isopentyl pyrophosphate and dimethylallyl pyrophosphate undergoes a “head-to-tail” condensation in which one pyrophosphate group is displaced and a 10-carbon chain, geranyl pyrophosphate is formed. Geranyl pyrophosphate undergoes another head-to-tail condensation with isopentenyl pyrophosphate, yielding the 15-carbon intermediate farnesyl pyrophosphate. Finally, two molecules of farnesyl pyrophosphate join head to head forming squalene.

1.2.3.4 Conversion of squalene to the four-ring steroid nucleus

The action of enzyme squalene mono oxygenase adds one oxygen atom from O₂ to the end of the squalene chain, forming an epoxide, squalene 2,3-epoxide, which is cyclised to a steroid nucleus, resulting in the formation of lanosterol. Lanosterol is finally converted into cholesterol in a series of 20 reactions, including the migration of some methyl groups and removal of others.

1.2.4 Cholesterol is transported to plasma lipoproteins

Cholesterol and cholesteryl esters, like triacylglycerols and phospholipids are insoluble in water. Those lipids must be moved from the tissues where they are synthesized/absorbed, liver/intestine to the tissues in which they will be stored or consumed. They are carried in the blood plasma from one tissue to another as plasma lipoproteins, molecular aggregates of specific carrier proteins called **apolipoproteins** with various combinations of phospholipids, cholesterol, cholesteryl esters and triacylglycerols. Apolipoproteins combine with lipids to form several classes of lipoprotein particles, spherical aggregates with hydrophobic lipids at the core and the hydrophilic side chains of protein amino acids at the surface. Differing combinations of lipid and protein produce particles of different density and sizes such as **very low density lipoproteins** (VLDL), **low density lipoproteins** (LDL) and **high density lipoproteins** (HDL). Each class of

lipoprotein has a specific function, determined by its point of synthesis, lipid composition and apolipoprotein content. The protein components act as signals, targeting lipoproteins to specific tissues or activating enzymes that act on the lipoproteins.

When the diet is rich in fatty acids than what are needed immediately as fuel, they are converted into triacylglycerols in the liver and packaged with cholesterol, cholesteryl esters as well as specific apoproteins such as apoB-100, apoC-I, apoC-II, apoC-III and apoE into very low density lipoproteins (VLDL). Excess carbohydrates in the diet is also converted into triacylglycerols in the liver and exported as VLDLs. The lipoproteins are transported in the blood from liver to the adipose tissues where activation of lipoprotein lipase by apoC-II causes the release of free fatty acids from triacylglycerols of the VLDLs. Adipocytes take up these fatty acids, resynthesizes triacylglycerols from them and store triacylglycerols in intracellular droplets.

The loss of triacylglycerols converts VLDL to low density lipoprotein, LDL. These are very rich in cholesterol, cholesteryl esters and apoB-100 as the major apolipoprotein. LDL carry cholesterol to peripheral tissues (other than liver) that have specific surface receptors called LDL receptors and recognize apoB-100.

The high density lipoprotein, HDL, is synthesized in the liver as small protein rich particles, containing little cholesterol, cholesteryl esters and apoC-I and apoC-II as the major apolipoproteins as well as the enzyme lecithin-cholesterol acyl transferase (LCAT) which catalyzes the formation of cholesteryl esters from lecithin (phosphatidylcholine) and cholesterol. The nascent HDL in the blood stream collects cholesteryl esters from other circulating lipoproteins and LCAT on their surface converts phosphatidylcholine and cholesterol from lipoproteins to cholesteryl esters, which enter the interior of nascent HDL, converting it from flat disc to sphere- a mature HDL. These cholesterol esters rich HDL then returns to liver, where the cholesterol is unloaded and some of it converted into bile salts and the rest stored as cholesteryl esters in lipid droplets in the cytosol.

1.2.5 Influx of exogenous cholesterol

Cholesterol can be endocytosed from lipoproteins in the circulation by mechanisms involving desorption- transfer of cholesterol from lipoproteins to the exoplasmic leaflet of the plasma membrane bilayer- or by receptor-mediated uptake. The best understood process is the one involving serum low density lipoprotein (LDL), and its LDL-receptor. Cholesterol is endocytosed in LDL via LDL receptors in the clathrin- coated pits in the plasma membrane to sorting

endosomes where it is released from its receptor and the LDL-receptor recycles to the cell surface. In the sorting endosomes cholesteryl esters are hydrolyzed to cholesterol by cholesterol esterase and transported to the cell surface via a rapid route or through slower circuits involving recycling endosomes. Cholesterol is transported to late endosomes and then to lysosomes with NPC 1 protein [Neufeld, *et al*, 1996 Higgins, *et al*, 1999 Puri, *et al* 1999] that can fuse with each other. These endosomal compartments then communicate with the exocytic pathway with the help of Trans Golgi Network (TGN) [Cruz, *et al*, 2000 Lange, *et al*. 1989]. The NPC 1 protein is a multispinning membrane protein that contains a putative sterol-sensing domain in the membrane spans [Davies, *et al* 2000]. One potential function of the sterol-sensing domain in NPC 1 is to direct cholesterol binding and NPC 1 protein may function to remove cholesterol from the degradative endosomal compartments by facilitating sterol transport to the Golgi or other destinations in vesicular carriers [Liscum, *et al*, 2000 Blanchette-Mackie, *et al*. 2000]. Some of the cholesterol is also transported to the ER, where it is esterified by the enzyme acyl-coenzyme A: cholesterol acyl transferase (ACAT) [Liscum, *et al*., 1999]. This esterification is activated as a means to detoxify excess free cholesterol and the esters are deposited in cytosolic lipid droplets, from where cholesterol can be mobilized upon ester hydrolysis. This transport to

the ER can be mediated by two pathways. One involves the Golgi complex whereas the other pathway bypasses the Golgi and the cholesterol from the endosomes reaches ER by a protein carrier [Neufeld, *et al.*, 1999. Underwood, *et al.*, 1998].

1.2.6 Cholesterol efflux from cells

Cellular cholesterol is effluxed by release of cholesterol to circulating lipoproteins at the rate of 0.1% of total cholesterol per min [Johnson, *et al.*, 1991]. The release from plasma membrane can take place by desorption into lipoproteins or be induced after HDL binding to membrane receptors [Rothblat, *et al.*, 1999]. Liver and intestine release cholesterol to the circulation mostly as esters by synthesizing and secreting lipoproteins [Olofsson, *et al.*, 1999]. Cholesterol can be removed by plasma membrane by shedding [Dolo, *et al.*, 2000]. The candidate protein involved in cholesterol efflux by HDL is the ATP- binding cassette transporter (ABCA 1) [Bodzioch, *et al.*, 1999. Brooks- Wilson, *et al.*, 1999. Rust, *et al.*, 1999]. ABCA 1 helps in translocating cholesterol from cytoplasm to the exoplasmic bilayer- leaflet from where efflux takes place.

1.2.7 Regulation of cellular cholesterol levels

The best known mechanism involved in cholesterol homeostasis is the control of cholesterol biosynthesis. This control system involves membrane-

bound transport factors called sterol regulatory element binding proteins (SREBPs) that activate genes upregulating cholesterol uptake and synthesis. The SREBP is present in the ER membrane and cycles between ER and the Golgi. It can be released from the ER membrane by two proteolytic cleavage. The movement of SREBP is dependent on a factor, the SREBP cleavage activating protein (SCAP) that contains a sterol- sensing domain regulating the transport. When cholesterol levels fall, the SREBP-SCAP complex moves from the ER to the Golgi, where two site specific proteases S1P and S2P to liberate the active SREBP for transport to the nucleus. The sterol deprivation discharges SREBP-SCAP complex into the Golgi [Nohtufft, *et al.*, 2000].

Another point of regulation is at the plasma membrane level. Plasma membrane contains cholesterol in the lipid raft domain and in the liquid disordered domain. In the liquid ordered or the lipid raft domain, cholesterol is in 1:1 balance with sphingomyelin. Increasing cholesterol levels beyond saturation limit of rafts would lead to an increased cholesterol concentration in the liquid- disordered phase. This latter pool of cholesterol is free to move back to the ER, thus blocking transport SREBP-SCAP to the Golgi. This slows down cholesterol synthesis and leads to push extra cholesterol from plasma membrane to ER for esterification and is stored as cholesteryl esters in cytosolic lipid droplets. The enzyme

sphingomyelinase regulates this process which degrades sphingomyelin that leads to a rapid increase in ER cholesterol and eventually cholesteryl ester formation [Slotte, *et al.*, 1988. Scheek, *et al.*, 1997].

The sphingomyelin and cholesterol levels are controlled together with oxysterols. [Ridgway, *et al.*, 2000]. Oxysterols are produced by sterol hydrolases from cholesterol. The molecule 25-OH-cholesterol is known to bind to the oxysterol-binding protein (OSBP). OSBP resides in the cytosol or the Golgi and is regulated by the cellular cholesterol content. Cholesterol depletion leads to translocation of OSBP to the Golgi complex and to activation of both cholesterol and sphingomyelin synthesis [Ridgway, *et al.*, 1992. Ridgway, *et al.*, 1998].

Cholesterol is also metabolized in most tissues of the body. The liver plays a key role in eliminating cholesterol that has been removed from the periphery by incorporation into circulating high-density lipoproteins. These are taken up by scavenger receptor B1 in the liver [Trigatti, *et al.*, 2000], and then part of the released cholesterol is metabolized to bile salts and eliminated by secretion [Cohen, *et al.*, 1999. Oude Elferink, *et al.*, 1999].

1.3 Nitric Oxide

Over the past decade or so, NO a free radical gas has been implicated in many physiological and pathological processes [Moncada, *et al.*, 1991]. NO plays a central role in cardiovascular system as the endothelium derived relaxing factor [Furchgott, *et al.*, 1980], within the central nervous system in the signal transduction pathways for memory formation, sensory processing and the regulation of cerebral blood flow [Xu, *et al.*, 1998] and also in the immune defence network [Wagner, *et al.*, 1984]. NO is a diatomic free radical molecule and is produced by a family of NOS enzymes. These enzymes require a panel of substrates and cofactors to fully function. NO-generating reaction requires L-arginine, NADPH and oxygen as substrates and tetrahydrobiopterin (BH₄), thiol, flavin adenine dinucleotide (FAD) and flavin mononucleotide (FMN) as cofactors (Figure 1.3). In addition to NO, NOS catalyzed reaction produces citrulline and NADP as co-products. The family of isoforms consists of: nNOS (the first to be purified and cloned, hence also called NOS1), iNOS (NOS2), and eNOS (NOS3). Each isoform is the product of a distinct gene [Hammadi, *et al.*, 2008]. Historically, NOS have been classified into two distinct categories, constitutive (nNOS and ecNOS) and inducible [Nathan, *et al.*, 1994]. Generally, nNOS and eNOS are produced **constitutively** in the cells, respectively, and require elevation

in intracellular Ca^{2+} and attendant activation of calmodulin to produce NO. These isoforms are regulated primarily by Ca^{2+} influx and generate low levels of NO for brief periods of time [Moncada, *et al.*, 2002. Bredt, *et al.*, 1992]. On the other hand, iNOS is an **inducible** form of NOS and needs to be induced by cytokines in essentially every cell type, and can generate locally high concentrations of NO for prolonged periods of time. The thesis dissects a very important aspect of eNOS in endothelial dysfunction therefore; it would be worthwhile to understand eNOS in detail.

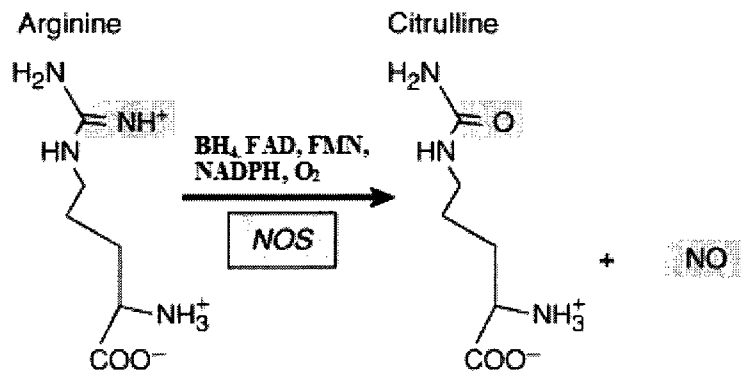


Figure 1.3 Nitric oxide synthesis by nitric oxide synthase (NOS)

Nitric oxide (NO) produced from eNOS serves as an endogenous vasodilator, platelet inhibitor, antioxidant, and regulator of vascular endothelium by sustaining its anti-coagulant and antithrombogenic properties [Dudzinski, *et*

al., 2006]. Endothelial nitric oxide synthase (eNOS) is expressed not only in endothelial cells, but also in cardiac myocytes and blood platelets, where the enzyme subserves key roles in cardiovascular physiology [Dudzinski, *et al.*, 2005]. eNOS has also been reported to be expressed in diverse tissues including mast cells, renal epithelium, erythrocytes, and leukocytes. Because NO production must be carefully titrated to respond to diverse physiologic and pathophysiologic stimuli, eNOS is regulated by multiple interdependent control mechanisms and signaling pathways.

1.3.1 Post-translational modifications to the eNOS

1.3.1.1 Acylation

In quiescent cells, eNOS is specifically targeted to small invaginations of the plasmalemma called caveolae. Caveolae are invaginated membrane microdomains defined by the presence of a scaffolding protein caveolin. The caveolae are enriched in cholesterol and sphingolipids [Govers, *et al.*, 2001]. Caveolae sequester diverse receptors and signalling proteins from a variety of signal transduction pathways, including G protein coupled receptors, G proteins, growth factor receptors, Ca^{2+} regulatory proteins in microdomains, may serve to position eNOS to receive signals from these upstream signaling pathways and facilitate communication with downstream activators [Dudzinski, *et al.*, 2006]. Localization

of eNOS to caveolae is dependent on irreversible, co-translational myristoylation of its N-terminal glycine (after removal of true N-terminal methionine) by N-myristoyltransferase [Dudzinski, *et al.*, 2006]. Myristoylation initially targets N-Myr-eNOS to the cell membrane in general, where reversible post-translational palmitoylation of the Cys 15 and Cys 26 residues occurs by palmitoyltransferase [Shaul, *et al.*, 2002]. Myristoylation and palmitoylation confer on eNOS three acyl anchors that anchor it firmly to the caveolar lipid bilayer.

1.3.1.2 Intracellular Ca^{2+} levels and calmodulin binding

Intra-cellular Ca^{2+} level are a critical determinant of eNOS activity because maximal catalytic function of eNOS requires calmodulin binding [Chen, *et al.*, 2000]. Binding of calmodulin simultaneously disrupts the inhibitory caveolin–eNOS interaction [Michel, *et al.*, 1997]. Numerous pathways converge on mobilization of intracellular Ca^{2+} transients to provide the most rapid mechanisms of eNOS activation via calmodulin. A diverse group of agonists, including bradykinin and acetylcholine [Goetz, *et al.*, 1999], activate a G protein-dependent signaling pathway that ultimately releases intra-cellular Ca^{2+} stores [Loscalzo, *et al.*, 1995]. In this pathway, phospholipase C (PLC) cleaves membrane component phosphatidylinositol 4,5-triphosphate into diacylglycerol (an activator of protein kinase C) and inositol 1,4,5-triphosphate (IP3), which

binds to IP3 receptors that are found in high concentrations in caveolae and regulate intra-cellular Ca^{2+} through pleiotropic effects on ion channels [Fujimoto, *et al.*, 1992].

1.3.1.3 Phosphorylation

Phosphorylation and de-phosphorylation are also important regulatory factors on eNOS activity. Key serine and threonine residues in eNOS constitute regulatory loci: phosphorylations at Ser 1177 (primary sequence numbering corresponds to human eNOS), Ser 1179 (bovine), Ser 635, and Ser 617 are stimulatory while phosphorylations at Thr 495 and Ser 116 are inhibitory [Bauer, *et al.*, 2003]. The activation of eNOS catalytic function by Ser 1177 phosphorylation is due to inhibition of calmodulin dissociation from eNOS and also enhancement of the internal rate of eNOS electron transfer. Ser 1177 phosphorylation is catalyzed by numerous kinases, including kinase Akt (protein kinase B) as well as the cyclic AMP-dependent protein kinase (PKA), AMP-activated protein kinase (AMPK), PKG, and Ca^{2+} /calmodulin dependent protein kinase II (CaM kinase II) [Fulton, *et al.*, 2001] Phosphorylation at Ser 617, occurring downstream of either PKA or Akt, appears to sensitize eNOS to calmodulin binding [Michell, *et al.*, 1997] and possibly modulate phosphorylation at other eNOS sites [Bauer, *et al.*, 2003]. Phosphorylation at Ser 635 is responsive

to PKA and increases eNOS activity in response to PKA dependent agonists as well as basal stimuli like shear stress [Michell, *et al.*, 2001] Phosphorylation at Thr 495, downstream of protein kinase C (PKC) and AMPK [Fulton, *et al.*, 1999], attenuates the binding of calmodulin by eNOS; accordingly, agonist-mediated de-phosphorylation of Thr 495, probably due to protein phosphatase 2A or protein phosphatase 1, enhances the interaction of eNOS and calmodulin. The phosphorylation state of Thr 495 helps adjust the product mix of eNOS output between superoxide and NO [Lin, *et al.*, 2003]. Phosphorylation of eNOS at Ser 116 inhibits enzyme activity, and de-phosphorylation of eNOS at this site is promoted by the eNOS agonist VEGF, but not by several other eNOS agonists [Kou, *et al.*, 2002].

1.3.1.4 **S-Nitrosylation**

Reversible S-nitrosylation is recognized as an additional *in vivo* post-translational control of eNOS activity [Erwin, *et al.*, 2005]. Quiescent eNOS is inhibited by S-nitrosylation at cysteine residues Cys 94 and Cys 99 that comprise a zinc-tetrathiolate cluster [Erwin, *et al.*, 2005]. S-nitrosylation of eNOS leads to inhibition whereas de-nitrosylation stimulated by eNOS agonists is associated with increase in enzyme activity. Sub-cellular location also affects eNOS S-nitrosylation and de-nitrosylation. Membrane targeting is required for S-

nitrosylation owing to the facilitation of NO and gaseous reaction in the hydrophobic milieu of the membrane made of lipids. De-nitrosylation occurs intracellularly, facilitated by the cytosolic reducing environment and lack of proximity to membrane-bound enzymes that catalyze nitrosylation.

1.3.2 Protein partners of eNOS in the caveolae

1.3.2.1 Caveolin

Caveolins are a 22 KDa proteins integrally linked to membrane owing to membrane-spanning domains and reversible post-translational triple C-terminal palmitoylation [Parat, *et al.*, 2001]. Caveolin-1 and caveolin-2 are ubiquitously expressed in endothelial cells; caveolin-3 is a muscle-specific isoform in cardiomyocytes and skeletal muscle [Rothberg, *et al.*, 1992]. Caveolin-1 and eNOS bind to each other by protein-protein interaction. Caveolin inhibits eNOS both by impeding the signalling of caveolae-targeted receptors that transducer eNOS-stimulatory signals as well as by sterically blocking the calmodulin binding site to eNOS [Michel, *et al.*, 1997].

1.3.2.2 Endoglin

Endoglin (CD105) is a 180 KDa glycoprotein highly expressed on endothelial cell membranes. It is enriched in caveolae and stabilizes eNOS by promoting its association with hsp90 [Toporsian, *et al.*, 2005].

1.3.3 Signalling partners of eNOS

1.3.3.1 PI3K/Akt

Kinase Akt (protein kinase B) phosphorylates eNOS at Ser1177. Kinase Akt is localized in the cytosol in inactive form and must translocate to the membrane for its own activation and eNOS phosphorylation [Gonzalez, *et al.*, 2002]. It is controlled by the phosphoinositide-3-kinase (PI3K)-dependent phosphorylation pathways and it appears PI3K recruits Akt to the membrane for phosphorylation [Vanhaesebroeck, *et al.*, 1997].

1.3.3.2 hsp90

The role of heat shock protein 90 (hsp90), a chaperone involved in protein trafficking and folding, extends to agonist-dependent eNOS activation. eNOS becomes robustly associated with hsp90 as hsp90 undergoes reversible tyrosine phosphorylation in response to diverse eNOS agonists [Venema, *et al.*, 1996]. Hsp90 binding stimulates eNOS activity by cooperatively enhancing the affinity of eNOS for binding calmodulin. Hsp90 also affects eNOS specific activity by means of effects on Akt. Hsp90 can bind both inactive and active Akt and is required for the interaction of Akt with eNOS [Garcia-Cardena, *et al.*, 1998]. Furthermore, hsp90 maintains levels of phospho-Akt and thus Akt

phosphorylation activity by protecting PI3K from proteasomal degradation [Wei, *et al.*, 2005] as well as inhibiting Akt deactivation by protein phosphatase 2A. Synergistic activation of eNOS can be seen following formation of a ternary complex containing hsp90, Akt, and calmodulin-bound eNOS [Takahashi, *et al.*, 2003]. Finally, NO itself may negatively modulate hsp90 by Snitrosylation of a cysteine residue that inhibits the hsp90 ATPase function and may disrupt eNOS–hsp90 binding; this mechanism might provide negative feedback to regulate the amount of NO generation and/or facilitate cyclic eNOS activity [Martinez-Ruz, *et al.*, 2005].

1.3.3.3 Phosphatases

Depending on the site, dephosphorylation of eNOS could either activate the enzyme (e.g. Ser 116 or Thr 495), or attenuate enzyme activity (e.g. Ser 1177), perhaps returning NOS to basal activity after stimulatory phosphorylation. Several phosphatases, including serine–threonine protein phosphatase 1 (PP1), serine–threonine protein phosphatase 2A (PP2A), and calcineurin participate in eNOS regulation. PP1 primarily de-phosphorylates Thr 495 and may activate eNOS [Fulton, *et al.*, 2001]. A pathway involving the phosphatase calcineurin leads to de-phosphorylation of Ser 116 and to the activation of eNOS, while downstream of bradykinin calcineurin also de-phosphorylates Thr 495 [Harris, *et al.*, 2005].

PP2A functions as an overall negative regulator of eNOS due to its primary roles in de-phosphorylating phospho-Akt and de-phosphorylating Ser 1177 despite the fact that it can also de-phosphorylate Thr 495 [Wei, et al., 2006]. Possibly because of its high abundance and robust constitutive activity, the influence of PP2A on eNOS is regulated partly by the proteasome [Wei, *et al.*, 2005]. Proteasomal inhibition causes PP2A ubiquitination and redistribution of PP2A from the cytosol to the membrane, thus leading to the association of PP2A with eNOS, and thereby reducing both phosphorylation of Akt and of eNOS at their respective stimulatory phosphorylation sites [Wei, *et al.* 2005].

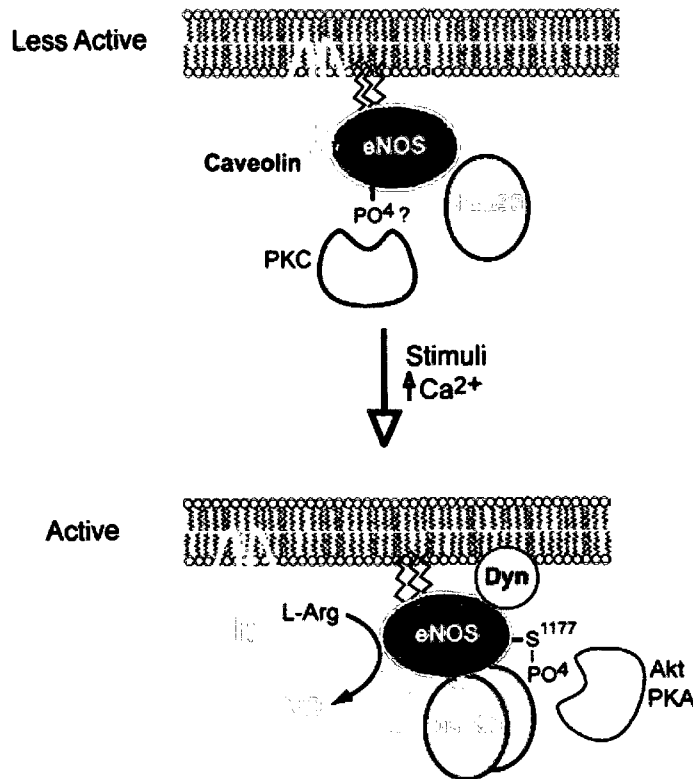


Figure 1.4 Post-translational activation of eNOS: In the top panel, eNOS under basal condition is less active. Under basal condition, eNOS is associated with caveolin, hsp90 and protein kinase C (PKC), which phosphorylates it. eNOS association with caveolin and PKC renders it less active. Endothelial cell stimulation by various stimuli (bottom panel) activates eNOS catalysis [ie the conversion of L-arginine (L-Arg) to nitric oxide (NO)] through its association with calcium-activated calmodulin (CaM). More calcium fluxes in cytoplasm recruits more CaM to eNOS. The action of CaM may be facilitated by the recruitment of hsp90 to eNOS and from the dissociation of eNOS from caveolin. eNOS Ser 1177/1179 phosphorylation can be induced by both calcium-dependent and independent stimuli. Phosphorylation of these residues by Akt, protein kinase A (PKA) is associated with increased eNOS activity.

1.3.4 eNOS sub-cellular localization and trafficking

In endothelial cells, eNOS appears to localize at peripheral region of the Golgi complex and cholesterol-rich microdomains of the plasma membrane (PM) such as caveolae. Co-translational N-myristoylation and posttranslational cysteine palmitoylation of eNOS determine its membrane targeting [Sessa, *et al.*, 2004]. It has been proposed that eNOS membrane localization may bring eNOS in close proximity to factors that are required for its proper function, such as L-arginine, BH4, CaM, and Akt which are less accessible to the Golgi-eNOS [Govers, *et al.*, 2001].

1.3.4.1 NOSIP

One eNOS-associated protein identified is the eNOS Interacting Protein (NOSIP), a 34 kDa protein that binds the carboxy-terminal of the eNOS oxygenase domain and appears to assist in translocation of eNOS from plasma membrane caveolae to intra-cellular membranes [Dedio, *et al.*, 2001]. Association of eNOS and NOSIP is inhibited by caveolin-1.

1.3.4.2 NOSTRIN

The second protein identified is the eNOS TRafficking INducer protein NOSTRIN, a 58 kDa protein of the PCH family (pombe *cdc15* homology) that is robustly expressed in endothelium and highly vascularised tissue [Schilling, *et al.*,

2006]. NOSTRIN shares the characteristic domain structure of PCH proteins, which includes an N terminal cdc15 domain (consisting of an FCH region [Fes/CIP homology] followed by a coiled-coil structure) and C-terminal coiled coil and SH3 domains [Icking, *et al.*, 2006]. The FCH region is sufficient to direct membrane targeting of NOSTRIN (to plasmalemma and peripheral vesicles), while FCH deletion mutants are found in the cytosol fraction [Icking, *et al.*, 2006]. The NOSTRIN SH3 domain not only binds the oxygenase domain of eNOS. NOSTRIN interacts (via its C-terminus) with eNOS (oxygenase domain) and via its central domain with caveolin-1 (at its N-terminus). Caveolin-1 and NOSTRIN each enhance the binding of the other to eNOS on unique sites; accordingly, a ternary eNOS–NOSTRIN–caveolin-1 complex of unknown stoichiometry has been demonstrated in vivo; this ternary complex may localize at the plasma membrane [Schilling, *et al.*, 2006].

1.4 Endoplasmic Reticulum stress (ER stress)

Endoplasmic Reticulum (ER) is a well designed site for the synthesis and folding of proteins. It is composed of protein chaperones, proteins that catalyze protein folding and sensors which detect the presence of misfolded or unfolded proteins. ER has several important functions involving glycosylation, formation of disulphide bonds, folding and assembly of newly synthesized proteins. All the proteins must undergo these processes properly in the ER before transit to the Golgi compartment. A Quality Control which is sensitive surveillance mechanism exists in the ER that permits only properly folded proteins to exit the ER and reach other intracellular organelles and cell surface. Misfolded or unfolded proteins are either retained within the ER lumen in complex with molecular chaperones or are directed toward degradation through the 26S proteasome in a process called ER-associated degradation (ERAD) or through autophagy.

Accumulation of misfolded or unfolded proteins in ER disturbs ER function and cell survival can be threatened. Overload of these abnormal proteins in the ER triggers an ER stress response, termed as the unfolded protein response (UPR) [Marciniak, *et al.*, 2004]. The UPR is an intracellular signalling pathway that coordinates ER protein folding demand with protein-folding capacity and is essential to adapt to homeostatic alterations that cause protein misfolding. These

include changes in intraluminal Ca^{2+} , altered glycosylation, and nutrient deprivations, pathogen infection, expression of folding-defective proteins and changes in redox status. ER serves as a cellular Ca^{2+} store and plays an important role in Ca^{2+} homeostasis by pumping Ca^{2+} into ER lumen via sarco-endoplasmic reticulum Ca^{2+} -ATPase (SERCA) and by releasing Ca^{2+} from the ER by inositol 1,4,5- triphosphate (IP_3) receptor and/or ryanodine receptor (RyR) [Oyadonaari, *et al*, 2004. Schroder, *et al.*, 2005]. High concentration of Ca^{2+} in ER is necessary for folding and disulphide bond formation of newly synthesized proteins and is required for the function of ER chaperones such as calreticulum, calnexin and protein disulphide isomerase (PDI). The ER also provides an oxidizing protein folding- environment that favors the formation of disulphide bond formation and results in the generation of reactive oxygen species (ROS) as a by-product of protein oxidation.

When ER function is disturbed and unfolded or misfolded proteins accumulate in ER, the ER stress response pathway or the UPR is activated to restore normal ER functions. There are three ER stress sensors (Ire1, ATF6 and PERK) on the ER membrane [Wang, *et al.*, 1996]. In unstressed conditions, ER chaperone GRP78/BiP binds to the ER luminal domain of 3 ER stress sensors. When unfolded or misfolded proteins are accumulated in ER, GRP78/BiP

dissociates from ER stress sensors, and then binds to those abnormal proteins [Bertolotti, *et al*, 2000. Okamura, *et al.*, 2000]. Dissociation of GRP78/BiP induces the activation of ER stress sensors.

Four distinct ER stress response phases have been identified [Yoshida, *et al.*, 2003]- (1) Attenuation of translation (2) Induction of ER chaperones (3) Degradation of unfolded/misfolded proteins by ubiquitin-proteasome system (4) Apoptosis. Under ER stress condition, these 4 stages show a time-dependent transition [Yoshida, *et al.*, 2002].

1.4.1 Attenuation of translation

Under ER stress condition, PERK is activated by dimer formation and autophosphorylation. The activated PERK brings phosphorylation of eIF2 α (α subunit of eukaryotic initiation factor 2) [Harding, *et al.*, 2000]. The phosphorylated eIF2 α blocks the binding of initiator Met-tRNA to ribosomes and so adenine-uracil-guanine (AUG) initiation codon recognition is reduced and the general translation is attenuated. However, translation of the transcription factor ATF4 is upregulated by eIF2 α through induction of GADD34 (regulatory subunit of protein phosphatase) and activation of protein phosphatase 1 (PP1c) (Marciniak, *et al.*, 2004). PP1c catalyzes the dephosphorylation of eIF2 α . The first

stage of ER stress response is terminated by the re-binding of BiP to PERK and dephosphorylation of eIF2 α .

1.4.2 Induction of ER chaperones

Protein folding in the ER is facilitated by ER chaperone proteins such as GRP78/BiP and GRP94 and by enzymes such as protein disulphide isomerase and peptidyl-prolyl isomerase [Schroder, *et al.*, 2005]. Under ER stress conditions, the ER stress sensor ATF6 inactive form (p90ATF6) is transported to the Golgi and is activated by a 2-step cleavage by Site-1 protease (S1P) and Site-2 protease (S2P), then ATF6 active form (p50ATF6) is produced [Ye, *et al.*, 2000]. The active p50ATF6 binds to the cis-acting ER stress response element (ERSE) of ER stress-related genes such as GRP78/BiP and XBP1, then the transcription of those genes are activated [Yoshida, *et al.*, 2003]. ER stress sensor Ire1 which on activation by dimer formation and autophosphorylation, splices out a small fragment of XBP1 and activates it [Yoshida, *et al.*, 2002. Calton, *et al.*, 2002. Lee, *et al.*, 2002]. XBP-1 active form binds to ERSE to increase the transcription of ER stress-related genes such as GRP78/BiP and XBP1 itself. Therefore, ATF6 and XBP1 play the key role to enhance the folding activity in the second stage of ER stress response.

1.4.3 Degradation of unfolded/misfolded proteins by ubiquitin-proteasome system

When the first two ER stress response phases are not able to rectify the unfolded /misfolded proteins, then the remainder of these are detected by the quality control system in ER, transported from the ER to cytosol and degraded by ERAD [Meusser, *et al.*, 2005]. These proteins are retro-translocated to cytosol and degraded through the ubiquitin-proteasome system in cytosol [Gardner, *et al.*, 2001]. On ER stress, expression of ERAD-related molecules including EDEM is induced through active Ire1 and XBP1 signaling and ERAD activity is enhanced.

1.4.4 Apoptosis

When ER functions are severely impaired, apoptotic pathway is induced to eliminate the damaged cells [Oyadomari, *et al.*, 2002]. There are 3 pathways involved in ER stress mediated apoptosis. The first is the transcriptional activation of the gene for C/EBP homologous protein (CHOP) [Zinszner, *et al.*, 1998]. The second is the activation of the Ire1-TRAF2-ASK1-MAP kinase pathway [Nishitoh, *et al.*, 2002]. The third is activation of ER-associated caspase 12 [Nakagawa, *et al.*, 2000].

CHOP/GADD153 is expressed at low levels under physiological conditions but is strongly induced at the transcription level in response to ER

stress. There are at least 4 ER stress-responsive transcriptional enhancer elements (AARE1, AARE2, ERSE1 and ERSE2) in the transcriptional regulatory region of CHOP gene [Ubeda, *et al.*, 2000]. The translational activation of ATF4 as a result of eIF2 α is phosphorylation by activates PERK binds to the AARE1 and AARE2 [Fewcett, *et al.*, 1999]. XBP1 active form induced via the cooperation of ATF6 and Ire1 pathway binds to ERSE and enhances the transcription of ER stress-related genes including CHOP. Under ER stress conditions, the activity of CHOP is enhanced through the phosphorylation of Ser78 and Ser81 of CHOP protein by the p38 MAP kinase [Wang, *et al.*, 1998]. Under ER stress condition, it is reported that p38 MAP kinase is activated through Ire1-TRAF2-ASK1 signaling pathway. Therefore, it is speculated there may be a crosstalk between the CHOP pathway and ASK1 pathway.

c-Jun N-terminal kinase (JNKs) and p38 MAP kinases are classified as stress-responsive MAP kinase family [Matsukawa, *et al.*, 2004]. The apoptosis signal-regulating kinase 1 (ASK1) belongs to MAPKKK family and activates both the JNK and p38 pathways by phosphorylating and activating MAPKK family molecule SEK1/MKK7 and MKK3/MKK6/ASK1. ASK1 is activated by interaction with the TNF receptor-associated factor 2 (TRAF2). Under ER stress conditions, activated Ire1 recruits TRAF2 and then ASK1 directly binds to

TRAF2 and is activated [Nishitoh, *et al.*, 2002]. The activation of ASK1 is also redox-dependent (Liu, *et al.*, 2000). In unstressed condition, thioredoxin (Trx) directly binds to ASK1 and inhibits kinase activity. Trx is a ubiquitously expressed reduction/oxidation (redox)- regulatory protein and oxidized Trx cannot bind to ASK1.

Caspase 12 belongs to the ICE (Caspase-1) subfamily of caspase cysteine protease family [Oyadomari, *et al.*, 2004]. ICE subfamily members function as activator of other caspases and cytokines by cleaving them. Caspase family molecules are produced as inactive pro-forms and are activated by cleavage when activating signals including apoptosis-inducing signals are transmitted. Pro-caspase-12 is localized on the cytosolic side of the ER membrane and is activated by ER stress [Nakagawa, *et al.*, 2000]. In ER stress condition, Ca^{2+} is released from ER to cytosol, then calpain, which is Ca^{2+} -dependent cysteine protease, is activated which activates caspase-12 by cleavage [Nakagawa, *et al.*, 2000]. The cytosolic caspase-7 is translocated from cytosol to ER in ER stress condition, and caspase-7 activates caspase-12 by cleavage [Rao, *et al.*, 2001]. The activated Ire1 in ER stress conditions recruits TRAF2, which interacts with pro-caspase-12 and promotes its clustering and activation [Yoneda, *et al.*, 2001]. Activated caspase-12

cleaves procaspase-9 and activated caspase-9 activates procaspase-3 by cleavage. Activated caspase-3 activates apoptosis promoting molecules such as DNase.

1.4.5 NO-Induced ER Stress

NO- mediated apoptosis has been observed in diseases such as septic shock, autoimmune diseases, cerebral infarction and diabetes mellitus [Ignarro, *et al.*, 2000. Kroncke, *et al.*, 1997. Dimmeler, *et al.*, 1997]. NO has several cytotoxic effects including reactions with proteins and nucleic acids and causes apoptosis. NO induces DNA damage leading to cell death through induction of p53 and activation of poly (ADP-ribose) polymerase (PARP) (Messmer, *et al.*, 2005). In unstressed condition, p53 is rapidly degraded, and the protein level of p53 within cells is low [Harris, *et al.*, 2001]. p53 is induced in response to DNA damage through suppression of rapid degradation, then the upregulated p53 either blocks cellular proliferation by cell cycle arrest at G1 stage or induces programmed cell death in the case of severe DNA damage. DNA damage also activates PARP, which results in depletion of NAD⁺ and ATP, subsequently, necrosis takes place.

NO- induced apoptosis can be mediated by ER stress pathways. Calreticulin is a Ca²⁺ binding ER chaperone and maintenance of Ca²⁺ homeostasis in the ER is essential for protein folding because some of ER chaperones are Ca²⁺ dependent proteins [Schroder, *et al.*, 2005]. NO is reported to inhibit Ca²⁺ -

ATPase activity of SERCA by tyrosine nitration [Xu, *et al.*, 1999], or increase the activity of RyR through S-nitrosylation [Xu, *et al.*, 1998]. Therefore, NO depletes ER Ca^{2+} either by inhibiting Ca^{2+} uptake from cytosol through SERCA or by activating Ca^{2+} release to cytosol through RyR.

Another proposed mechanism for NO and ER stress- mediated apoptosis involves the effects of NO on mitochondria cytochrome c oxidase (complex IV). In physiological concentrations, NO bind to mitochondrial enzyme complex IV and inhibit it in a manner that is reversible and in competition with oxygen [Xu, *et al.*, 2004]. Cytochrome c oxidase is the terminal enzyme of the mitochondrial respiratory chain. Therefore, increases in NO concentration can prevent the enzyme from using any available oxygen, prevent respiratory chain and can cause the production of ROS, changing the redox status of the cell [Xu, *et al.*, 1998]. Protein folding process in the ER is highly redox-dependent, and can disturb ER function and activate ER stress pathway. As NO changes Ca^{2+} concentration in the ER, ATF6 is activated by proteolytic cleavage by the S1P and S2P proteases and the active ATF6 translocates to the nucleus to upregulate the ER stress- responsive genes.

1.4.6 ER stress and oxidative stress in diseases

1.4.6.1 Diabetes

The type 2 diabetes is associated with a combination of insulin resistance in fat, muscle and liver and the failure of pancreatic β cells to increase insulin production [Saltiel, *et al.*, 2001]. Oxidative damage is associated with the development of insulin resistance and diabetic state. Insulin signalling is also very sensitive to alterations in ER homeostasis and redox status. ER stress and oxidative stress as well as inflammatory cytokines and free fatty acids activate Ire1, an ER stress sensor and which activates the JNK pathway. JNK then phosphorylates the Insulin Receptor Substrate-1 (IRS-1) on Ser307 which reduces insulin receptor-stimulated Tyr phosphorylation and insulin signalling.

1.4.4.2 Neurodegenerative diseases

Neurodegenerative diseases, such as Alzheimer disease (AD) and Parkinson disease (PD), represent a class associated with accumulation of abnormal protein aggregates in and around affected neurons. Oxidative stress and protein misfolding play critical roles in the pathogenesis of these diseases and are characterized by fibrillar aggregates composed of misfolded proteins. At the cellular level, neuronal death or apoptosis may be mediated by oxidative stress and ER stress or both.

1.4.6.3 **Hyperhomocysteinemia and atherosclerosis**

Elevated plasma levels of homocysteine (Hcy), sulphur-containing amino acids are linked to the development of ischemic heart disease, stroke and peripheral vascular disease. Hcy induces protein misfolding in the ER and triggers the UPR [Huang, *et al.*, 2006]. In causing ER stress Hcy brings cholesterol dysregulation and triglyceride biosynthesis and leads to the accumulation of cholesterol in the cell [Werstuck, *et al.*, 2001].

Atherosclerosis is caused by the abnormal deposition of cholesterol in the coronary arteries. Cholesterol accumulation in macrophages plays a critical role in the progression of atherosclerosis. Excess cholesterol must accumulate in specific pools within the cell to elicit cytotoxicity, by UPR signalling and caspase activation resulting in apoptosis [Feng, *et al.*, 2003].

1.5 Sphingomyelase

1.5.1 Sphingomyelin

The sphingomyelin molecule is composed of a polar phosphorylcholine head group, an amide linked acyl chain, and a long chain sphingoid base. The polar head group of sphingomyelin is similar to the phosphorylcholine head group of phosphatidylcholines. The amide-linked acyl chains of sphingomyelin are usually saturated or monounsaturated and contain 14–24 carbons (Figure 1.5).

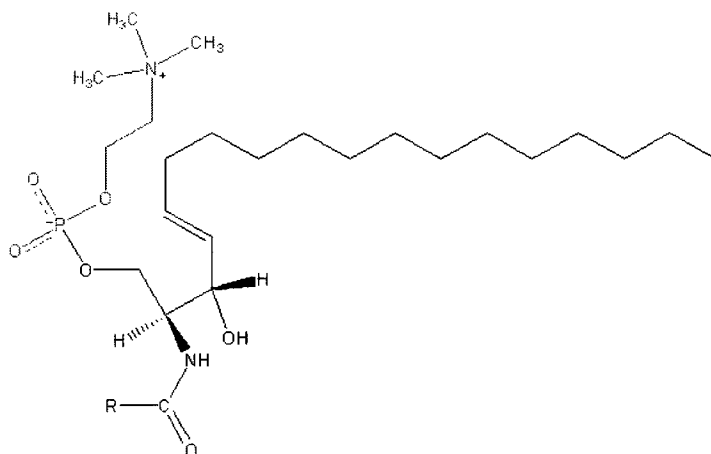


Figure 1.5 **Structure of sphingomyelin.** Black is sphingosine, red is phosphorylcholine and blue is fatty acid.

The subcellular distribution of sphingomyelin mass is confined to the plasma membrane (with most of it being in the exoleaflet). Sphingomyelin (SM) is synthesized by the reversible enzymatic transfer of phosphorylcholine group of phosphatidylcholine to ceramide, thus yielding Sphingomyelin and

Diacylglycerol. This reaction is catalyzed by Sphingomyelin synthase [Ullman, *et al.*, 1974]. This event occurs mainly in the *cis* and *trans* Golgi network [Fulterman, *et al.*, 1990]. The synthesized SM then reaches plasma membrane via vesicular flow. However, other subcellular sites have been described including endosomes and the nucleus [Kallen, *et al.*, 1994]. An alternative route for SM biosynthesis has been reported involving CDP-choline as the phosphocholine donor [Diringer, *et al.*, 1972]. Sphingomyelin synthase (SMS) which catalysis this reaction occurs in two isoforms in mammals SMS 1 and SMS 2 with SMS 1 predominant in Golgi and SMS 2 in Plasma Membrane [Fulterman, *et al.*, 1990 and Kallen, *et al.*, 1994]. The regulation of SMS depends on the levels of Ceramide and Diacylglycerol in the cell. Sphingomyelin is hydrolysed by sphingomyelinases (SMases) releasing ceramide and a cascade of bioactive lipids. These lipids include sphingosine and sphingosine-1-phosphate which have specific signalling capacity. Sphingomyelinases are present in various types of cells including cardiac myocytes, endothelial and vascular smooth muscle cells bringing about cell proliferation, cell death and contraction of cardiac and vascular myocytes. SMases have different isoforms according to their pH optima- alkaline, acid and neutral, localization and cation dependence. These isoforms are- Alkaline SMase, confined to the intestinal mucosa, bile and liver. Acid SMases (ASMases)

and neutral SMases (NSMases), however are crucially involved in cardiovascular physiology and pathophysiology.

1.5.2 Acid sphingomyelinase

Acid sphingomyelinase is further classified into two on the basis of their localization in the cell- Lysosomal sphingomyelinase (L-SMase) and secretory sphingomyelinase (A-SMase).

1.5.2.1 Lysosomal Acid sphingomyelinase

Lysosomal ASMase is 70 kDa glycoprotein with oligosaccharide side chains containing mannose-6-phosphate residues, typical of lysosomal proteins. It's in vitro pH optimum is between 4.5 and 5, and SM accumulation in the lysosomes of Niemann Pick Deficient (NPD) patients further supports its classification as a lysosomal protein [Fowler, *et al.*, 1969]. L-SMase requires Zn^{2+} for activity and is tightly bound to Zn^{2+} .

1.5.2.2 Secretory Acid sphingomyelinase

S-ASMase contains complex N-linked oligosaccharides. Its activity is highly dependent on the availability of Zn^{2+} and requires exogenous Zn^{2+} for its optimum activity [Tabas, *et al.*, 1999].

1.5.3 Lysosomal Acid sphingomyelinase and vascular tone

In human lymphocytes, TNF receptor superfamily receptors triggers L-ASMase translocation from lysosomes to the extracellular surface of the cell membrane. The translocated L-ASMase localizes to sphingolipid-rich membrane lipid rafts and releases extracellularly orientated ceramide. This allows the formation of larger ceramide-enriched platforms, which serve to cluster the receptors determining the initiation of apoptosis signalling [Gulbins, *et al.*, 2003]. The mechanism involves phosphorylation of L-ASMase by PKC δ [Zeidan, *et al.*, 2008]. L-ASMase dependent formation of ceramide-enriched lipid macrodomains in VSMCs and EC contributes to FasL-induced impairment of the vasodilator response [Jin, *et al.*, 2008. Zhang, *et al.*, 2007] and muscarinic-1 receptor-mediated coronary artery constriction [Jia, *et al.*, 2008] which are both major aggravating factors in atherosclerosis.

1.5.4 Secretory Acid sphingomyelinase in atherosclerosis

Both proliferation and death of VSMCs contribute to the progression of the atherosclerotic lesions. The sphingomyelin/ceramide pathway in atherogenesis, through a mitogenic effect on VSMCs. Endothelial cells, which cover the atherosclerotic lesions, secrete S-ASMase. Enzyme secretion is enhanced by atherogenic pro-inflammatory cytokines [Marathe, *et al.*, 1998].

Secreted ASMase hydrolyses SM to ceramide on the surface of atherogenic lipoprotein particles, even at neutral pH [Schissel, *et al.*, 1998]. The resulting increase in lipoprotein ceramide promotes fusion and subendothelial aggregation of the lipoprotein particles, increasing their affinity for arterial wall proteoglycans and leading to foam cell formation [Tabas, *et al.*, 2007]. Also, oxidized phospholipids that are found in atherosclerotic lesions may promote VSMC death via ASMase activation [Loidl, *et al.*, 2003].

1.5.5 Secretory Acid sphingomyelinase in heart failure

In addition to neuro-hormonal activation, inflammation and oxidative stress are key mediators in chronic heart failure (HF) progression [Keith, *et al.*, 1998. Castro, *et al.*, 2002. McMurray, *et al.*, 1993] and severity [Mallat, *et al.*, 1998]. The ability of pro-inflammatory cytokines to trigger S-ASMase secretion from ECs [Marathe, *et al.*, 1998] combined with the stimulatory effect of reactive oxygen species (ROS) on enzyme activity [Grammatikos, *et al.*, 2007] are possible mechanisms explaining the increase in plasma S-ASMase activity in patients with HF [Doehner, *et al.*, 2007].

1.5.6 Neutral Sphingomyelinase

Neutral Sphingomyelinase (NSMase) has 3 isoforms- two of them are Mg^{2+} dependent that are termed as NSMase1 and NSMase2 and the third form is Mg^{2+} independent (NSMase3).

1.5.6.1 Neutral, Mg^{2+} -dependent sphingomyelinase

Neutral Mg^{2+} -dependent sphingomyelinase (~92kDa) is integral membrane protein. The enzyme has pH optima near pH 7.0 and requires mM amounts of Mg^{2+} and Mn^{2+} for activity. Mg^{2+} -NSMase has several locations in the cell, NSMase1 is localized in the nucleus, ER and Golgi [Mizutani, *et al.*, 2001. Tomiuk, *et al.*, 2000] and NSMase2 in the inner leaflet of the plasma membrane [Tani, *et al.*, 2007].

1.5.6.2 Neutral, Mg^{2+} -independent sphingomyelinase

This enzyme is termed as NSMase3 and is present in the cytosol. It is a small protein of 53 KDa molecular weight.

1.5.7 Neutral sphingomyelinase signalling pathways and cardiovascular dysfunction

In isolated cardiac myocytes, NSMase mediates apoptosis elicited by TNF- α [Krown, *et al.*, 1996. Oral, *et al.*, 1997] or IL-1 β [Radin, *et al.*, 2008].

Glutathione inactivates NSMase and lower levels of glutathione are required for

the binding of NSMase to TNF α receptor [Defer, *et al.*, 2007]. In cultured VSMC, apolipoprotein C-1 (apoC-1)-enriched high-density lipoproteins (HDLs) stimulate NSMase, triggering an apoptotic response via the release of cytochrome c from mitochondria and caspase-3 activation [Kolmakova, *et al.*, 2004]. Apoptosis of VSMCs is a critical event in the rupture of atherosclerotic plaque, leading to thrombosis, myocardial infarction and possible death. Oxidized low density lipoproteins (oxLDLs) and TNF- α also stimulate NSMase in VSMCs. However, these stimuli do not trigger apoptosis, but instead contribute to VSMC proliferation resulting from the metabolism of ceramide into Sphingosine-1-phosphate (S1P) and the downstream activation of ERK1/2 MAPKinases [Auge, *et al.* 2002]. In cultured VSMCs, the NSMase2 isoform is involved in the ROS and oxLDL induced proliferation and the process of NSMase2 activation that relies on a proteolytic cascade involving furin/membrane type 1-matrix metalloprotease (MT1-MPP)/MMP-2 proteases [Coatrieux, *et al.*, 1997]. Through NSMase activation, oxLDLs induce cultured VSMC proliferation which *in situ* contributes to the formation and progression of atherosclerotic lesions. OxLDLs are present in both animal and human atherosclerotic lesions and trigger the progression of atherosclerosis and plaque rupture.

Objectives of the study:

Objective 1. How increased plasma membrane cholesterol content can affect nitric oxide diffusion, dynamics and signalling?

To achieve this objective we carried out the study by having the knowledge about the basic property of nitric oxide that it tends to partition in the hydrophobic milieu in the biological membrane. This property of nitric oxide led us to think that if nitric oxide favors hydrophobicity then what would be the consequences on nitric oxide diffusion from plasma membrane and its subsequent intracellular signalling brought by cGMP activation and VASP (Ser²³⁹) phosphorylation, if this hydrophobicity was further increased in the form of more cholesterol content in the plasma membrane. From this study, we drew the conclusion that nitric oxide diffusion from plasma membrane, cGMP response and VASP (Ser²³⁹) phosphorylation was significantly reduced under conditions where there was more cholesterol in the plasma membrane. This important finding can serve as a platform for the studies which involve cancer, neurodegeneration and cardiovascular disorders where the bioavailability of nitric oxide is severely decreased leading to adverse consequences.

Objective 2. (i) Can endoplasmic reticulum stress (ER stress) lead to increase in plasma membrane cholesterol content?

(ii) How ER stress causes increase in plasma membrane cholesterol content?

(iii) Whether increase in plasma membrane cholesterol can influence nitric oxide production/diffusion and eNOS localization in the endothelial cells?

The study was performed by bearing the rationale that if ER stress upregulates genes for cholesterol synthesis leading to increase in the accumulation of intracellular cholesterol then can ER stress also give rise to plasma membrane cholesterol, as plasma membrane not only holds ~90% cellular cholesterol but also is the site from where influx and efflux of cholesterol takes place. The result of this study showed that there was a huge increase in cholesterol content in the plasma membrane under ER stress condition. To investigate as to how this dysregulation in plasma membrane cholesterol is brought through, we found that neutral sphingomyelinase2, a plasma membrane resident enzyme responsible for maintaining cholesterol balance in plasma membrane is inactivated by S-nitrosation of Cys thiols and nitration of Tyr residues under ER stress. Part (iii) of Objective 2 was carried out as a follow up of Objective 1 and here we wanted to determine nitric oxide release under increased plasma membrane cholesterol brought by ER stress. We found that there was a gradual decline in nitric oxide release as the ER stress was prolonged. Then we wanted to investigate the issue of eNOS localization in the Golgi, where eNOS is known to produce less nitric oxide and the studies performed till the time showed that under ER stress condition,

intracellular vesicular transport is obstructed with proteins getting trapped in the ER and Golgi. With the available knowledge we hypothesized that could the gradual decline in nitric oxide production as a result of ER stress be due to eNOS getting trapped in the Golgi. And consistent to our expectation we determined that there was some eNOS getting localized in the Golgi under ER stress.

The study can give important insights in the development of endothelial dysfunction, where hypercholesterolemia and decrease in bioavailability of nitric oxide lead to cardiovascular and neurological disorders.

Part II

Chapter 2

Cloning and characterization of Perfringolysin O- Domain 4 (PFO-D4) with cholesterol on Bilayer Lipid Membrane (BLM)

2.1 Introduction

Thiol-activated cytolysins comprise a large family of bacterial protein toxins that are secreted by Gram-positive bacteria [Alouf, *et al.*, 1991.]. They share 40-70% homology in their amino acid sequences and have common functions, cholesterol binding and pore-formation through oligomerization on plasma membrane [Tweten *et al.*, 1988. Shimuzu, *et al.*, 1991. Kehoe, *et al.*, 1987]. Perfringolysin O is a 472 amino acid residues cytolysin produced by *Clostridium perfringens* type A bacteria. Its cytolytic activity is mainly brought about by 4 steps which occur in sequential order: 1. Binding to plasma membrane cholesterol 2. Insertion into the membrane 3. Oligomerization 4. Pore formation [Shatursky, *et al.*, 1999]. The three dimensional structure of theta-toxin elucidated by X-ray diffraction studies revealed that it is a β -sheet rich, elongated rod-shaped molecule and consists of four discontinuous domains [Sugahara, *et al.*, 1996]. Domain 4 or the C-terminal domain, is an autonomous structure comprising of amino acid residues 363-472. The Domain 4 has a highly conserved undecapeptide sequence ECTGLAWWW (amino acid residues 430-440) having a single cysteine and PFO has only one cysteine in the whole protein. This single cysteine is essential for the oligomerization of monomers of theta-toxin to form a prepore assembly onto the plasma membrane followed by pore formation

[Hotze, *et al.*, 2001]. Recently, there was a report suggesting that the three short hydrophobic loops (L1-L3) at the tip of Domain 4 of the PFO are responsible to anchor the molecule onto the cholesterol-rich membrane [Soltani, *et al.*, 2007].

There are several different kinds of probes available for visualizing cellular cholesterol such as filipin, NBD-cholesterol, dehydroergosterol (DHE) etc. But all of these probes suffer from limitations that they can indiscriminately target cholesteryl esters, can quickly photobleach, can permeabilize the cell and cannot differentiate between the intracellular cholesterol pool and plasma membrane cholesterol where ~90% of the cellular cholesterol resides [Lange, *et al.*, 2000]. The purpose of the present study was to generate a cholesterol probe which can target exclusively plasma membrane cholesterol and for this we exploited the cholesterol binding property of the Domain 4 of PFO. Although there has been several studies done to characterize the binding capacity of PFO/PFO-D4 with cholesterol by using large unilamellar liposomes, intact cells or isolated cholesterol-rich microdomains [Alouf, *et al.*, 1984. Ohno-Iwashita, *et al.*, 1988. Ohno-Iwashita, *et al.*, 1990], but all these studies have limitations in that these studies could not be utilized to estimate cholesterol levels in the membrane. In the present study, we have used a bilayer lipid membrane chamber and fluorescence microscopy to make a bilayer membrane over a 1 mm hole using a

canonical lipid raft mixture [Fidorra, *et al.*, 2006. Nicolini, *et al.*, 2006. Veatch, *et al.*, 2003]. By performing titration with increasing [PFO-D4-GFP] on bilayer lipid membrane made with varying mol% of cholesterol we obtained a saturation curve. The dissociation constant (K_D) of PFO-D4 was obtained from the saturation curve at the point of saturation and the K_D values clearly showed the PFO-D4 specifically binds to cholesterol and show a stronger binding with higher mol% of cholesterol in the membrane.

2.2 Materials and equipment

2.2.1 Materials

Tris-HCl, NaCl, Imidazole, Lysozyme, DNaseI, Phenylmethanesulphonylfluoride (PMSF), Ampicillin, Isopropyl β -D-1-thiogalactopyranoside (IPTG) and 1-palmitoyl 2- oleyl phosphatidylcholine (POPC) was purchased from Sigma-Aldrich Canada (Oakville, ON). Sphingomyelin (chicken egg derived) and cholesterol (plant derived) was purchased from Avanti Polar lipids Inc. (Alabaster, AL, USA). Methonal and chloroform was purchased from Merck KGaA (Darmstadt, Germany). Restriction enzymes and Phusion™ High-Fidelity DNA Polymerase were purchased from New England Biolabs (Pickering, ON, Canada). Plasmid GFPuv was purchased from Clontech (Mountain View, CA, USA). pTrcHisB vector was purchased from Invitrogen (Carlsbad, CA, USA). XL-1 Blue supercompetent cells were purchased from Stratagene (Cedar Creek, TX, USA).

2.2.2 Equipment

Northern Eclipse 6.0 Imaging Software; Empix Imaging Inc., Mississauga, ON.

Zeiss Axiovert 200 Inverted Fluorescence Microscope, Empix Imaging Inc., Mississauga, ON.

Agilent 8453 UV-VIS Spectrophotometer, Agilent Technologies, Canada, Inc,
Mississauga, ON

Mettler AJ1000 Balance; Mettler, Toledo Canada, Mississauga, ON

Orion Model 420A pH Meter, Thermo Electron Corp. Canada, Burlington, ON

2.3 Methods

2.3.1 Cloning of truncated PFO:

To make truncated PFO, we used the plasmid pRT10 (a generous gift from Dr. Rodney Tweten) containing the perfringolysin O gene (pfoA) in the pTrc HisC vector. The pRT10 plasmid was restriction digested between BamHI and BglII restriction sites and the DNA fragment from Phe₂₅₂-Asn₅₀₀ with the cohesive ends was treated with mung bean nuclease at 37 °C for 20 min to generate blunt ends. The blunt ended DNA fragment was then self ligated and the vector was transformed into XL-1 blue supercompetent cells for amplification and sequenced.

2.3.2 Cloning of PFO-D4 in pTrcHisB vector:

The pRT10 plasmid containing the perfringolysin O gene (pfoA) was used to construct the pfoA derivative D4 encoding the C-terminal region of the toxin. The DNA fragment containing the D4 (Lys₃₉₁-Asn₅₀₀) encoding region was PCR amplified using pRT10 plasmid as the template and ligated into the pTrcHisB expression vector, inserting it between the BamHI and KpnI restriction sites on the 3'-end of the sequence encoding the His tag site. The polymerase chain reaction primers used were as follows: Forward primer, 5'-CCCGGATCCGTCTACAGAGTATTCTAAGG-3'; reverse primer, 5'-

CCCGGTACCGGATTGTAAGTAATACTAGATCC-3'. The cloned vector was transformed into XL-1 blue supercompetent cells for amplification and sequenced.

2.3.3 Cloning of PFO-D4-pTrcHisB plasmid with GFP:

The PFO-D4-pTrcHisB plasmid was used to insert the GFP gene. The GFP insert was isolated from the pGFP vector by restriction digesting the vector between KpnI and EcoRI sites and ligated between these sites in the PFO-D4-pTrcHisB vector, thus inserting it at the 3'-end of the PFO-D4-pTrcHisB vector. The cloned vector was transformed into the XL-1 blue supercompetent cells and sequenced.

2.3.4 Transformation and protein expression of PFO-D4-GFP in XL-1 Blue supercompetent cells:

A 50µl aliquot of XL-1 blue supercompetent cells was added to prechilled polypropylene round bottom tubes. Approximately, 2µl of PFO-D4-GFP plasmid was added to the cells and the tubes and swirled gently. The mixture was incubated on ice for 30 min. Following incubation the cells were heat shocked in 42 °C water bath for 45 s and incubated on ice for 2 min. Approximately, 200µl of the preheated SOC medium was added to the cells and the cells were incubated at 37 °C for 1 h under shaking at 225 rpm. The mixture was then plated on LB agar

plates containing 50µg/ml ampicillin and incubated at 37 °C for 16-18 h. A single colony from the plate was streaked into 50ml of Terrific Broth (TB) containing 50µg/ml ampicillin and grown overnight at 37 °C under 250 rpm. The overnight grown culture was transferred into 1L TB+Amp (50µg/ml) and incubated for 6 h at 37 °C under 250 rpm with an optical density of 0.6. To induce PFO-D4-GFP protein expression 1mM IPTG in 50% glycerol was added to the cells and again incubated for 6 h at 37 °C under 250 rpm.

2.3.5 Purification and quantification of PFO-D4-GFP protein:

The induced culture was centrifuged at 5000Xg for 30 min and the pellet was resuspended in 20 ml of the lysis buffer (100 mM Tris-HCl, 250 mM NaCl with 30 mM Imidazole pH 8.0, 100µg/ml lysozyme, 50µg/ml DNaseI, 2mM PMSF and 1% Triton X-100). The suspension was incubated on ice for 30 min, sonicated at level 4 for 8 pulses (20 s each pulse) and then centrifuged at 17000Xg for 30 min at 4 °C. The clear supernatant was added to the nickel column, which was equilibrated with 10 mM Imidazole buffer (100 mM Tris-HCl, 250 mM NaCl pH 8.0). After loading the sample, the column was again equilibrated with 3 column volumes of 10 mM Imidazole buffer. The protein was eluted with 2 column volumes of 300 mM Imidazole buffer (100mM Tris-HCl, 250 rpm NaCl

pH 8.0). Imidazole was removed and the buffer was exchanged with Hepes buffer pH 7.4 in the eluted protein using Amicon centrifugal filters. The protein was aliquoted into 50 μ l and stored at -80 ⁰ C for future use. The quantification of the purified protein was done by measuring optical density at 280 nm with PFO-D4-GFP having an extinction coefficient of 59740 M⁻¹cm⁻¹.

2.3.6 Bilayer Lipid Membrane (BLM) setup:

To access the cholesterol specificity of PFO-D4-GFP we made a bilayer membrane (BLM) setup that had a teflon film with a 1mm diameter hole on which the artificial lipid membrane was made. The teflon film rested on a trough filled with Hepes buffer pH 7.0 (aqueous phase) maintained at 37 ⁰ C, the lipids used to make the bilayer were dissolved in organic solution and that constituted the organic phase and with and after overlay of PFO-D4-GFP in Hepes buffer pH 7.0 there was an organic phase in the middle with aqueous milieu on top and bottom making a lipid bilayer.

2.3.7 Cholesterol specificity of PFO-D4-GFP on BLM:

The lipids in the organic phase consisting of POPC, 10 mol% sphingomyelin and varying mol% of cholesterol (5 mol%, 10 mol%, 20 mol%, 30 mol% and 40 mol%) keeping the number of moles of POPC constant was

dissolved in 2:1 chloroform:methanol was used to make the membrane. A small aliquot of 2 μ l of the lipid mixture was added on top of 1mm hole in the Teflon film, held at 37 $^{\circ}$ C. After the organic solvents were evaporated, 1 μ l of PFO-D4-GFP with different concentrations was laid over the dried lipid membrane and incubated for 15 min, followed by washing with Hepes buffer pH 7.0. Thereafter, the bilayer lipid membrane was imaged in the fluorescent microscope to see the binding of PFO-D4-GFP on cholesterol in the membrane interpreted as means of average fluorescence of PFO-D4-GFP with excitation/emission at 390 nm/510 nm.

2.3.8 Cholesterol specificity of PFO-D4-GFP with Methyl β -cyclodextrin treatment on the BLM:

A lipid raft mixture with POPC:sphingomyelin and 20 mol% of cholesterol was made as described above. Thereafter, the membrane was treated with different concentrations of methyl- β -cyclodextrin dissolved in Hepes buffer pH 7.0 (0mM, 2.5mM, 5mM and 10mM) and then probed for cholesterol with 720nM PFO-D4-GFP. The bilayer lipid membrane was imaged in the fluorescent microscope to see the binding of PFO-D4-GFP with cholesterol in the membrane, interpreted as means of average fluorescence of PFO-D4-GFP.

2.4 Results

Lipid raft mixture consisting of POPC:sphingomyelin:cholesterol with following mol%- 85:9:5 mol%, 84:8:10 mol%, 30:3:20 mol%, 22.8:2.3:30 mol%, 18:2:40 mol% was used to make the horizontal bilayer membrane (BLM) designed for an inverted microscope. The number of moles of POPC was kept constant and the mol% for each lipid was calculated by taking the total number of moles of the lipids. As mentioned above, that PFO contains one cysteine residue at amino acid position 431 residing in D4 of the PFO and this cysteine is essential for the oligomerization of monomers to form prepore complex on the plasma membrane, the PFO plasmid which was a generous gift to us from Dr. Rodney Tweten was mutated by replacing Cys₄₃₁ with Ala at this position keeping the total number of amino acids in the protein same as 472 residues. In order to test the cholesterol specificity of PFO-D4-GFP, the above mentioned BLM mixtures were exposed to increasing concentration of PFO-D4-GFP construct. As can be seen from Fig. 2.1.1 (a-e) that there was an increase in the fluorescence when increasing concentration of PFO-D4-GFP was added to the BLM mixtures of each ratios and at a certain concentration of PFO-D4-GFP there was no further increase in the fluorescence Fig 2.1.1 (a-e) and a plateau was reached with further addition of higher PFO-D4-GFP concentration thus generating a saturation curve Fig.

2.1.2. This showed the fluorescence increase, as a function of concentration of PFO-D4-GFP, displayed saturation behaviour. The specificity of PFO-D4-GFP for cholesterol, on the lipid raft mixtures with varying mol% of cholesterol (5 mol%, 10 mol%, 20 mol%, 30 mol% and 40 mol%) was made and used to determine its apparent dissociation constant K_D and any change in K_D values with increasing mol% of cholesterol in the BLM. As the fluorescence increase and PFO-D4-GFP concentration showed saturation behaviour, the apparent K_D of the various sphingomyelin to cholesterol mixtures for PFO-D4-GFP estimated from the fit of the data to a saturation function, indicated that as the mol% of cholesterol increased the apparent K_D decreased. And as can be seen from Fig.2.1.1 (a-e) and Fig 2.1.2 as the mol% of cholesterol was increased the plateau with the fluorescence was reached at a lower concentration of PFO-D4-GFP and thus displays a decrease in the K_D values (5 mol% K_D = 2.3 μ M, 10 mol% K_D = 1.02 μ M, 20 mol% K_D = 0.52 μ M, 30 mol% K_D = 0.43 μ M, 40 mol% K_D = 0.16 μ M) Fig. 2.1.2 inset. The cholesterol specificity of PFO-D4-GFP was further verified in another way where methyl- β - cyclodextrin was used to extract cholesterol from the raft mixture on the model membrane. Methyl- β -cyclodextrin at concentrations (0mM, 2.5mM, 5mM and 10mM) was incubated with the model membrane prior to the addition of PFO-D4-GFP and the fluorescence was measured. Fig 2.2 (a) shows a

decrease in the fluorescence as the concentration of methyl- β -cyclodextrin was increased thus showing that with less cholesterol PFO-D4-GFP displays a less binding characteristic in the model membrane.

2.5 Discussion

Lipid rafts are microdomains on the plasma membrane which are formed of sphingolipid (mainly sphingomyelin) and cholesterol and phospholipids and scattered on the plasma membrane. We used raft mixtures with varying mol% of cholesterol to determine the binding specificity of PFO-D4-GFP to cholesterol and our data clearly indicate that PFO-D4-GFP binds specifically to cholesterol and prefers higher cholesterol concentrations for tighter binding.

Our study with the raft mixture showed that PFO-D4 requires more cholesterol to strongly bind to the membrane. As can be seen from Fig.2.1.1(a-e) and Fig. 2.1.2 there is a decrease in the K_D values with increase in the mol% of cholesterol. Most of the studies performed on PFO till date on its dynamics of cholesterol binding are with erythrocytes and erythrocytes have huge amount of cholesterol in plasma membrane. The present and the previous studies converge at the same point that PFO binding is specific to cholesterol on the plasma membrane and the present study shows the cholesterol specificity of PFO in terms of its dissociation constant, K_D . The relationship between apparent K_D was non-linear and could be fit by the equation **apparent K_D = 11.14/ [Cholesterol mol%]** Fig 2.2 (f) inset. Rafts contain a 1:1 mixture of sphingomyelin to cholesterol. The fact that the apparent K_D decreased or the interaction between PFO and cholesterol

increased at the point when the cholesterol to sphingomyelin ratio increased above one i.e. (~10 mol %) supports the recent findings that PFO-D4 interacts with free cholesterol in the plasma membrane [Flanagan, *et al.* 2009]. Furthermore, these results suggested that we could use the equation obtained from the model membrane studies to estimate free cholesterol concentrations in the cell membranes by simply performing a PFO-D4-GFP titration.

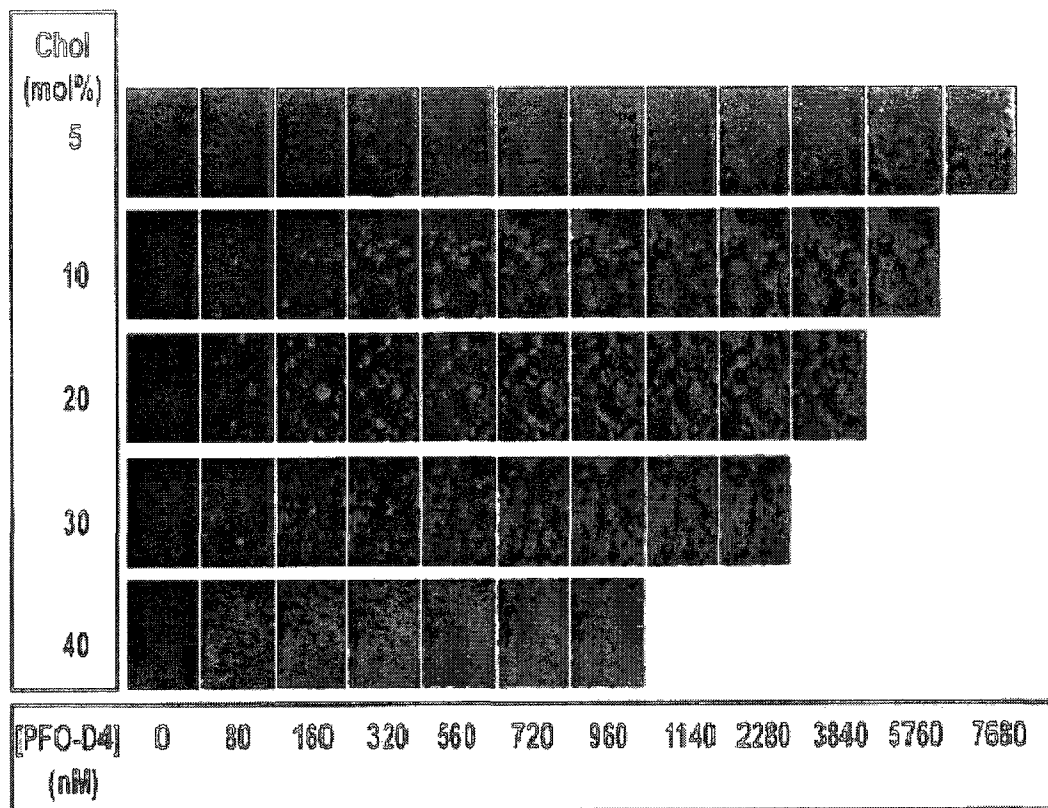


Figure 2.1.1 Pictures displaying the titration of cholesterol in bilayer lipid membrane (BLM) with PFO-D4-GFP. BLM made of POPC: sphingomyelin: cholesterol with varying mol% of cholesterol (5mol%, 10mol%, 20mol%, 30mol%, 40mol%) where the mol% of POPC and sphingomyelin were kept constant and the mol% for each lipid were calculated by taking the total number of moles of the lipids.

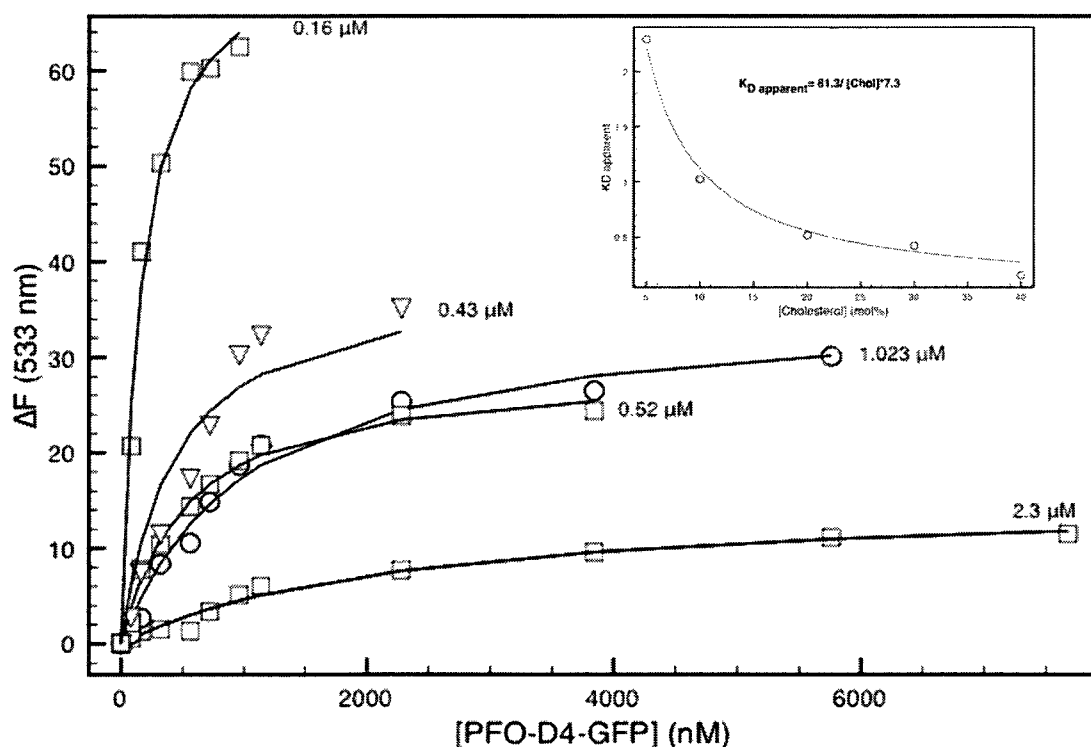


Figure 2.1.2 Titration of cholesterol in bilayer lipid membrane (BLM) with PFO-D4-GFP. Bilayer lipid membrane chamber designed was used to make horizontal bilayer membrane with the following POPC:Spingomyelin:cholesterol mol% ratios- 85:9:5 mol% □, 84:8:10 mol% ⊗, 30:3:20 mol% ◻, 22.8:2.3:30 mol% ▼, 18:2:40 mol% ■. The number of moles of POPC and Spingomyelin was kept constant and the mol% was calculated by taking the total number of moles of the lipids. Various [PDO-D4-GFP] were incubated with the bilayer membrane at 37° C in Hepes buffer pH7.4 and the apparent dissociation constant, K_D was determined at the saturation limit of [PFO-D4-GFP]. The inset shows the apparent K_D of PFO-D4-GFP as a function of [cholesterol] (mol%) in the bilayer membrane. The error bars show S.D. (n=5).

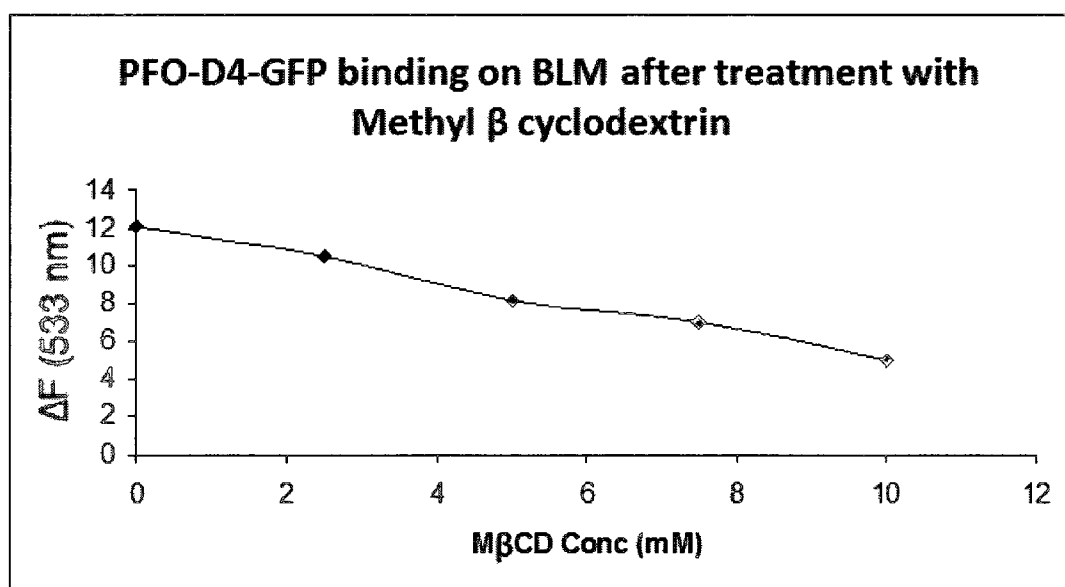
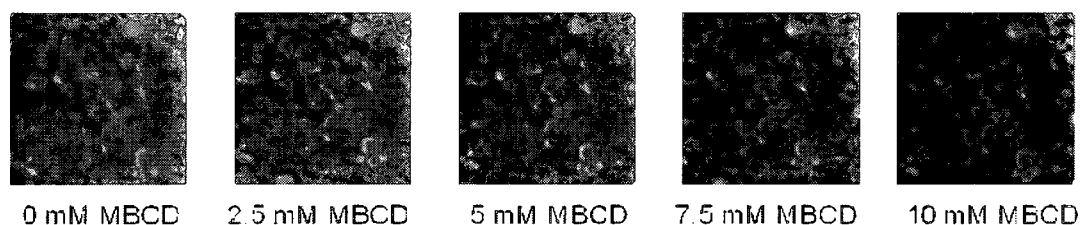


Figure 2.2 Cholesterol specificity of PFO-D4-GFP on BLM cholesterol after extraction from methyl- β -cyclodextrin. The cholesterol extraction from the raft mixture with POPC: sphingomyelin: cholesterol with the ratio 30:3:20 mol%, by methyl- β -cyclodextrin extraction and incubated with 720nM of PFO-D4-GFP. The plot depicts the decrease in average fluorescence of PFO-D4-GFP.

Part III

Chapter 3

Plasma membrane cholesterol content affects nitric oxide diffusion, dynamics and signalling

Published as original in The Journal of Biological Chemistry, (2008) 283, 18513-21.

3.1 Introduction

Nitric oxide (NO) is a small, gaseous free radical and is produced by nitric oxide synthase. Several regulatory factors at the level of nitric oxide synthase catalysis influence the rate of NO generation. The lifetime of NO molecules is governed by their relative abundance in relation to other radicals [Issner, *et al.*, 1997. Lima, *et al.* 2003], transition metal centers [Chiang, *et al.*, 2006. Mason, *et al.*, 2006] and oxygen (O₂) [Caccia, *et al.*, 1999. Lewis, *et al.*, 1994]. Also, NO being a very small molecule, its diffusional path of NO from the point of origin is affected by its hydrophobic solubility [Wood, *et al.*, 1994. Philippides, *et al.*, 2000], resulting in an enrichment of NO in biological membranes in relation to the aqueous milieu. In the present work, the hypothesis that the cells may utilize plasma membrane cholesterol to further orchestrate spatial heterogeneity in NO biological signalling activity was tested.

Cholesterol, a major lipid component of the plasma membrane in eukaryotic cells, plays an essential role in maintaining membrane fluidity and architecture [Hao, *et al.*, 2001. Rukmini, *et al.*, 2001]. Cells tightly control the ratio of cholesterol and phospholipids in plasma membrane, segregate with sphingolipids and proteins to form distinct lipid raft complexes that are ordered

platforms for communicating signals into and out of the cells [Simons, *et al.*, 1997]. Dysregulation of cholesterol synthesis and transport acts as a contributing factor to pathophysiological changes [Mason, *et al.*, 2003. Chen, *et al.*, 1995], which are of particular importance in cardiovascular disease, chronic inflammation and lipid disorders such as Niemann-pick disease. The influence of cholesterol on NO diffusion and signalling dynamics was seen by soluble guanylyl cyclase (cGCs) activation and VASP phosphorylation (Ser²³⁹). These data show that one effect of plasma membrane cholesterol content on modulation of the level and type of NO signalling; pathological alterations in levels and distribution of cellular cholesterol may contribute a mechanism of errant NO signalling.

3.2 Materials and Equipment

3.2.1 Materials

Tris-HCl, EDTA, PMSF, L-NMMA, DMEM were purchased from Sigma Canada (Oakville, ON). DEA/NO was purchased from Calbiochem (Los Angeles, CA, USA) Amplex Red cholesterol assay kit was obtained from Invitrogen (Carlsbad, CA, USA). The cGMP enzyme immunoassay kit was purchased from Amersham Biosciences (Piscataway, NJ, USA). Normal human fibroblasts (HFF-1) were obtained from ATCC (Manassas, VA, USA). NPC1 fibroblasts (GM17923) were obtained from the Coriell Cell Repository (Camden, NJ, USA).

3.2.2 Equipment

Agilent 8453 UV-VIS Spectrophotometer, Agilent Technologies, Canada, Inc, Mississauga, ON

Mettler AJ1000 Balance; Mettler, Toledo Canada, Mississauga, ON

NUAIRE Biological Safety Cabinet Class II Type A/B3; Thermo Electron Corp. Canada, Burlington, ON

Orion Model 420A pH Meter, Thermo Electron Corp. Canada, Burlington, ON

Varian Eclipse Fluorescence Spectrophotometer, Varian Canada, Mississauga,
ON

3.3 Methods

3.3.1 Cell Culture:

Normal Human Fibroblasts (HFF-1) and NPC 1 fibroblasts were maintained in Dulbecco's minimal essential medium (DMEM) supplemented with 10% fetal calf serum (FCS) and cultivated at 37 °C under an atmosphere of 5% CO₂.

3.3.2 Cloning of PFO-D4 in pTrcHisB vector and purification:

Cloning of PFO-D4 in pTrcHisB vector was performed as mentioned in section 2.3.2 and purification of PFO-D4 protein by Ni²⁺ affinity chromatography was performed as described in section 2.3.5. The labelling of the purified protein with Alexa 532 and subsequently staining on HFF-1 and NPC1 fibroblasts and imaging of cellular plasma membrane cholesterol was done by Dr. Shane Miersch.

3.3.3 Preparation of cholesterol-loaded cyclodextrin:

Excess of cholesterol (50mM) was dissolved in 1:1 (v/v) MeOH : chloroform and dried under a stream of argon in a glass tube. 5mM M β CD was dissolved in serum free DMEM and added to the dried cholesterol film and was kept under nutation for overnight at room temperature. The M β CD-cholesterol complex was filtered by 0.45 μ m sterile filter and cholesterol was quantified.

3.3.4 Cholesterol analysis:

The quantification of cholesterol loaded in cyclodextrin was done using a cholesterol oxidase enzymatic assay and interpolation from a standard curve. In brief, solubilised cholesterol is oxidized by cholesterol oxidase to the cholest-4-en-3-one, producing hydrogen peroxide as a reaction by-product. Cholesterol oxidase mediated production of H_2O_2 is coupled to the oxidation of 10-acetyl-3,7-dihydroxy phenoxazine to the highly fluorescent resorufin product by horseradish peroxidase. Cholesterol determination was performed according to the manufacturer's instructions to monitor resorufin formation in 96-well plate at 37 °C with an excitation/emission couple of 545/595 nm on a Perkin Elmer Life Sciences Victor 3 fluorescent plate reader.

3.3.5 Modulation of cellular plasma membrane cholesterol:

Cellular cholesterol was augmented by treatment with cholesterol loaded methyl- β -cyclodextrin (M β CD) adduct. In brief, 1×10^6 cells in complete DMEM medium were incubated with 100 μ M adduct for 1 h at 37 °C and 5% CO_2 . Alternately, cellular cholesterol was depleted using an apo-MBCD. Thus, 1×10^6 cells were incubated with 5 mM MBCD for 1 h at 37 °C and 5% CO_2 . Following cellular

treatment, cholesterol-modulating agents were removed and the cells were used for experimentation.

3.3.6 cGMP production and VASP phosphorylation as measures for intracellular NO signalling:

Cells were cultivated at ~85% confluence and treated with 500µM L-NMMA for 2 h to inhibit endogenous NO production. The cells were incubated a further 2 min with SOD mimetic Mn(III)TMPyP (5µM) and exposed to the NO donor DEA/NO (1 µM and 3 µM) and left undisturbed for 10 min in the incubator. Cells were trypsinized, collected, washed once with PBS containing 500µM DTPA and counted. After being adjusted for cell density (~ 5×10^5 cells/ml), the cells were centrifuged and lysed with buffer containing phosphodiesterase and protease inhibitors. The lysates were then analyzed for either cGMP with an enzyme immunoassay kit or VASP and phospho-VASP by Western immunoblotting with VASP and phospho-VASP (Ser²³⁹) antibodies.

3.4 Results:

3.4.1 Cellular Plasma Membrane Cholesterol Content Shifts the Threshold for NO activation of cytoplasmic Soluble Guanylyl Cyclase and the downstream cGMP-dependent Phosphorylation of VASP

NPC1 fibroblasts have been shown to exhibit a marked increase in plasma membrane cholesterol content [Vainio, *et al.*, 2005] and decreased membrane fluidity relative to normal human fibroblasts [Vainio, *et al.*, 2005, Koike, *et al.*, 1998]. Therefore, NHF and NPC1 fibroblast model system was used to test the hypothesis that cholesterol levels in cellular plasma membranes affect NO signaling of intracellular targets. Activation of cytoplasmic sGC was utilized as a sensitive biosensor for changes in the level of extracellular NO diffusion through the plasma membrane. The contribution from endogenous NOS activity was negated by the presence of the NOS inhibitor N^G -monomethyl-L-arginine (500 μ M). The levels of cGMP that accumulated in response to exogenous 1 and 3 μ M DEA/NO exposures were 64% lower (*, $p < 0.001$; two-tailed t test) and 52% lower (*, $p < 0.001$; two-tailed t test), respectively, in NPC1 fibroblasts in comparison with that observed in an equivalent number of NHF (Fig. 3.2). When NHF were treated with M β CD-cholesterol to augment plasma membrane

cholesterol to NPC1-equivalent levels, production of cGMP elicited by subsequent DEA/NO exposure was similar to NPC1 fibroblast responses (Fig. 3.2, *white to gray bars*). M β CD-cholesterol treatment decreased NHF cGMP levels 72% (**, $p < 0.001$; two-tailed t test) and 81% (**, $p < 0.001$; two-tailed t test) following either 1 or 3 μ M DEA/NO exposure, respectively. In the reverse experiment, decreasing the plasma membrane in NPC1 by M β CD treatment increased cGMP production by 2.9-fold (***, $p < 0.001$; two-tailed t test) and 2.3-fold (***, $p < 0.001$; two-tailed t test) in response to 1 and 3 μ M DEA/NO, respectively. In contrast, when the plasma membrane was ruptured by cellular lysis immediately prior to DEA/NO exposure, NPC1 produced 91% (1 μ M DEA/NO) and 93% (3 μ M DEA/NO) of the cGMP produced by NHF (Fig 3.3). These data support the hypothesis that plasma membrane cholesterol levels can modulate the degree of cytoplasmic sGC activation by NO.

These data were extended to test whether variations in plasma membrane cholesterol affected downstream cGMP-mediated signaling. VASP is an actin-binding regulatory protein that is a substrate for both cGMP-protein kinase (at Ser²³⁹) and cAMP-protein kinase (at Ser¹⁵⁷) [Linder, *et al.*, 2005. Garcia, *et al.*, 2002]. Consistent with cGMP data (Fig. 3.2), VASP Ser²³⁹-phosphorylation in NPC1 cells exposed to DEA/NO (1 μ M) was 40% less (*, $p = 0.033$, two-tailed t

test) than levels observed in an equal number of identically treated NHF cells. Depletion of plasma membrane cholesterol from NPC1 cells with M β CD resulted in a proportionate increase in VASP Ser²³⁹-phosphorylation (38%; **, $p = 0.087$, two-tailed t test) following NO exposure. Conversely, augmentation of plasma membrane cholesterol in NHF with M β CD-cholesterol resulted in the attenuation VASP phosphorylation by 50% ($p = 0.0034$, two-tailed t test) (Fig. 3.3, A and B). These results clearly demonstrate that plasma membrane cholesterol content can influence NO engagement with intracellular targets, such as sGC, thereby modulating downstream signaling through cGMP-protein kinase and VASP phosphorylation.

3.5 Discussion:

The aim of this study was to investigate whether plasma membrane cholesterol levels can modulate NO diffusion and cellular signalling. Niemann-Pick C1 disease is an autosomal-recessive neurovisceral disorder characterized by defective endosomal cholesterol trafficking due to NPC1 gene mutation [Zhang, *et al.*, 2001]. Analysis of NPC1 fibroblasts revealed increased levels of plasma membrane cholesterol (2 fold) and cholesterol-enriched lipid rafts (3.7 fold) relative to NHF (Fig. 3.1). In support of the hypothesis, cGMP levels elicited in NPC1 fibroblasts exposed to NO donor were ~50% lower than that observed in their NHF counterparts (Fig. 3.2). Importantly, synthetic enrichment of NHF plasma membrane cholesterol (4-fold) by incubation with MBCD-cholesterol adducts resulted in a similar (~80%) decrease in cGMP elicited by NO compared with NHF with basal cholesterol (Fig. 3.2). Conversely, the depletion of plasma membrane cholesterol from NPC1 fibroblasts resulted in and ~ 2-3fold increases in the amount of cGMP produced. Responses to NO by both NPC1 cells and NHF were within 93% of each other when plasma membrane was ruptured prior to NO exposure. These data are consistent with a diminished capability of exogenous NO molecules to permeate cellular plasma membranes as a function of increased

cholesterol content, which was directly related to the activation of intracellular sGC.

Changes in membrane cholesterol were shown to influence targets downstream of sGC, such as the protein kinase-G substrate VASP, a mediator of cell motility, angiogenesis, vascular permeability and platelet aggregation [Garcia, *et al.*, 1998. Mo *et al.*, 2004. Bellamy, *et al.*, 2002. Ohno-Iwashita, *et al.*, 1990]. Fig. 3.3 shows that the level of VASP phosphorylation elicited by NO exposure could be manipulated by either augmentation or depletion of plasma membrane cholesterol. These results suggest that hypercholesterolemia may globally infringe upon numerous cGMP-mediated signalling pathways.

The spatial heterogeneity that cholesterol adds to the plasma membrane may act to modulate sGC at several levels. Interestingly, Ca^{2+} promotes sGC association with plasma membrane caveolae, specialized microdomains enriched with cholesterol [Linder, *et al.*, 2005]. Due to the steep response curve of sGC to NO in the low nanomolar concentration range [Mo, *et al.*, 2004. Bellamy, *et al.*, 2002], small decreases in NO transit through the membrane imposed by cholesterol could act to raise the threshold for sGC activation. In this light, Schmidt and co-worker found that membrane-associated sGC exhibited and

enhanced sensitivity to low levels of NO, whereas maximal sGC activity in response to high levels of NO was decreased in the membrane pool compared with the cytoplasmic fraction. In contrast with our findings, cholesterol depletion of endothelium-intact aortic rings by MBCD treatment disrupted sGC, protein kinase G and caveolin-1 co-localization and impaired relaxation by sGCs agonists [Linder, *et al.*, 2005]. These studies and the present data together illustrate that plasma membrane cholesterol is dynamically linked to sGC signalling, with the direction and magnitude of its effect probably determined by configurations unique to cell types and activation states.

Our findings show that increased plasma membrane cholesterol content raises the threshold for exogenous NO to activate sGC and affect the downstream protein kinase G target VASP. Therefore, this study raises the possibility that the physical partitioning of NO by membrane cholesterol rafts could be a contributing factor in the pathobiology of diseases beyond Niemann-Pick disorder, including cancer, neurodegeneration and cardiovascular diseases.

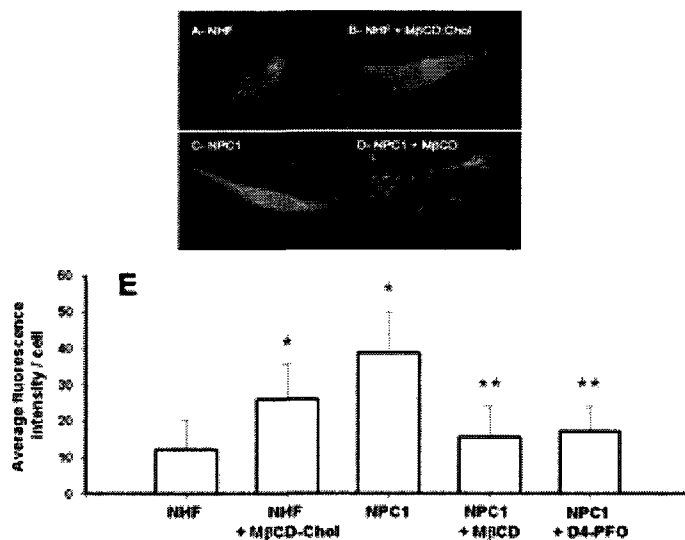


Figure 3.1: PM cholesterol of NHF *versus* NPC1 fibroblasts by fluorescence imaging of Alexa 532 labelled D4. Fixed normal (A) and NPC1-deficient fibroblasts (C) stained with 400 nM Alexa 532-labeled D4 and imaged under identical exposure conditions exhibited cholesterol-dependent fluorescence. Normal human fibroblasts repeatedly stained less intensely than their NPC1-deficient counterpart. Importantly, treatment of NHF with 100 μ M cholesterol-loaded M β CD was associated with an increase in cellular staining (B) and staining observed in NPC1-deficient cells could be largely abrogated by treatment with 10mM M β CD prior to fixation (D). Data taken from 3–5 independently stained cell populations are summarized numerically from average intensities per cell for at least 50 cells (E). *Error bars*, S.D. *, $p < 0.005$ compared with NHF; **, $p < 0.001$ compared with NPC1; two-tailed t test. Cholesterol and phospholipid levels were determined from plasma membrane isolates obtained by sucrose gradient ultracentrifugation and are representative of two separate experiments with *error bars* showing S.D. (F).

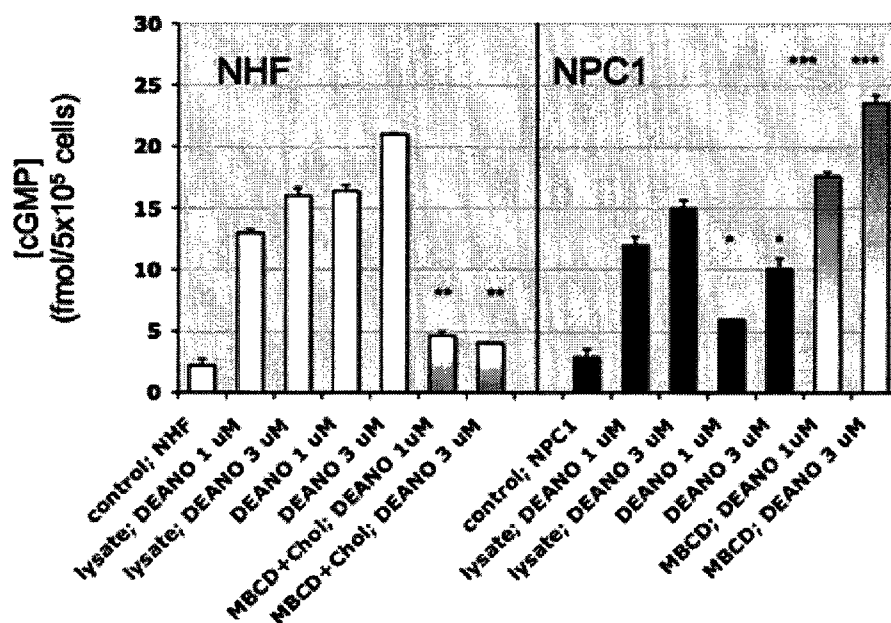


Figure 3.2: **Differential cGMP response of NHF and NPC1 fibroblasts to exogenous NO.** Cyclic guanosine monophosphate was measured by an enzyme immunoassay following stimulation of NHF (*white bars*) and NPC1-deficient fibroblasts (*black bars*) with the NO donor DEA/NO (1 and 3 μ M). Shown is a comparison of [cGMP] in NPC1 fibroblasts with that observed in an equivalent number of NHF (*, $p < 0.001$; two-tailed t test); $n = 3$. Also shown is a comparison of [cGMP] in M β CD-cholesterol-treated NHF with NHF (*white to gray bars*; **, $p < 0.001$; two-tailed t test) and a comparison of [cGMP] in M β CD-treated NPC1 with NPC1 (*gray to white bars*; ***, $p < 0.001$; two-tailed t test); $n = 3$. In addition, [cGMP] levels in response to DEA/NO (1 and 3 μ M) were compared in cell lysates of equal numbers of NHF and NPC1. *Error bars*, SD.

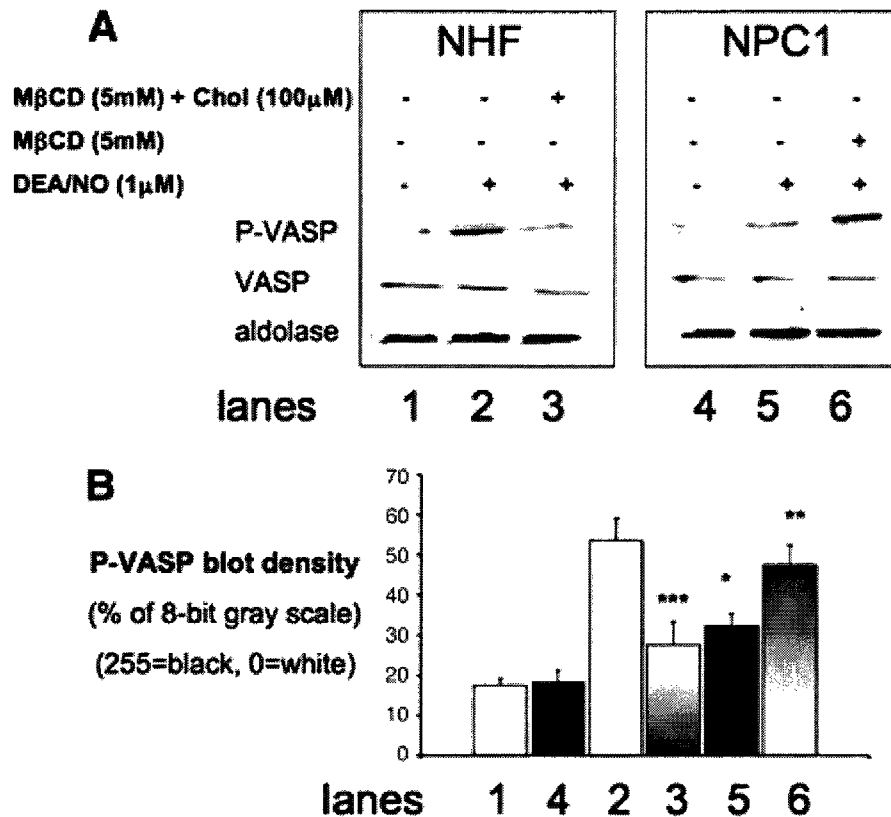


Figure 3.3: **Differential VASP Ser²³⁹ phosphorylation response of NHF and NPC1 fibroblasts to exogenous NO.** A, the amount of VASP and phospho-Ser239 VASP was estimated from Western immunoblots using equivalent numbers of NHF (*lanes 1–3*) and NPC1-deficient fibroblasts (*lanes 4–6*) probed with antibodies for phospho-VASP (*P-VASP*), VASP, and aldolase (loading control) in separate blots, subsequent to the exposure of the cells to DEA/NO (1 μ M) (*lanes 2, 3, 5, and 6*), NHF pretreated with M β CD-cholesterol (*lane 3*), or NPC1 pretreated with M β CD (*lane 6*). B, density plots of P-VASP data from Fig. 5A. Comparison of phospho-VASP in NPC1 fibroblasts with that observed in an equivalent number of NHF (*, $p < 0.033$; two-tailed t test); $n = 2$. Shown is a comparison of phospho-VASP in M β CD-treated NPC1 with NPC1 (*gray to white bars*; **, $p < 0.087$; two-tailed t test); $n = 2$. Also shown is a comparison of phospho-VASP in M β CD-cholesterol-treated NHF with NHF (*white to gray bars*; ***, $p < 0.0034$; 2-tailed t test); $n = 2$. Band density was estimated with ImageJ (1.39t) software. Error bars, S.D.

Part IV

Chapter 4

**Endothelial dysfunction can be induced by
endoplasmic reticulum stress mediated inhibition
of neutral sphingomyelinase 2.**

4.1 Introduction:

Endothelial dysfunction is a common occurrence in the pathogenesis of many cardiovascular diseases such as hypertension, coronary artery disease, chronic heart failure, diabetes, peripheral artery disease and chronic renal failure [Hua CAI, *et al.*, 2000]. Endothelial dysfunction is also an initiation factor in atherosclerosis [Davignon, *et al.*, 2004]. The hallmark of endothelial dysfunction which is common to all kinds of cardiovascular pathologies is the dominance of vasoconstriction over vasodilation in the endothelium. The pathologic mechanisms attributed to reduced vasodilation are reduced nitric oxide generation by eNOS, increased stress and hypercholesterolemia.

Endothelial dysfunction is the outcome of various kinds of stresses around the endothelium- endoplasmic reticulum stress (ER stress), oxidative and nitrosative stress [Mete, *et al.*, 2009. Outinen *et al.*, 1999. De'cio, *et al.*, 2007. Ohara, *et al.*, 1993. Keaney, *et al.*, 2005. Pa'l, *et al.*, 2005]. ER stress is an important early event in the progression of endothelium dysfunction. ER stress is also known to raise intracellular cholesterol thus bringing about cholesterol imbalance in the cell [Jin, *et al.*, 2000. Kyosuke, *et al.*, 1999, Werstuck, *et al.*,

2001. Colgan, *et al.*, 2007. Lee, *et al.*, 2004. Cheng, *et al.*, 2006]. Interestingly, the factors which lead to the rise in cellular cholesterol are the same which are also activated during ER stress. Site specific proteases S1P and S2P localized in the Golgi cleaves ATF6, an effector protein responsible to restore normal ER function and also SREBP-2 a transcription factor when activated by cleavage upregulate genes for cholesterol synthesis [Jin, *et al.*, 2000. Kyosuke, *et al.*, 1999]. Studies from some groups have shown that hypercholesterolemia increases oxidative stress near the endothelium [Prasad, *et al.*, 1997. Ohara, *et al.*, 1993. Prasad, *et al.*, 2003]. Oxidative stress together with the nitrosative stress causes dysfunctionality of endothelial vessel wall in many ways. The superoxide anion produced in oxidative stress reacts with nitric oxide, which is produced constitutively by endothelial nitric oxide synthase (eNOS) leading to the formation of the strong oxidant peroxynitrite which attacks various biomolecules in the vascular endothelium, vascular smooth muscle and myocardium leading to endothelial dysfunction [Pa'l, *et al.*, 2005].

Studies by many groups have shown that hypercholesterolemia contributes to abnormal endothelium-dependent vasodilation, thus bringing about endothelial dysfunction, which may be due to the attenuation of the eNOS activity [Robert, *et al.*, 1997. Olivier, *et al.*, 1999. Hayakama, *et al.*, 1999. Zulli, *et al.*, 2003]. The

activity of eNOS is regulated by many factors in the cell, availability of Ca^{2+} -calmodulin complex [Michel, *et al.*, 1997], eNOS Ser (1179) phosphorylation [Yasuko, *et al.*, 2002] and cellular localization [Carlos, *et al.*, 2006. Qian, *et al.*, 2006. Davin, *et al.*, 2005]. Impairment in any of these factors renders eNOS less active. Studies have revealed that where in endothelial dysfunction less eNOS activity may be attributed to less eNOS phosphorylation [Smith, *et al.*, 2003 Naoyuki, *et al.*, 2006] or more eNOS localization in the Golgi [Mukhopadhyay, *et al.*, 2007], stress can be an important contributor in lowering eNOS phosphorylation [Ruqin, *et al.*, 2007] or eNOS localization in the golgi [Murata, *et al.*, 2002].

The cellular site which needs special attention is the plasma membrane as it holds almost 50-90% cellular cholesterol [Lange, *et al.*, 2000] in free or bound form and is also a relay station for several signal transduction pathways serving as an anchorage for several kinds of receptors and proteins. The point of interest in the current study is that plasma membrane harbours eNOS in the detergent resistant microdomains called caveolae where it is known to be most active and is also a docking site for many proteins that mediate cholesterol influx/efflux and intracellular trafficking to maintain cholesterol homeostasis in the cell]. Neutral Sphingomyelinase 2 (NSMase2) is one such protein, it is a Mg^{2+} - dependent

enzyme showing optimum activity at neutral pH and is known to reside in the caveolae in the plasma membrane [Zhou, *et al.*, 2004. Liza, *et al.*, 2003. Veldman, *et al.*, 2001]. There is growing evidence which suggests that NSMase2 maintains cellular cholesterol balance by pushing excess cholesterol to the intracellular ER site to be stored as cholesteryl esters [Scheek, *et al.*, 1997. Slottle, *et al.*, 1988. Liza, *et al.*, 2003]. Apart from maintaining cholesterol balance NSMase2 is also known to mediate in vaso-relaxation by bringing about eNOS phosphorylation [Clara, *et al.*, 2006. Barsacchi, *et al.*, 2003. Kimiko, *et al.*, 2005].

Here we present evidence showing that the inhibition of NSMase2 by S-nitrosation of cysteine thiols and nitration of tyrosine residues, results in the build up of plasma membrane cholesterol, which we have previously shown to diminish the trans-bilayer diffusion of NO thus limiting its bioavailability [Miersch, *et al.*, 2008]. We chose two of the well known ER stressors Tunicamycin (*Tm*) and Palmitate (*Pm*) which causes ER stress in very different ways. *Tm* causes ER stress by blocking protein glycosylation and Palmitate incorporates into ER membrane, disrupting the structure and integrity of ER membrane and impairment of SERCA resulting in depletion of Ca^{2+} stores. Furthermore, our data indicates that ER stress-mediated NSMase2 inhibition results in decreased levels of eNOS phosphorylation, increased eNOS localization in the Golgi and less NO

production. This study is first of its kind which shows how ER stress can lead to elevation in plasma membrane cholesterol which in turn can cause impairment of eNOS activity and eventually leads to endothelial dysfunction.

4.2 Materials and Equipment

4.2.1 Materials

Bovine Aortic Endothelial Cells were purchased from Coriell Research Repository (Camden, NJ, USA). Fetal Bovine Serum and Lipofectamine LTX transfection reagent were purchased from Invitrogen (Carlsbad, CA, USA). Streptomycin and Penicillin were purchased from GIBCO (Carlsbad, CA, USA). F12K medium was purchased from ATCC (Manassas, VA, USA). Tunicamycin, Palmitate, L-NMMA and acetylcholine were purchased from Sigma (Oakville, ON, Canada). U18666A, DEA/NO and GW4869 were purchased from Calbiochem (Los Angeles, CA, USA). 24-well glass bottom plates were purchased from MatTek Corporation (Ashland, MA, USA). pGIPZ NSMase2 expression plasmid was purchased from Open Biosystems (Huntsville, AL, USA). Antibodies to eNOS and phospho (Ser1179) eNOS and VASP and phospho (Ser239) VASP were purchased from Cell Signaling Technologies (Danvers, MA, USA). Antibodies for GM130, GRP78/BiP, Caveolin1, β -cop, aldolase, CD36, SREBP-2, Nitrotyrosine, anti-rabbit phycoerythrin and anti-mouse fluorescein isothiocyanate were purchased from Abcam Inc. (Cambridge, MA, USA).

Antibody to NSMase2 was purchased from Santa Cruz Biotechnolgy Inc. (Santa Cruz, CA, USA). Protein G beads were purchased from GE Healthcare (Piscataway, NJ, USA). Peroxidase conjugated streptavidin was purchased from Peirce (Rockford, IL, USA). Polyvinylidene (PVDF) membrane was purchased from Millipore (Billerica, MA, USA). carboxy-H₂DCFDA was purchased from Molecular Probes (Carlsbad, CA, USA). Bradford Protein assay kit was purchased from Bio-rad (Mississauga, ON, Canada). Sphingomyelinase assay kit was purchase from Echleon Inc. (Salt Lake City, UT, USA).

4.2.2 Equipment

Agilent 8453 UV-VIS Spectrophotometer, Agilent Technologies, Canada, Inc, Mississauga, ON

Mettler AJ1000 Balance; Mettler, Toledo Canada, Mississauga, ON

NUAIRE Biological Safety Cabinet Class II Type A/B3; Thermo Electron Corp. Canada, Burlington, ON

Orion Model 420A pH Meter, Thermo Electron Corp. Canada, Burlington, ON

Varian Eclipse Fluorescence Spectrophotometer, Varian Canada, Mississauga, ON

Wallac 1420 Victor3 Fluorescent Plate Reader, Perkin Elmer, Woodbridge, ON

Haemocytometer; Reichert Co, Buffalo, NY, USA

Northern Eclipse 6.0 Imaging Software; Empix Imaging Inc., Mississauga, ON.

Zeiss Axiovert 200 Inverted Fluorescence Microscope, Empix Imaging Inc.,
Mississauga, ON.

Mini SDS-PAGE gel apparatus, Bio-rad, Mississauga, ON, Canada

Sievers Nitric Oxide Analyzer (NOA) 280i, Boulder, Co, USA

MLA-80 fixed angle rotor Optima Ultracentrifuge, Beckman Coulter Inc.,
Mississauga, ON, Canada

4.3 Methods

4.3.1 Cell Culture and treatment conditions:

Bovine Aortic Endothelial Cells, BAECs were maintained in F12K complete medium supplemented with 10% FBS, 100µg/ml Streptomycin, 100U/ml Penicillin. Cells from passages five to ten were used in these studies. All cells were maintained in a humidified incubator at 37 °C with 5% CO₂. The compounds Tunicamycin, Palmitate, L-NMMA, acetylcholine and U18666A were prepared fresh in culture medium, sterilized by filtration and added to the cell cultures. In most of the experiments the cells were treated with Tm (10µg/ml) and/or Palmitate (500µM) for 3 and 24 h unless mentioned, cells which were mock treated with culture medium at the corresponding times were taken as control.

For overexpression of NSMase2, BAECs were grown to 4X10⁴ cells per well in 24 well glass bottom plates and transiently transfected with 5µg of the pGIPZ NSMase2 expression plasmid using 100µl of the Lipofectamine LTX transfection reagent and transfection was followed as per manufacturer's instructions. The transfection was carried out for 24 h until 80% of the cells were transfected and

the transient transfectants were seen for overexpression of NSMase2 by indirect immunofluorescence. After getting transient transfectants, the cells were thereafter treated with the ER stressors for the indicated time points.

For the inhibition of NSMase2, BAECs were grown to 4×10^4 cells per well in 24 well glass bottom plates and incubated with 20 μ M with NSMase2 inhibitor GW4869. NSMase2 inhibition was assessed by indirect immunofluorescence. Following incubation of cells with GW4869 for 30 min, the cells were treated with the ER stressors for the indicated time points. However, the inhibition was stable for upto 24 h.

4.3.2 Animal care and treatments:

C57BL6 mice were purchased from Charles River and were fed a standard chow diet (Harlan Teklad). At 15 weeks of age mice were injected intraperitoneally with tunicamycin (0.25 μ g/kg body weight) or palmitate (20 μ g/kg body weight) or an equal volume (100 μ L) of saline. After 24 h the mice were sacrificed and perfusion fixed and en face aortas were mounted on glass slides, as previously described [Khan, *et al.*, 2009], for further analysis. All procedures were pre-approved by the McMaster University Animal Research Ethics Board.

4.3.3 Plasma membrane cholesterol estimation by cholesterol specific probe (PFO-D4-GFPuv) and cholesterol oxidase assay:

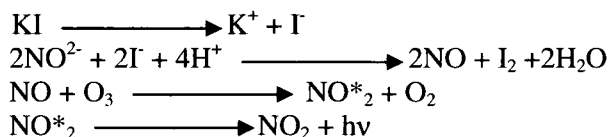
Imaging of Cellular Plasma Membrane Cholesterol with D4-GFPuv- The aortic sections and BAECs were stained with 250 nM and 1 μ M of PFO-D4-GFPuv respectively for 30 min under 37 °C, 5% CO₂, washed three times with Hepes buffer and imaged on an Axiovert epifluorescence microscope with 535 nm/550 nm excitation/emission under identical exposure conditions. Images were pseudo colored green using Northern Eclipse 6.0 imaging software and the average fluorescence intensity per unit of image area was measured for 50-80 cells from not less than 3 independent experiments.

Plasma membrane cholesterol analysis- Plasma membrane cholesterol isolation was done as described in [Miersch, *et al.*, 2008]. Briefly, 5×10^5 cells/10 cm plates were trypsinized and washed once with 100 mM Tris buffer, pH 7.4 and then with 10 mM hypotonic Tris buffer pH 7.4. A 1 ml suspension was homogenized by 50 strokes in a Dounce homogenizer and then spun at 190 X g for 10 min. Subsequently, the method described in [Vainio, *et al.*, 2005] was followed. Lipid suspension isolated in buffer was extracted twice with 200 μ l of 1:1 MeOH/CHCl₃ and back extracted once with 1M NaCl and the solvent was evaporated in a glass tube under a gentle stream of Ar. The lipid film was sonicated in 200 μ l of

CHAPS/Triton/Sodium Cholate buffer and cholesterol was quantified using a cholesterol oxidase enzymatic assay and interpolated from standard curve. Cholesterol estimation was performed according to the manufacturer's instructions in a 96-well plate at 37 °C with an excitation/emission of 545 nm/595 nm on a Perkin Elmer Life Science Victor 3 Fluorescent plate reader.

4.3.4 Nitric oxide release:

BAECs were seeded at a density of 4×10^4 cells per well in 24 well plate and treated with the ER stressors for 3, 6, 12 and 24 h. There were 2 sets of cells, in the first set thirty minutes prior to the termination of the treatment times, the cells were stimulated with the Ca^{2+} ionophore acetylcholine (100 μM) by removing the culture medium and replacing with a fresh medium having acetylcholine, in the other set the culture medium treated with the ER stressors were left without any replacement with acetylcholine. The nitric oxide released was measured in the form of nitrite in the medium. 10 μl of the culture medium containing nitrite was injected into Sievers Nitric Oxide Analyzer (Model 280i). The concentration was calculated by interpolation from a sodium nitrite standard curve. The NO released is measured by the following reactions occurring in the purge vessel.



Nitrite reduced to NO by KI in the acidic solution rapidly reacts with ozone (O_3) which yields NO^*_2 in an excited state. As the excited electron returns to the ground state, a photon is emitted and is detected by chemiluminescence.

4.3.5 Endothelial nitric oxide synthase localization by double immunofluorescence assay and by differential sucrose density gradient fractionation:-

Immunocytochemistry- Formalin fixed aortic cross-sections and BAECs were processed for fluorescence microscopy to determine colocalization of eNOS and GM130 a Golgi marker. The sections and the cells were incubated with primary rabbit anti-eNOS and FITC conjugated anti-GM130, in a humidified chamber for 2 h at 1:200 dilutions. Phycoerythrin conjugated anti-rabbit secondary antibody incubated, for 1 h at 1:400 dilutions in the humidified chamber was used to detect eNOS. The sections and the cells were imaged on the epifluorescence microscope with 495 nm/528 nm with Ex/Em for FITC and 488 nm/575 nm with Ex/Em for Phycoerythrin. The images were pseudocolored red and green and merged using Northern Eclipse 6.0 imaging software.

Differential Sucrose Density Fractionation- Plasma membrane caveolar microdomains and the Golgi were prepared by differential sucrose density

gradient fractionation, essentially as described [Macdonald, *et al.*, 2005] with slight modifications and adjustments for smaller volumes. BAECs were plated in 10 cm culture plates were washed and scraped in phosphate buffered saline. After pelleting the cells for 2 min at 250xg, 1 ml of 500mM sodium carbonate, pH 11.0 containing protease inhibitor cocktail was mixed with the pellet and incubated on ice for 20 min. Cells were lysed by 20 strokes in a Dounce homogenizer for 45 sec in a Branson sonifer 250. A step gradient of 5-30% (5% steps) sucrose with 250 mM sodium carbonate in HBS was established in an ultracentrifuge tube (1.3 ml each) and the homogenate was layered on top of the gradient. After centrifugation at 200,000xg, 4 °C for 18 h in a MLA-80 fixed angle rotor, nine equal fractions were taken, starting from the top of the gradient and subjected to Trichloroacetic acid precipitation, gel electrophoresed and immunoblotted.

4.3.6 Assay for Neutral Sphingomyelinase 2 activity:-

Isolation of NSMase2 from plasma membrane- Plasma membranes were prepared from 5×10^5 BAECs per 10 cm culture plates as previously described [Kinya, *et al.*, 1976]. Purified plasma membranes were sonicated at 4 °C for 30 sec in 10 volumes of 0.1% TritonX-100, 10 mM Tris/HCl (pH 7.5) and 0.2 mM MgCl₂ with protease inhibitor cocktail. The concentration of Triton X-100 was then

raised to 1.0%, kept at 4 °C under rotation overnight; the membrane fraction was centrifuged at 30,000Xg for 10 min. The resulting supernatant containing the solubilised proteins was used for the immunoprecipitation of NSMase2. 25 µL of polyclonal rabbit anti-NSMase2 antibody was added to the supernatant and rocked for 90 min at 4 °C. Protein G beads which were equilibrated and precleared previously were added to the supernatants' and rocked for 90 min at 4 °C. The beads were then harvested by centrifugation at 400Xg for 5 min. The supernatant which did not contain any enzyme (analyzed by western blot) was discarded and the beads were washed once in wash buffer (20 mM Tris HCl pH 7.5 and 0.2% Triton-X 100), spun down at 400Xg for 5 min. The supernatant was discarded and the NSMase2 was eluted with the elution buffer (20 mM Tris HCl pH 7.5, 0.2% Triton-X 100 and 4% SDS) by gently rocking at 250 rpm for 15 min. The beads were then spun down at 400Xg for 5 min and the supernatant (s1) was stored. The elution was carried out again for 5 min and the supernatant (s2) was stored. The two supernatants (s1 & s2) were pooled together and were analyzed for NSMase2 by western blot. Protein quantification was done by Bradford Protein assay.

Activity- From the purified NSMase2 20µg was used to assess the activity by the chromogenic sphingomyelinase assay kit, 100ul of the purified enzyme was mixed with 100µl of the enzyme mix provided by the manufacturers in 96-well microtitre

plate. Briefly, the hydrolysis of sphingomyelin yielded phosphorylcholine and ceramide. Alkaline phosphatase catalyzed the hydrolysis of phosphorylcholine and choline oxidase caused oxidation of choline producing hydrogen peroxide. DAOS plus 4-Aminoantipyrine (4-AAP) in the presence of hydrogen peroxide and peroxidase resulted in the oxidative coupling of DAOS and 4-AAP to form a blue chromogen that was detected by measuring the absorbance of light at 595 nm. NSMase2 activity (mU/ml) was calculated by interpolation from the standard curve.

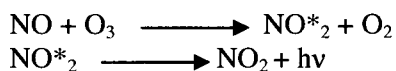
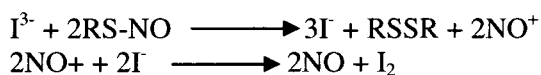
4.3.7 S-nitrosation, denitrosation and nitration of NSMase 2:-

S-nitrosation- The isolation of NSMase2 was carried out in the same way as described in the section “Isolation of NSMase2 from plasma membrane” with difference from the elution step. The elution was carried out in the biotin switch blocking buffer (2.5% w/w SDS and 30 mM NEM). The beads were resuspended in the blocking buffer and incubated at 50 °C for 25 min with frequent vortexing. The beads were spun at 400Xg for 5 min and the supernatant was stored. The supernatant was analyzed by immunoblotting and quantified by Bradford protein assay. The immunoprecipitated NSMase2 was then subjected to Biotin Switch Assay as described in [Yanhong, *et al.*, 2005]. Briefly, NEM was removed from the supernatant by precipitating the protein with 2 vol of prechilled (-20 °C)

ethanol, incubated at -20 °C for 1 h and centrifuged at 8000 X g, 4 °C for 10 min. Protein pellets were washed twice with prechilled ethanol to remove traces of NEM and resuspended in 0.1 ml HENS buffer per mg of protein (250 mM Hepes pH 7.7, 1 mM DTPA, 100 µM neocuproine, 1% SDS), 1mM Biotin-HPDP and 15 mM sodium ascorbate were added to the protein solution. The mixture was incubated in dark for 3 h at room temperature. The protein was precipitated and washed with prechilled ethanol. Protein pellets were resuspended in HENS buffer and mixed with 2X sample buffer without reducing agent. Protein was separated by SDS-PAGE, transferred to a PVDF (Millipore) membrane and incubated with peroxidase conjugated streptavidin (1:50,000 dilution) at 4 °C, overnight. The blot was developed by chemiluminescent horseradish peroxidase substrate.

Denitrosation- NSMase2 was isolated from plasma membrane essentially the same as described in the “Isolation of NSMase2 from plasma membrane”. The amount of protein in each sample was adjusted to 50µg by diluting with phosphate buffered saline pH 7.4 and 10µl of the sample was taken for the denitrosation assay. Denitrosation was carried out by reductive tri-iodide chemiluminescence as described [Peter, *et al.*, 2007] with smaller volumes adjustments. Acidic tri-iodide (I_3^-) reagent was freshly prepared with 200 mg of potassium iodide and 130 mg iodine in 4 ml of dH₂O and 11 ml of glacial acetic acid. 10µl of the sample were

injected into the purge vessel containing the acidic tri-iodide reagent of Sievers NOA (Model 280i). The total NO released was measured by the following reaction in the purge vessel.



The concentration was calculated by interpolation from a sodium nitrite standard curve.

Nitration- The formalin fixed aortic sections were processed to determine nitration of NSMase2 by double immunofluorescence assay. Sections were incubated with primary antibodies for NO₂-Tyr antibody (1:100) and NSMase2 (1:100). Secondary goat anti-mouse Phycoerythrin (1:200) and secondary donkey anti-rabbit FITC (1:200) were used for NO₂-Tyr and NSMase2 detection respectively. Images were captured using Axiovert epifluorescence microscope. The amount of nitration was also determined on immunoprecipitated NSMase2 from plasma membrane by western immunoblotting with NO₂-Tyr antibody.

4.3.8 Oxidative Stress:-

A cell permeant free radical sensitive 5-(and-6)-carboxy-2',7'-dichlorodihydrofluorescein diacetate (Carboxy-H₂DCFDA) probe was used to measure reactive oxygen species (ROS). The cell culture supernatant and the cell pellets which were formed by scraping the cells in phosphate buffered saline and spinning at 12000 rpm for 5 min were mixed with 100µl of 10µM of carboxy-H₂DCFDA (reconstituted in PBS). The samples were loaded in 96 well microtitre black optical bottom plate, incubated at 37°C for 1 h and read in plate reader with 492 nm/525 nm Excitation/Emission filter.

4.3.9 Western Blot analysis:-

Phospho Ser (1179) eNOS, eNOS and Caveolin1- Plasma membrane caveolar microdomains were isolated as described above "Differential sucrose density fractionation". The fractions having the caveolar microdomains were pooled together, TCA precipitated and the protein quantification was done with Bradford protein assay and the protein in each sample was adjusted equal by phosphate buffered saline pH 7.4. 20µg of the protein samples were mixed in SDS-PAGE sample buffer and separated on 10% SDS PAGE gels under reducing conditions and transferred to PVDF membranes. Immunoblots were incubated with primary

antibodies to phospho Ser (1179) eNOS, eNOS and caveolin1, followed by appropriate horseradish peroxidase conjugated secondary.

GRP78/BiP and SREBP-2- Cell lysates from BAECs were prepared in modified RIPA buffer. Protein lysates were subjected to SDS PAGE, transferred to PVDF membrane with primary antibodies to GRP78/BiP and SREBP-2 followed by horseradish peroxidase conjugated secondary.

VASP phosphorylation- BAECs were cultivated to approximately 85% confluency and treated with 500 μ M L-NMMA for 6 h to inhibit endogenous NO production. The cells were treated with the ER stressors for 24 h and 2 min prior to the end of the treatment time the cells were incubated with 1 μ M DEA/NO and left undisturbed for 10 min in the incubator. Cells were lysed in the modified RIPA buffer containing protease inhibitor. The lysates were then analyzed for VASP and phospho VASP Ser²³⁹ by immunoblotting with VASP and phospho VASP Ser²³⁹ antibodies.

4.3.10 Statistics:-

Results are shown as a mean \pm SD. Data was analysed with an impaired two-tailed Student's t test, a value of $P < 0.05$ was considered significant.

4.4 Results

4.4.1 ER Stress induces the increase of cholesterol in the plasma membranes of BAEC and mouse aortas:

BAEC were treated with ER stressors palmitate (*Pm*) and tunicamycin (*Tm*). The plasma membranes were isolated by sucrose density centrifugation and their cholesterol content was determined by an Amplex red cholesterol assay that utilized cholesterol oxidase/horseradish peroxidase/ATBS. The cholesterol determinations indicated that the PM-cholesterol levels increased by ~4-fold to ~5.3-fold 24h post exposure to *Tm* and *Pm* respectively (Figure 4.1A – white bars). This was testified in another way where ER stressed BAECs plasma membrane were stained with cholesterol specific probe PFO-D4-GFP and then imaged under fluorescence microscope. The ER stressed BAECs showed an increase in plasma membrane cholesterol as viewed by the increase in the fluorescence of PFO-D4-GFP on the plasma membrane (Figure 4.1B). To determine if acute exposure to ER stress could affect membrane cholesterol in vivo, C57BL6 mice were injected with *Pm* (20µg/Kg bodyweight), *Tm* (0.25µg/Kg bodyweight) or an equal volume of saline. Mice were sacrificed and aortas were removed, mounted en face and probed with PFO-D4-GFP. PFO-D4-

GFP titrations (Figure 4.1C, 4.1D), coupled with the equation derived from K_D vs. mol % plot (Figure 4.1B-inset), were used to estimate the changes in plasma membrane cholesterol upon exposure of the mice to ER stressors.

The *apparent* K_D estimated from for control cells was 1.2 mM. Upon *Tm* and *Pm* exposure these values decreased to ~0.19 mM and ~0.26 mM respectively. These decreases in apparent K_D s correspond to an estimated increase in mol % of cholesterol from ~9.4 mol% to 58 mol% and 42 mol% respectively upon *Tm* and *Pm* exposure. These *in vivo* results are very similar to those obtained for BAEC *in vitro* (Figure 4.1A). This was tested in another way in which aortic wall sections were stained with 250nM of PFO-D4-GFP which also showed increased fluorescence in the ER stressed aortic sections as compared to control (saline treated) in aortic sections (Figure 4.1E).

4.4.2 ER Stressed cells are less responsive to extracellular NO mediated signaling:

Next we tested whether ER stress mediated elevations in plasma membrane cholesterol affected downstream cGMP-mediated signaling. VASP is an actin-binding regulatory protein that is a substrate for both cGMP-protein kinase (at Ser²³⁹) and cAMP-protein kinase (at Ser¹⁵⁷) [Linder, *et al.*, 2005,

Garcia, *et al.*. 2002]. To do this, we exposed control and ER stressor exposed cells first to eNOS inhibitor L-NMMA for 6h then these cells were incubated for 10 min with the NO donor DEA/NO (1 mM). The cells were then probed for the levels of VASP and phospho-VASP by western blotting. The ER stressed cells yielded ~3.5-fold and ~4.7-fold lower levels of phospho-VASP in response to extracellular NO indicating that elevated plasma membrane cholesterol attenuates the transmembrane diffusion of NO (Figure 4.2). This translates into significantly lower intracellular signaling by NO.

4.4.3 Neutral Spingomyelinase 2 activity in BAEC is inhibited by nitration and S-nitrosation by ER stressors:

Neutral Sphingomyelinase 2 (NSMase2) is one of the key enzymes that regulate plasma membrane cholesterol levels. In view of the fact that ER stressors increased plasma membrane cholesterol both *in vivo* and *in vitro*, we sought to determine whether the activity of NSMase2 in BAEC was altered by ER stress. Our results showed that upon 24h of exposure to *Tm* or *Pm* NSMase2 activity was inhibited by ~40 % and ~58 % respectively (Figure 4.3A). We also exposed the IPd enzyme to GSNO (0.1 mM) in order to S-nitrosate it. The enzyme activity

subsequent to GSNO-exposure decreased by ~82% indicating that *S*-nitrosation can inhibit the enzyme (Figure 4.3A).

It is well established that oxidative stress is associated with the onset of ER stress [Célio, *et al.*, 2009]. This was confirmed here where the levels of reactive oxygen species (ROS) determined by the carboxy-H₂DCFDA probe indicated that exposure to either *Tm* or *Pm* resulted in ~3 to 4 fold increase in intracellular reactive oxygen species (ROS) (Figure 4. 3: B-dark gray bars) and ~9 to 12 fold increase in extracellular ROS (Figure 3: B-light gray bars). Peroxynitrite is a highly reactive compound produced by the reaction of NO and superoxide, a component of ROS, that irreversibly modifies proteins by tyrosine nitration and/or thiol nitrosation. To determine if NSMase2 was susceptible to modification by peroxynitrite the NSMase2 immunoprecipitates (IPs) were probed by antinitrotyrosine antibodies (Figure 4.3C) and subjected to the biotin shift assay as well as to the direct denitrosation (i.e. release of NO from nitrosated thiols) of the samples in a chemiluminescent NO analyzer, to determine the thiol nitrosation status (Figure 4.4A, B). The IPs of NSMase2 exposed to ER stressors were also positive for nitrotyrosine (Figure 4.3C).

To determine the thiol nitrosation status of NSMase2 in vivo, the en face aortas of mice injected with ER stressors were co-stained with antibodies against nitrotyrosine and NSMase2 (Figure 4.3D). Results showed that anti-nitrotyrosine antibodies (red fluorescence) were colocalized (yellow fluorescence) with anti-NSMase2 antibody (green fluorescence) (Figure 4.3D).

In terms of thiol (*S*-) nitrosation status, biotin shift assay revealed that NSMase2 was *S*-nitrosated (SNO) in control cells (Figure 4.4A). This level of *S*-nitrosation could be due to false positives associated with the use of ascorbate as a denitrosating agent in the biotin shift assay. However, upon 3h exposure to ER stressors the nitrosation levels (as estimated from blot densities) increased by 1.4- to 1.6-fold. And by 24h the level of SNO-NSMase2 increased by ~2.6- (*Tm*) to 3.1-fold (*Pm*) over controls (Figure 4.4B).

As a more direct measure of determining the levels of *S*-nitrosation levels of NSMase2, the enzyme was isolated from the control or ER stressor exposed samples by IP and their SNO content was determined by releasing the NO from the *S*-nitrosated thiols of NSMase2 by exposure to triiodide in a chemiluminescent NO analyzer (Figure 4.4C). By this method, it was evident that control enzyme had trace amounts of nitrosated thiols. But upon exposure to *Tm* or *Pm* the

amount of *S*-nitrosation increased by ~10-fold and ~30-fold respectively. These results strongly suggest that peroxynitrite produced by ER stress-induced ROS in combination with endogenous NO production can inactivate NSMase2.

4.4.4 NSMase2 overexpression or inhibition affects NO production and plasma membrane cholesterol levels in BAEC:

The present data showing that NSMase2 was inhibited as a consequence of ER stress coupled with the established pivotal role for this enzyme in the modulation of plasma membrane cholesterol and NO-biosynthesis, prompted us to overexpress or inhibit NSMase2 in order to clarify its role in endothelial dysfunction.

In control cells, the levels of plasma membrane cholesterol decreased by ~50% upon overexpression NSMase2 (Figure 4.1A: *24h data, black bars*). The effects of NSMase2 overexpression on plasma membrane cholesterol were more dramatic in the case of the *Tm* and *Pm* treated BAEC. The cholesterol levels that were increased by ~4-fold and ~5-fold in the presence of *Tm* and *Pm* decreased by ~2.5 and ~3-fold upon NSMase2 overexpression (Figure 4.1A: *24h data, black bars*).

The inhibition of NSMase2 with GW4869 in control cells, resulted in a ~1.4-fold increase in plasma membrane cholesterol. In *Tm* and *Pm* treated BAEC, the inhibition of NSMase2 increased plasma membrane cholesterol levels only by ~1.1 fold (Figure 4.1A: *24h data, light gray bars*). This is expected since ER stressors are already inhibiting the enzyme via nitration and *S*-nitrosation (Figures 4.3 and 4.4).

In the case of NO production, ER stressors gradually decreased both basal and Ca^{2+} ionophore-activated NO production (detected as nitrite). For ionophore activated cells, exposure to *Tm* and *Pm* decreased NO production by ~40 % and ~50% by 24h. Basal NO activity decreased by ~60% and ~76% respectively by 24h (Figure 4.5 A,B).

NSMase2 overexpression had minimal (~1.1-to ~1.6 fold) potentiation effect on ionophore-activated NO-production in control as well as *Tm* and *Pm* treated cells (Figure 4.5B: *24h data, black bars*). However, the basal NO-production was affected to a larger extent by NSMase2 overexpression where the control cells levels increased by ~1.3-fold (Figure 4.5B: *24h data, black bars*). In case of ER stressed cells, enzyme overexpression increased the ER stress-

attenuated NO-activity by ~1.36-fold and ~1.9-fold respectively for *Tm* and *Pm* treated cells (Figure 4.5A: 24h data, black bars).

4.4.5 ER stress-mediated inhibition of NSMase2 leads to decreased eNOS phosphorylation, and NO production but increased localization of eNOS in the Golgi:

It has been established that the ceramide formed during the NSMase2 catalyzed degradation of sphingomyelin acts as a second messenger for eNOS activation by phosphorylation at Ser 1179 [Clara, *et al.*, 2006]. We therefore probed the phosphorylation status of BAEC-eNOS as a function of ER stress as well as overexpression and inhibition of NSMase. eNOS is localized in the PM as well as in the Golgi. We first isolated the eNOS fractions by sucrose density fractionation where the PM and the Golgi fractions were first identified by their content by the organelle markers Caveolin1 and β -Cop respectively (Figure 4.6A). These fractions were then probed for eNOS in the absence and presence of *Tm* and *Pm*. The control levels of eNOS protein in the PM increased by ~1.3-fold % between 3h and 24h. Exposure of the BAEC to *Tm* and *Pm* did not significantly alter eNOS levels in the PM. In contrast, *Tm* and *Pm* exposure increased Golgi-eNOS by ~1.8- and ~2.5-fold, respectively (Figure 4.6 B, C).

This was also determined by double immunofluorescence assay by using antibodies for eNOS and GM130, a Golgi resident protein and we saw that with ER stress more eNOS localizes in the Golgi (Figure 4.6 D).

We next wanted to determine the extent to which ER stress as well as NSMase2 overexpression or inhibition affected eNOS phosphorylation at the PM. ER stressors *Tm* and *Pm* decreased eNOS phosphorylation by ~2.5- to 5-fold respectively in comparison to controls. The overexpression of NSMase2 increased phosphorylation levels by ~2-fold over wt cells. The exposure of the NSMase2 overexpressed BAEC to *Tm* and *Pm* decreased the phospho-eNOS by ~60% but brought phosphorylation levels to near those observed in the wt enzyme. The inhibition of NSMase2 activity by GW4869 nearly abolished all eNOS phosphorylation in the PM (Figure 4.7).

4.4.6 ER stress upregulates protein expression for GRP78 and SREBP-2 with no change in Caveolin1 protein expression:

We next did western blot analysis for three proteins which may directly or indirectly respond during stress- GRP78/BiP, SREBP-2 and Caveolin1. GRP78/BiP is an ER membrane bound protein under unstressed conditions. During ER stress it dissociates from the ER membrane and activates other ER

stress effector proteins that trigger alarm and adaptive signals to restore ER normal functions. The protein expression for GRP78/BiP was increased as a result of inducing ER stress for 3, 6 and 12 h in endothelial cells. L-aldolase was used as a loading control and GRP78/Bip protein was quantified as a ratio with L-aldolase at each time points (Figure 4.8). Sterol regulatory element binding protein (SREBP-2) is an ER membrane bound transcription factor that upon proteolytic cleavage with S1P and S2P proteases can activate genes for the biosynthesis of cholesterol. ER stress leads to the activation of SREBP-2 and thus cholesterol accumulation in the cell. We determined the activated form of SREBP-2 in the presence of both ER stressors Tm and Palmitate. U18666A was used as a positive control for SREBP-2 activation. Both the ER stressors activated SREBP-2 to different degrees post induction in ECs (Figure 4.9). L-aldolase was used as a loading control and activated SREBP-2 was quantified as a ratio of L-aldolase expression. We next aimed at determining the protein expression for Caveolin1, it being an important integral membrane component of caveolae and are known to regulate both eNOS activity and cellular cholesterol balance. We isolated the caveolar membrane fractions (3&4) by differential sucrose density fractionation from the untreated control and ER stressed ECs. The quantification of Caveolin 1

protein after western blotting as a ratio of CD36 did not show any increase/decrease in Caveolin 1 expression after inducing ER stress (Figure 4.10).

4.5 Discussion:

In summary, we have demonstrated that ER stress mediated by any route causes a rise in plasma membrane cholesterol in endothelial cells. Accumulation of cholesterol leads to oxidative stress generating reactive nitrogen oxide species (RNOS). The RNOS causes inactivation of NSMase2 resulting in a persistent increase in plasma membrane cholesterol. Inactivation of NSMase2 also leads to the lowering of eNOS activity by reduced eNOS Ser (1179) phosphorylation. Another important observation made is that with ER stress more eNOS localizes into the Golgi. However, this localization of eNOS into Golgi is not affected by the inactivation of NSMase2 and presumably there is some other signalling pathway responsible for it. This study establishes a specific framework by which an imbalance in plasma membrane cholesterol and eNOS activity are related and translated into an endothelial dysfunction response.

Plasma membrane is a prime site for the influx and efflux of cholesterol. Moreover, cholesterol synthesized in the ER is transported to the plasma membrane either by the Golgi complex or uses a pathway which bypasses the Golgi. Cholesterol endocytosed in the form of LDL- unesterified cholesterol and cholesteryl esters enters a complex series of endocytic compartments. The unesterified cholesterol is recycled back to the plasma membrane whereas

esterified cholesterol enters the lysosomes, where it is hydrolysed to cholesterol which moves to the ER to get re-esterified by ACAT and stored in cytosolic lipid droplets. Caveolae rafts in plasma membrane function in the uptake pathway for the HDL-cholesteryl esters in steroidogenic cells where cholesterol is needed in steroidogenesis. Exocytosis of cholesterol takes place by desorption of cell surface cholesterol into lipoproteins or is induced after high density lipoprotein binding to membrane receptors [Rothblat, *et al.*, 1999]. The whole process of cellular cholesterol synthesis, distribution and trafficking are highly regulated. This regulation is brought about by the SREBP-SCAP complex [Nohturfft, *et al.*, 2000]. Neutral sphingomyelinase action is also implicated in cellular cholesterol homeostasis. Increasing cholesterol levels beyond saturation in the plasma membrane activates NSMase which directs excess cholesterol into the ER where cholesterol is esterified by ACAT and inhibits SREBP cleavage [Slotte, *et al.*, 1988]. Anomaly in any of these regulators causes cholesterol imbalance which leads to cellular dysfunction. As evidenced in hepatic steatosis where hyperhomocysteinemia induces ER stress and activates SREBPs in cultured human hepatocytes and endothelial cells and leads to intracellular cholesterol accumulation [Werstuck, *et al.*, 2001]. Also induction of ER stress in HeLa and MCF7 cells increased SREBP-2 expression and intracellular cholesterol

accumulation [Colgan, *et al.*, 2007]. However, these studies were not extended to monitor the effect of ER stress on plasma membrane cholesterol. In the present study, we exposed BAEC to commonly employed ER stressors *Tm* and *Pm* and observed that plasma membrane cholesterol levels became elevated 4-5 fold (Figure 4.1A). In parallel *in vivo* studies with mice, the onset of ER stress also increased plasma membrane cholesterol to a similar extent to those observed *in vitro* (Figure 4.1C,D). There was also an increase in the expression of SREBP-2 (Figure 4.9).

We then determined that the ER stressed cells became 3.5- to 4.7-fold less responsive than controls to extracellular NO-induced VASP phosphorylation one of the many cGMP-mediated signaling pathways. These results fully substantiate our earlier observations showing that the level of VASP phosphorylation elicited by extracellular NO exposure could be manipulated by the augmentation or depletion of plasma membrane cholesterol [Miersch, *et al.*, 2008]. Our current study strongly suggests that ER stress-induced hypercholesterolemia can infringe upon various cGMP-dependent pathways by simply lowering the diffusion of NO across biomembranes and thus functionally lowering the bioavailability of NO.

Hypercholesterolemia increases oxidative stress by various ways, increases lipid peroxidation [Prasad, *et al.*, 1997], decreases anti-oxidant enzymes and

nonenzymatic antioxidants [Prasad, *et al.*, 2003]. Hypercholesterolemia initiates arachidonic acid pathway enzymes lipoxygenase and cyclooxygenase and in vascular cells it is associated with increased O_2^- production by xanthine oxidase and NADH/NADPH oxidase. These reactive oxygen species react with nitric oxide and generate RNOS. RNOS brings posttranslational modification of several proteome of endothelial cells by S-nitrosation of cysteine thiols or nitration of tyrosine residues. However, these modifications are reversible but they are involved in the inhibition of the function of the proteins [Diane *et al.*, 2006]. In an effort to determine pathological mechanism behind the elevations plasma membrane cholesterol we focused on NSMase2, a plasma membrane outer leaflet-resident enzyme that has been implicated in the fine regulation of plasma membrane cholesterol levels. We found NSMase2 activity was inhibited ~40 % and ~58 % by exposure to *Tm* and *Pm* respectively (Figure 4.3A). We then compared ROS production in the BAEC and observed very large increases in both intracellular and extracellular ROS upon induction of ER stress (Figure 4.3B). It is established that ROS in combination with the NO produced by BAEC can lead to the formation of peroxynitrite which can irreversibly inactivate proteins by nitration of tyrosine residues and the oxidation and/or S-nitrosation of cysteine thiols.

Our results did indicate that NSMase2 in ER stressed BAEC or in mice aortas had nitrotyrosine damage indicated by Western blots or by immunocytochemistry (Figure 4.3 C,D). NSMase IPs from ER stressed BAEC were also S-nitrosated as determined by 2 independent methods. In separate experiments we showed that the S-nitrosation of NSMase2 did inhibit its activity by ~80% (Figure 4.4A,B). Taken together, these lines of evidence strongly suggest that NSMase2 is susceptible to inhibition by of peroxynitrite during ER stress.

The next question we wanted to answer was how does the inhibition of NSMase2 bring about elevations in plasma membrane cholesterol? Sphingomyelin (SM) is preferentially localized in the outer leaflet of plasma membranes where it forms a 1:1 complex with cholesterol yielding microdomains termed rafts and caveolae. For this reason ~50-90% of cellular SM and cholesterol is concentrated in the plasma membranes [Lange, *et al.*, 2000]. In the plasma membrane free cholesterol is in equilibrium with microdomain cholesterol (Scheme I). As the work of Leppimäki *et al.* [Leppimäki, *et al.*, 1998] has elegantly shown, total plasma membrane cholesterol is intimately tied to SM metabolism, the key enzyme in SM biosynthesis serine C- palmitoyltransferase (SPT), was activated by 30% in cholesterol depleted cells but only slightly inhibited by 15% in cholesterol

loaded cells. This means that under conditions of ER stress, where cholesterol biosynthesis is upregulated via the SREBP pathway, SM biosynthesis will only be diminished by ~15%. The *de novo* synthesized SM was shown to be efficiently transported to the plasma membrane [Lange, *et al.*, 2000] where it will combine with the cholesterol to form microdomains pulling the equilibrium (Scheme I) to the right. Under normal conditions an active NSMase2 would disrupt microdomains by degrading SM to choline plus ceramide, which would release the SM-bound cholesterol. The free cholesterol would either effluxed from the cell or be internalized and acylated. In this manner, the cholesterol homeostasis would be maintained (Scheme I). Inhibition of NSMase2 under ER stress would shift the equilibrium to the right thus resulting in the buildup of plasma membrane cholesterol rafts. The fact that under ER stress, SM-biosynthesis is slightly inhibited would mean that the amount of free cholesterol would also increase in the plasma membrane since [SM] would be limited (Scheme I). It is also possible that ER stress and related effects could also attenuate the efflux or internalization of cholesterol thus contributing to its buildup in the PM.

We tested this hypothesis by either overexpressing or inhibiting NSMase2 in BAEC. As predicted the overexpression of the enzyme decreased plasma membrane cholesterol in control and ER stressed cells. Conversely, NSMase2

inhibition in control cells, increased plasma membrane cholesterol by ~1.4-fold. In the case of the ER stressed cells, where NSMase2 was already inhibited, further inhibition by GW4869 only increased cholesterol levels by a slight ~1.1 fold. These studies clearly indicate that attenuation of NSMase activity can result in elevated plasma cholesterol.

Hypercholesterolemia has other important manifestation which brings less vasodilatation of the endothelium. The abnormal vasodilatation may be due to less NO production and higher intracellular Ca²⁺ levels in smooth muscle cells [Roberts, *et al.*, 1997], inhibitory effects of caveolin abundance on eNOS after incubating ECs with serum LDL-C from hypercholesterolemic volunteers [Olivier, *et al.*, 1999], products of lipid peroxidation reduces NO bioavailability without affecting eNOS mass or catalytic activity in hypertension [Hayakawa, *et al.*, 1999], reduced eNOS Ser (1179) phosphorylation in high cholesterol fed animals [Suzuki, *et al.*, 2006]. However, all of these studies were performed where cholesterol was exogenously provided and there is no study till date which targets plasma membrane cholesterol and its subsequent effects on eNOS activity.

In a recent study [Miersch, *et al.*, 2008], we showed that there was an inverse relationship between the cholesterol content of the plasma membranes and the transmembrane NO-diffusion rate. In functional terms, elevations in plasma

membrane cholesterol translated into a significant attenuation of NO-mediated signalling. However, the extrapolation of these observations into common pathologies was not immediately obvious in view of the fact that in these studies we manipulated the plasma membrane cholesterol levels by chemical means or utilized cells from rare genetic diseases (sterol transport-defective Niemann-Pick type C1 fibroblasts). Neutral Sphingomyelinase action on selective degradation of sphingomyelin, yielding bioactive lipid intermediate- ceramide is also important for eNOS activity. Ceramide causes eNOS Ser 1179 phosphorylation by a variety of kinases including Akt [Fulton, *et al.*, 1999] and helps in regulating arterial wall tone independent of intracellular Ca^{2+} levels [Clara, *et al.*, 2006]. Here, we found that pathophysiological conditions induced by ER stress results in less eNOS activity due to less eNOS Ser 1179 phosphorylation mediated by inactivation of NSMase2. ER stress decreased phosphorylation by ~2.5 to 5-fold. The overexpression of NSMase2 followed by ER stress returned the phosphorylation to near *wt* levels. NSMase2 inhibition nearly abolished eNOS phosphorylation (Figure 4.7).

These results suggest that eNOS activity, and therefore NO production, should be attenuated by as a consequence of ER stress mediated NSMase inhibition. This was indeed the case, by 24h both basal and Ca^{2+} ionophore-activated NO production (detected as nitrite) decreased 50% to 76% respectively.

NSMase overexpression did increase basal, ER stress-inhibited activity by 1.4 to 1.9 fold. However enzyme overexpression did not have much effect on restoring NO-activity in ionophore-activated cells. This suggests that under non-stimulated conditions a larger fraction of eNOS is de-phosphorylated [OR “not phosphorylated”].

Another important observation made in the present study was the localization of eNOS into the Golgi after inducing ER stress. We observed that although the levels of eNOS protein were essentially unaffected at the plasma membrane, the amount of eNOS at the Golgi increased ~2 to 3-fold upon induction of ER stress (Figure 4.6). We also monitored the levels of caveolin 1 and found it not to be affected by ER stress. The functional significance of eNOS Golgi localization is not yet clear. In endothelial cells, eNOS localizes in the plasma membrane caveolar regions and in the intracellular Golgi site [Qian, *et al.*, 2006], eNOS within the caveolae is known to be in the most active state [Zheng *et al.*, 2000]. So far, few studies have shed some light into better understanding on the activity of PM-eNOS versus Golgi-eNOS. During pulmonary hypertension less NO produced by pulmonary arterial endothelial cells is due to the localization of eNOS into Golgi, mainly brought by the eNOS-Golgi blockade [Mukhopadhyay, *et al.*, 2007]. PM-eNOS is more accessible to agonist

stimulation, kinases and protein-protein interaction than the Golgi-eNOS [Qian, *et al.*, 2006], which may be a reason for less NO production by Golgi-eNOS. In the present study, the eNOS protein levels in the caveolae were largely the same after ER stress and localization into Golgi remained unaltered by overexpressing and inhibiting NSMase2, thus suggesting that NSMase2 does not have any role in eNOS localization. The fact that NSMase overexpression did not restore NO production to control levels in ER stressed cells, coupled with the observation that overexpression of NSMase2 under ER stress returned the phosphorylation to near *wt* levels suggests the ~50% loss in NO production is due to Golgi-trapped eNOS which cannot be activated by phosphorylation (Figures 4.5 and 4.7).

However, a detailed mechanism for this localization remains to be established whether it occurs by the translocation of eNOS from plasma membrane to Golgi with the help of an eNOS traffic inducer- NOSTRIN [Kirstin, *et al.*, 2002] or the “Golgi blockade hypothesis” comes into play here. The latter is shown where monocrotaline pyrrole induces megalocytosis and cell cycle arrest by blocking proteins in Golgi in endothelial cells mediated by unfolded protein response [Mukhopadhyay, *et al.*, 2006].

Caveolin1 is a coat protein for the caveolar microdomains of the plasma membrane. It serves as an eNOS inhibitor, forms ternary complexes with eNOS and

NOSTRIN for the subcellular translocation [Schilling, *et al.*, 2006] and is also an important trafficker during influx/efflux of cholesterol; it is highly upregulated during cholesterol loading in the cell. The caveolin1 protein levels in the isolated plasma membrane fractions were unaffected by the ER stress. The probable explanation for this could be that the earlier studies where caveolin 1 was upregulated with cholesterol were mainly done bearing the idea of cholesterol transport, when cholesterol was exogenously provided or when it was effluxed to HDL. However, in the present study cholesterol was *in situ* synthesized by pathophysiological conditions. Moreover, as the eNOS protein content was unchanged in the plasma membrane after ER stress, it seems quite possible that caveolin 1 was not directly involved in eNOS inhibition. Taken together with our data, there emerges a potential link between plasma membrane cholesterol and NO bioavailability by eNOS as a prelude to endothelial dysfunction brought by ER stress and can assist in designing better therapeutic targets to combat this dysfunction.

A

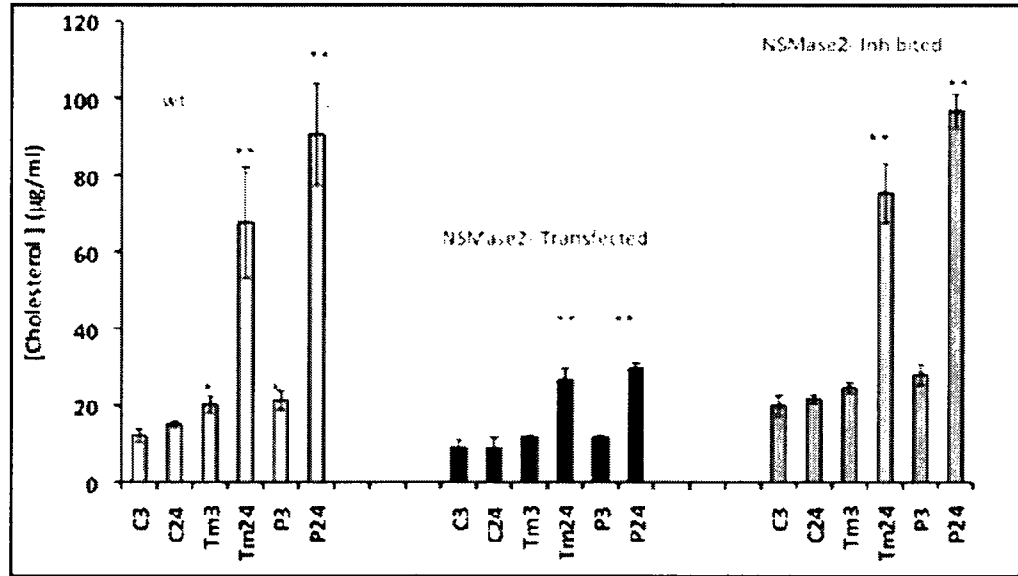


Figure 4.1 **Cholesterol analysis on PM isolates from BAECs and titration of PFO-D4-GFP on aortic wall cross-sections from C57BL6 mice.** (A) Cholesterol levels were determined from plasma membrane isolates obtained by sucrose gradient ultracentrifugation with 10µg/ml tunicamycin (*Tm*), 0.5mM palmitate (*Pm*) or mock treated (C) wild type (wt) BAECs (white bars), *Tm*, *Pm* or C treated p-GIPZ NSMase2 transfected BAECs (black bars) and *Tm*, *Pm* or C treated wt- GW4869 inhibited BAECs (gray bars) for 3 and 24 h respectively.

B

WT

p-GIPZ NSMase2

WT-GW4869

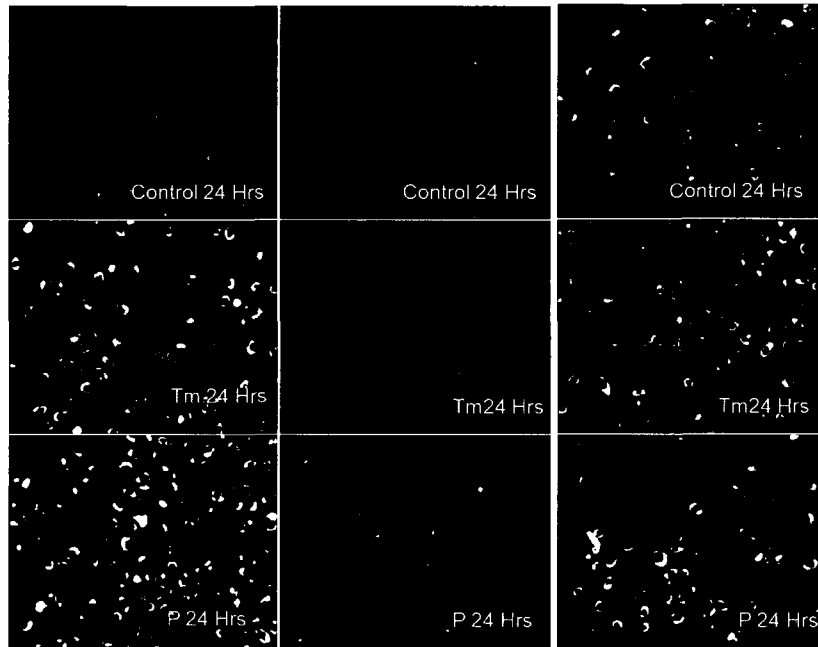
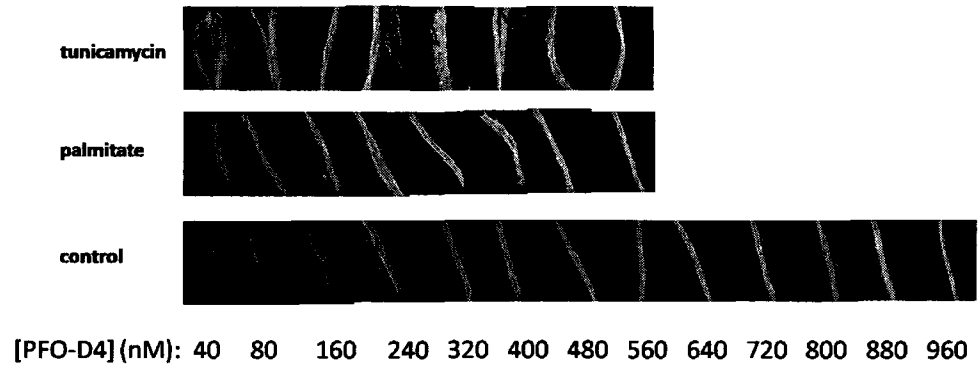


Figure 4.1: (B) **Visualizing cholesterol by staining with PFO-D4-GFP on BAECs** WT, p-GIPZ NSMase2 transfected and WT-GW4869 NSMase2 inhibited BAECs treated with ER stressors for 24 hours and stained for plasma membrane cholesterol with the cholesterol specific probe PFO-GFP-D4 (1uM).

C



D

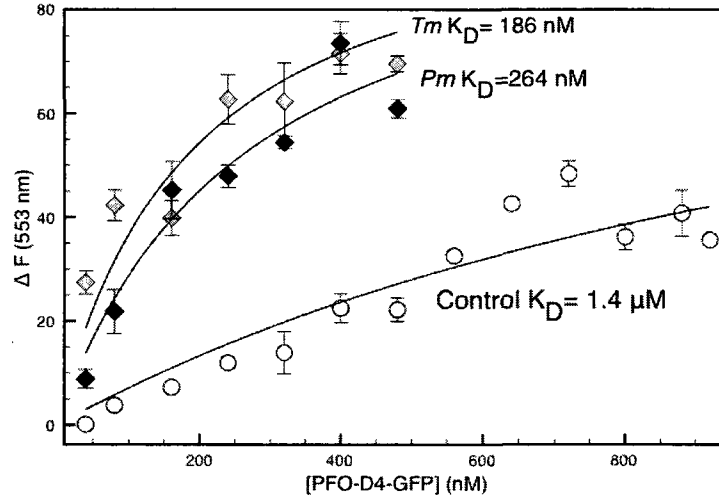


Figure 4.1 (C) **Titration of aortic cross-sections with PFO-D4-GFP** The aortic wall cross-sections from Tm treated (0.25 μ g/Kg bodyweight), Pm treated (20 μ g/kg bodyweight) and saline treated (control) C57BL6 mice were titrated with increasing [PFO-D4-GFP]. (D) Titration of aortic wall cross-sections with increasing [PFO-D4-GFP] from 3 independent experiments are summarized in the plot and the apparent K_D determined at the saturation limit of [PFO-D4-GFP]. The data shown is representative of 3 separate experiments with error bars showing S.D., * $p < 0.005$ and ** $p < 0.001$; two-tailed t-test.

E

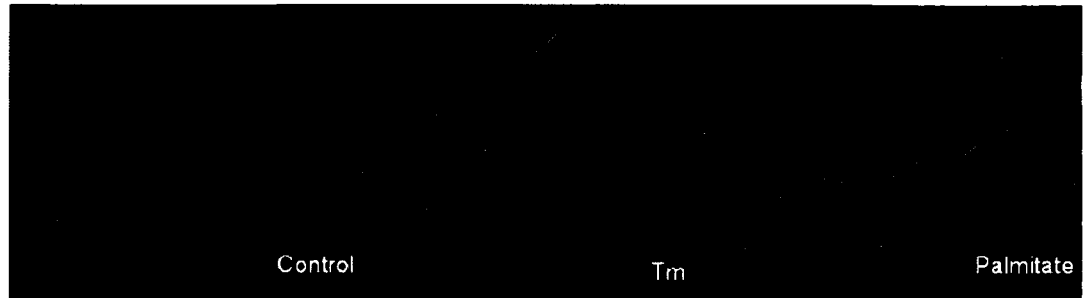


Figure 4.1 (E) Aortic cross-sections stained with PFO-D4-GFP The aortic wall sections obtained from C57BL6 mice treated with ER stressors *Tm*, Palmitate (*Pm*) or mock treated (Control) were stained with PFO-D4-GFP (green) at a concentration of 250nM. The nuclei were stained with DAPI (blue).

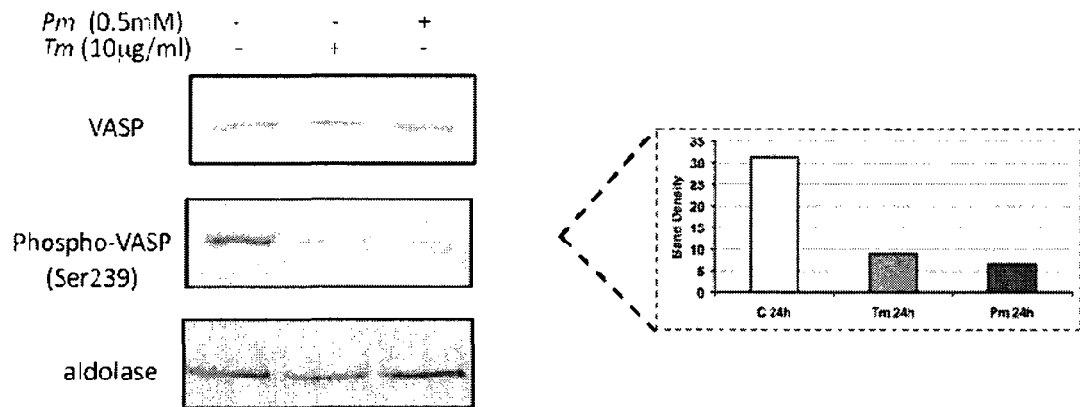
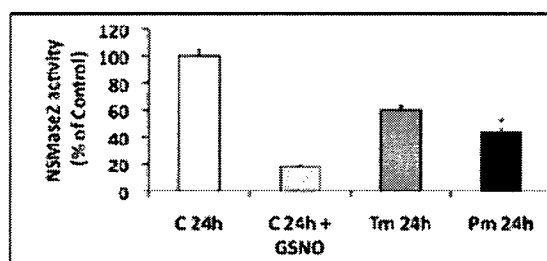


Figure 4.2 **Differential VASP Ser²³⁹ phosphorylation response of BAECs to exogenous NO.** The amount of VASP and \square phosphor Ser²³⁹ VASP was estimated from western immunoblots using equivalent numbers of BAECs treated with *Tm*, *Pm* or mock treated (C) and probed with antibodies for VASP, \square phosphor Ser²³⁹ VASP and aldolase (loading control) in separate blots, subsequent to the exposure of the cells to DEA/NO (1μM). The plot represents the density of \square phosphor Ser²³⁹ VASP blot with error bars showing S.D. and ** $p < 0.001$; two-tailed t-test; $n = 2$.

A



B

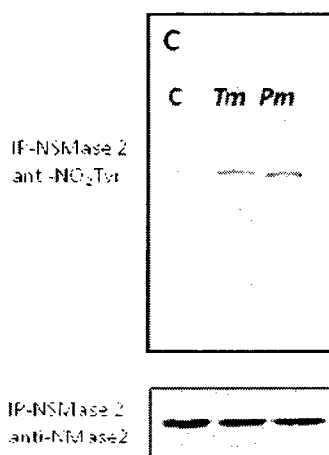
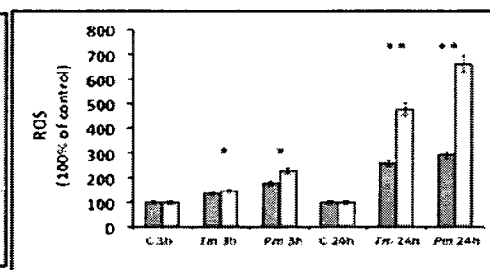


Figure 4.3 (A) **Activity of NSMase2 IP-isolated from BAECs, effects of ROS generation and nitration of tyrosine residues.** NSMase2 activity was measured in the immunoprecipitated NSMase2 from BAECs treated with *Tm*, *Pm* or mock treated (C) for 24 h. IP-NSMase2 exposed to GSNO was taken as a positive control. (B) ROS measured by carboxy-H₂DCFDA on cell culture supernatant (gray bars) and cell pellet (black bars) of BAECs treated with *Tm*, *Pm* and mock treated (C) for 3 h and 24 h respectively. (C) The amount of nitration on immunoprecipitated (IP) NSMase2 was estimated from western immunoblots with antibodies for NO₂-Tyr from BAECs treated with *Tm*, *Pm* or mock treated (C) for 24 h. Immunoblot of IP-NSMase2 was taken as the loading control.

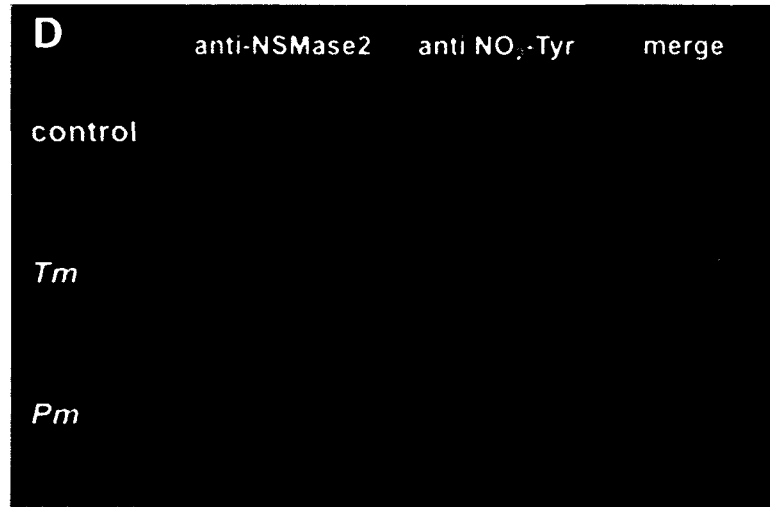


Figure 4.3 (D) **Double immunofluorescence assay to determine nitration on the aortas** Nitration was determined on the aortic wall cross-sections from Tm, Pm or saline (Control) treated C57BL6 mice. Secondary goat anti-mouse FITC and secondary donkey anti-rabbit Phycoerythrin were used for NSMase2 and NO₂-Tyr detection respectively. The data shown is representative of 2 independent experiments with error bars showing S.D.; * $p > 0.005$ and ** $p > 0.001$; two-tailed t-test.

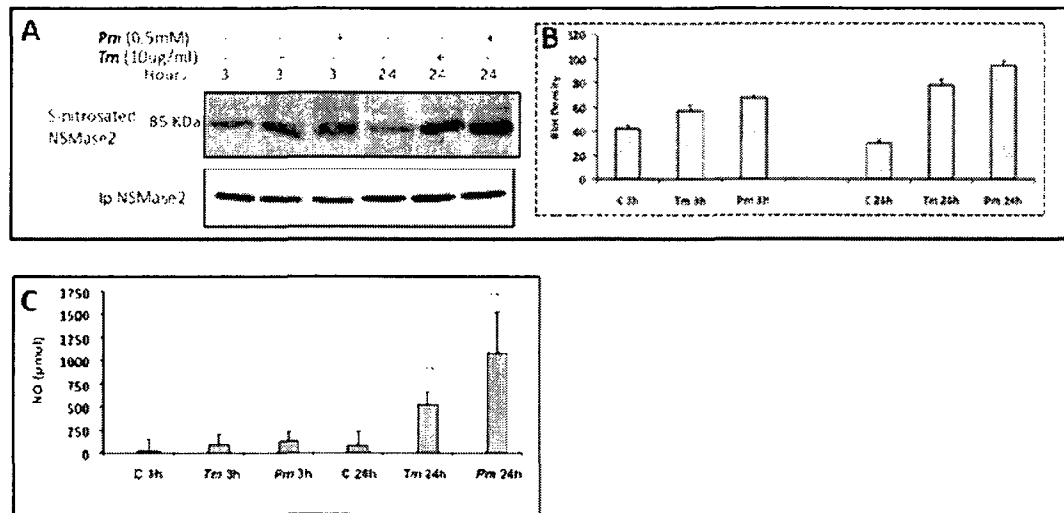


Figure 4.4 S-nitrosation and denitrosation of immunoprecipitated NSMase2 from BAECs determined by Biotin Switch Assay and reductive tri-iodide chemiluminescent assay respectively. (A) NSMase2 immunoprecipitated from BAECs treated with *Tm*, *Pm* or mock treated (C) for 3 and 24 h respectively was subjected to Biotin Switch Assay. Immunoblot of immunoprecipitated (Ip-NSMase2) was taken as loading control (B) Density plots of s-nitrosated BAECs treated with *Tm*, *Pm* or mock treated (C) for 3 and 24 h determined by reductive tri-iodide chemiluminescent assay. The data is representative of 2 independent experiments with error bars showing S.D.; ** $p > 0.001$; two-tailed t-test.

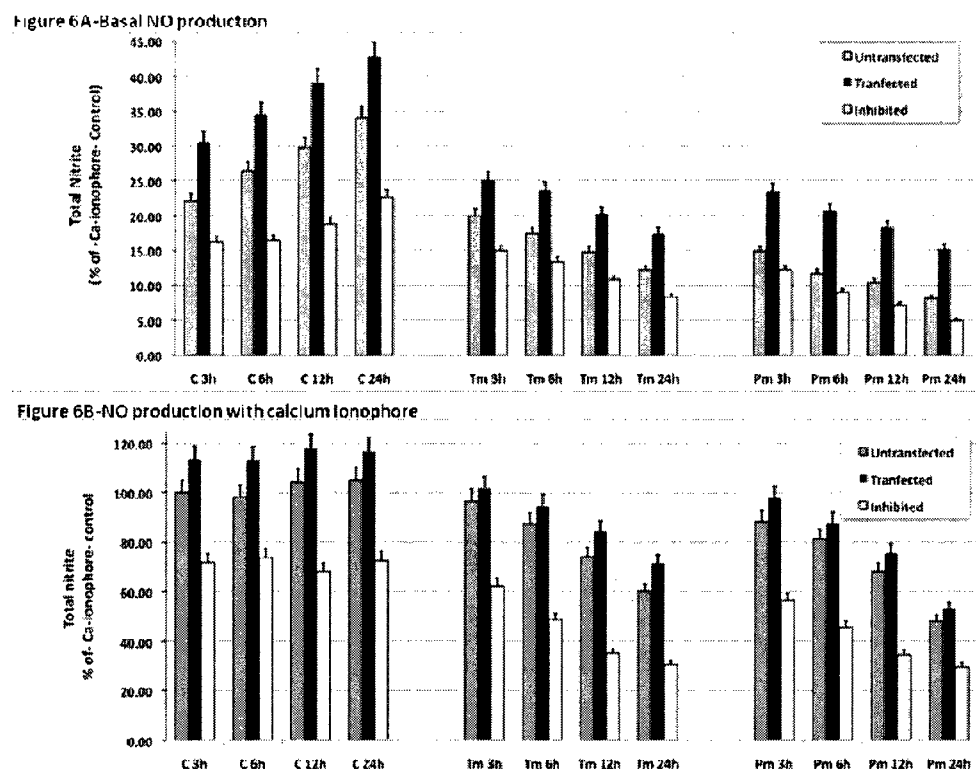


Figure 4.5 Nitric oxide production by BAECs measured in the form of total nitrite by Sievers Nitric Oxide Analyzer (NOA). (A) Total nitrite was measured with *Tm*, *Pm* or mock treated (C) wt BAECs (gray solid bars), *Tm*, *Pm* or mock treated p-GIPZ NSMase2 transfected BAECs (black solid bars) and *Tm*, *Pm* or mock treated wt- GW4869-inhibited BAECs (white bars) for 3, 6, 12 and 24 h respectively. (B) Thirty minutes prior to the measurement of nitrite at each time-points the cell culture supernatant was removed and replaced with Ca-ionophore, acetylcholine (100uM) containing cell culture medium. The data shown is representative of 13 independent experiments with error bars showing S.D.

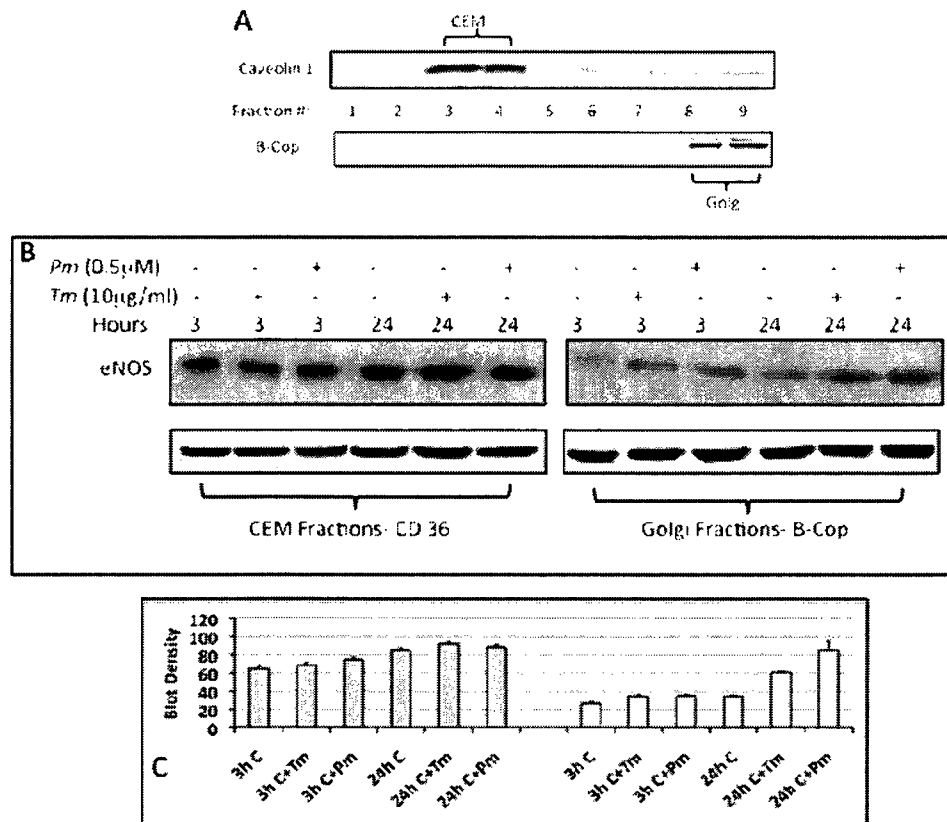


Figure 4.6 eNOS localization determined by differential sucrose density fractionation and Double Immunofluorescence assay. (A) BAECs were subjected to differential sucrose density fractionation with a step gradient 5-30% (5% steps) sucrose with 250 mM sodium carbonate in Hepes buffered saline to determine the caveolar enriched membrane (CEM) in fractions 3 and 4 and Golgi in fractions 8 and 9. Immunoblots with antibodies for caveolin 1 and β -cop were used to determine the organelle markers for CEM and Golgi respectively. (B) The CEM and Golgi fractions were pooled together from BAECs treated with *Tm*, *Pm* or mock treated (C) for 3 and 24 h and immunoblotted with anti-eNOS antibody. Immunoblots with CD36 and β -cop were used as loading controls for CEM and Golgi respectively. (C) Density plots of eNOS vs CD36 (gray bars) and eNOS vs β -cop (white bars) from Fig. 6(B). The data shown is representative of 3 independent experiments with error bars showing S.D.

D

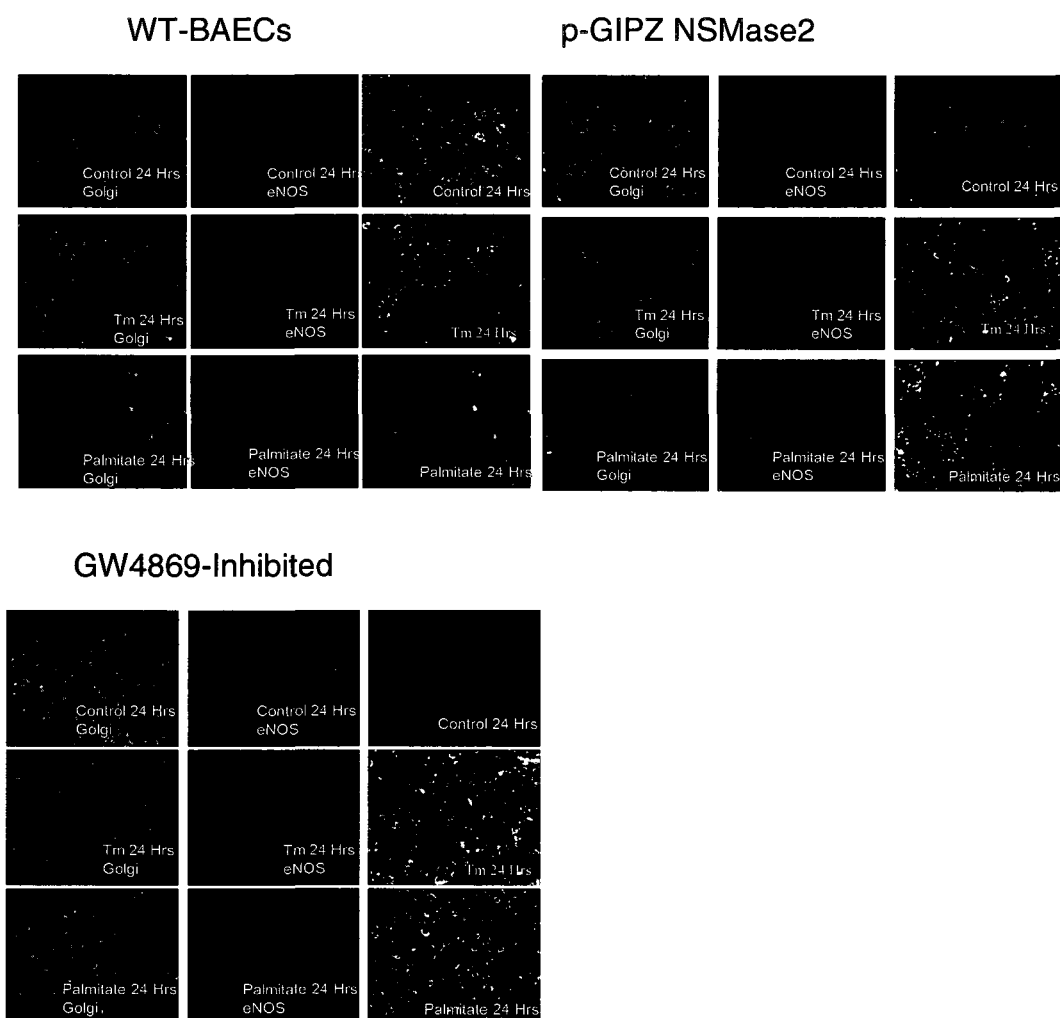


Figure 4.6 (D) Double immunofluorescence assay on WT BAECs, p-GIPZ NSMase2 transfected BAECs and GW4869 inhibited BAECs treated with ER stressors for 24 h. Antibodies for GM130, a Golgi marker and eNOS were probed with secondary antibodies conjugated with FITC (green) and Phycoerythrin (Red). The data is representative of 6 separate experiments.

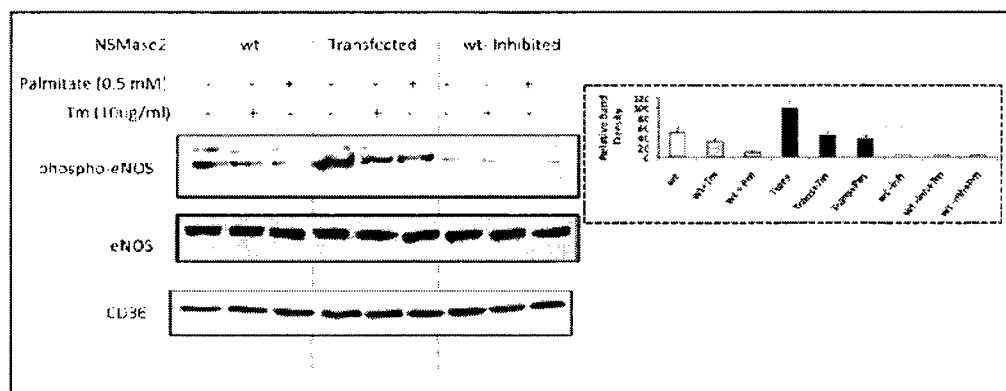


Figure 4.7 eNOS Ser¹¹⁷⁹ phosphorylation and total eNOS from isolated plasma membrane from BAECs. Plasma membrane isolates were obtained by sucrose density ultracentrifugation from Tm, Pm or mock treated (C) wt BAECs (gray bars), *Tm*, *Pm* or mock treated p-GIPZ Nsmase2 transfected BAECs (black solid bars) and *Tm*, *Pm* or mock treated wt-GW4869 inhibited BAECs (white bars) for 24 h and immunoblotted with antibodies for eNOS, phosphor Ser¹¹⁷⁹ eNOS and CD36 (loading control). Thirty min prior to the harvest of the cells the cell culture supernatant was removed and replaced with 100uM acetylcholine containing medium. The plots represent the relative density of phosphor Ser¹¹⁷⁹ eNOS vs CD36 and Total eNOS vs CD36. The data is representative of 3 separate experiments.

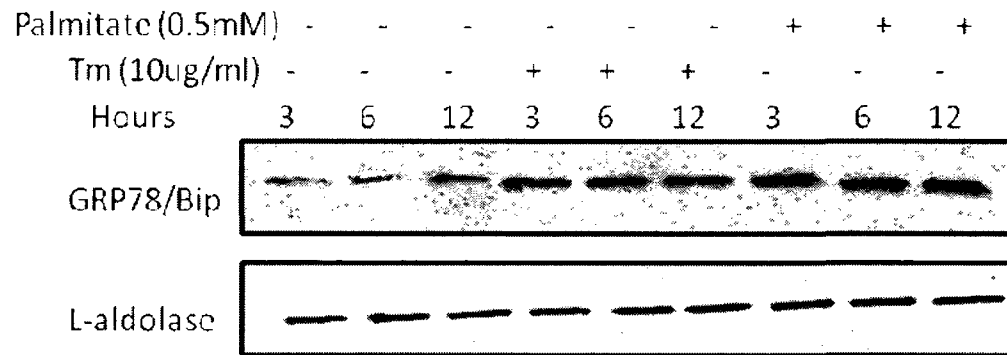


Figure 4.8 Western Immunoblot for GRP78/BiP Western immunoblot for ER stress marker GRP78/Bip from BAECs cell lysates treated with ER stressors for 3, 6, 12 h. L-aldolase was taken as a loading control.

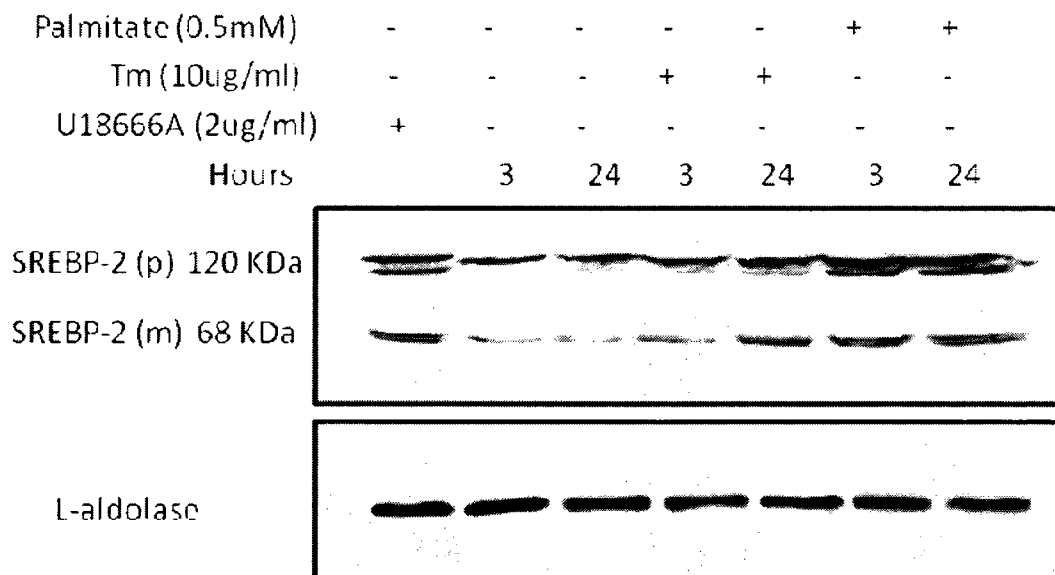
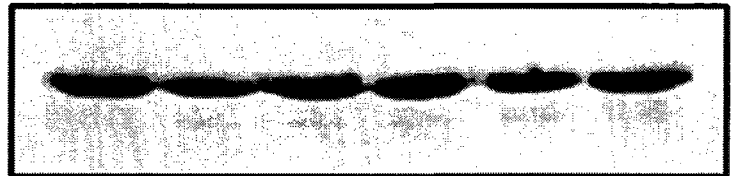


Figure 4.9. Western Immunoblot for SREBP-2 Western Immunoblot of SREBP-2, a transcription factor responsible for the upregulation of genes for cholesterol synthesis. Cell lysates from BAECs treated with ER stressors for 3 and 24 h were immunoblotted with antibodies for SREBP-2. U18666A was used as a positive control and L-aldolase as loading control. P is abbreviated for precursor form and m for mature form.

Palmitate (0.5mM)	-	-	-	-	+	+
Tm 10ug/ml	-	-	+	+	-	-
Hours	3	24	3	24	3	24

Caveolin 1



CD36

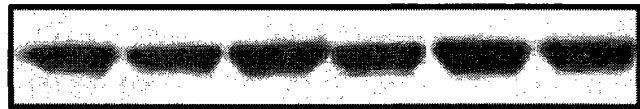
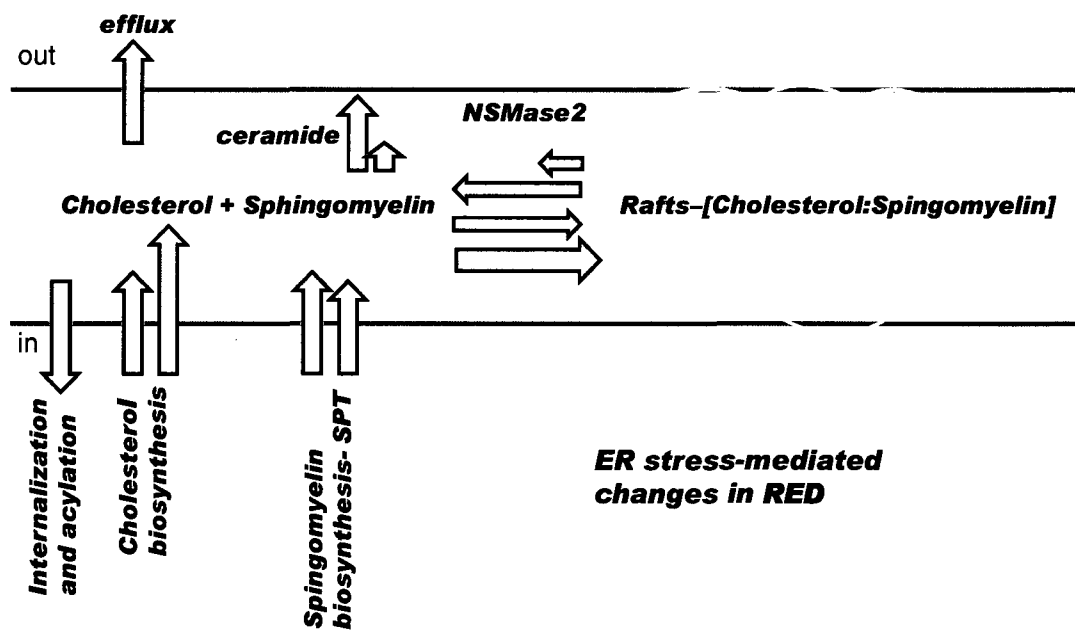


Figure 4.10. Western Immunoblot for Caveolin1 Caveolin 1 immunoblot from caveolae enriched plasma membrane isolated from BAECs treated with ER stressors for 3 and 24 h. CD36, a caveolae resident protein was taken as a loading control.



Scheme I

5.1 Conclusion

Endothelial dysfunction is associated with most forms of cardiovascular diseases and is also an important early event in the pathogenesis of atherosclerosis. The main characteristic of endothelial dysfunction which is common to all kinds of cardiovascular pathophysiology is the dominance of vasoconstriction over vasodilatation brought about by decreased biosynthesis and bioavailability of nitric oxide in the endothelial cell layer. The cardiovascular risk factors which give rise to endothelial dysfunction also cause ER stress in the endothelium. Interestingly, ER stress is known to upregulate genes for cholesterol bio-synthesis resulting in the accumulation of intracellular cholesterol. However, the relationship between endothelial dysfunction and ER stress is not firmly established and needs further investigation.

Nitric oxide (NO) is a hydrophobic molecule and tends to partition into the non-aqueous milieu in the plasma membranes. In objective 1 we hypothesized that plasma membrane ordering provided by cholesterol affects nitric oxide diffusion and signalling. The findings herein showed that sterol transport-defective Niemann- Pick type C1 (NPC1) fibroblasts which has increased plasma membrane cholesterol content, when exposed to exogenous NO were less responsive to

soluble guanylyl cyclase sGCs and subsequent cGMP production and VASP (Ser239) phosphorylation relative to their normal human fibroblast (NHF) counterparts. Furthermore, augmentation of plasma membrane cholesterol in NHF diminished production of both cGMP and VASP (Ser239) phosphorylation elicited by exogenous NO to NPC1 fibroblasts comparable levels. Conversely, decreasing membrane cholesterol in NPC1 fibroblasts resulted in the increased in both cGMP and VASP (Ser239) phosphorylation to levels similar to those observed in NHF. Therefore, this study raises the possibility that the physical partitioning of NO by membrane cholesterol rafts could be a significant contributing factor in the pathobiology of diseases beyond Niemann-Pick disorder, including cancer, neurodegeneration and cardiovascular diseases.

The objective 2 of this thesis was to understand the underlying ER stress-mediated mechanisms responsible for the induction of endothelial dysfunction. We observed that ER stress, in parallel with oxidative stress, caused elevations in plasma membrane cholesterol in bovine aortic endothelial cells (BAEC) as well as in the aortic wall of ER stressed C57BL6 mice. This study was a follow up of the objective 1 and here we wanted to examine the role of elevated plasma membrane cholesterol levels induced under pathological conditions of ER stress on the NO bioavailability. We observed that rise in plasma membrane cholesterol was

associated with decreased eNOS activity, eNOS phosphorylation and increased eNOS localization to the Golgi. In terms of NO bioavailability, ER stressed cells were 3 to 4 fold less responsive to extracellular-NO mediated signalling as measured by VASP phosphorylation. We also found that neutral sphingomyelinase 2 (NSMase2), a key enzyme in the control of plasma membrane cholesterol levels, was dysfunctional under conditions of ER stress as a result of S-nitrosation of its cysteine thiols and nitration of its tyrosine residues. In order to determine if the ER-stress induced effects on plasma membrane cholesterol were a direct consequence of altered NSMase2 activity, we over-expressed or inhibited the enzyme in BAEC. On the basis of these gain-and loss- of function experiments we observed that the over-expression of NSMase2 did decrease plasma membrane cholesterol while increasing basal nitric oxide levels. Conversely, the inhibition of this enzyme led to the attenuation of eNOS phosphorylation, NO production and an increase in plasma membrane cholesterol. Thus, this study signifies the role of neutral sphingomyelinase 2 under ER stress mediated increases in plasma membrane cholesterol and attenuation of endothelial NO production.

References

- Alouf, J. E., and Geoffroy, C. (1991) in *Sourcebook of Bacterial Protein Toxins* (Alouf, J. E., and Freer, J. H., eds) , pp. 147-186, Academic Press, London.
- Alouf JE, Geoffroy C, Pattus F, Verger R. (1984) *Eur J Biochem.* **141**, 205
- Arnout, J., et al. (2006) *Handb. Exp. Pharmacol.* **176(Pt. 2)**, 1-41
- Auge, N., Garcia, V., Maupas-Schwalm, F., Levade, T., Salvayre, R., Negre-Salvayre, A. (2002) *Arterioscler Thromb Vasc Biol.* **22**, 1990
- Balaban, R., S., Nemoto, S., et al. (2005) *Cell* **120**, 483
- Barsacchi, R., Perrotta, C., Bulotta, S., Moncada, S., Borgese, N., and Clementi, E. (2003) *Mol Pharmacol.* **63**, 886-895
- Bauer, P.,M., Fulton, D., Boo, Y.,C., Sorescu, G.,P., Kemp, B.,E., Jo, H., et al. (2003) *J Biol Chem.* **278**,14841
- Bellamy, T. C., and Garthwaite, J. (2002) *Mol. Cell Biochem.* **230**, 165–176
- Bendall, J. K., ALP, N. J., Warrick, N., Shijle, C., Adlam, D. et al. (2005) *Circ. Res.* **97**, 864-871
- Bertolotti, A., Zhang, Y., Hendershot, L., M., Harding, H., P., Ron, D. (2000) *Nat Cell Biol.* **2**, 326
- Blanchette-mackie, E., et al. (2000) *Biochim. Biophys. Acta* **1486**, 171
- Bodzioch, M., et al. (1999) *Nature Genet.* **22**, 347
- Boulanger, C., M., et al. (1992) *Circ. Res.* **70**, 1191
- Bredt, D.,S., and Snyder,S.H. (1992) *Neuron* **8**, 3–11.
- Brooks-Wilson, A., et al. (1999) *Nature Genet.* **22**, 336
- Busse, R., et al. (2006) *Handb. Exp. Pharmacol.* **176(Pt. 2)**, 43-78
- Caccia, S., Denisov, I., and Perrella, M. (1999) *Biophys. Chem.* **76**, 63–72
- Calfon, M., Zeng, H., Urano, F., Till, J., H., et al. (2002) *Nature* **415**, 92

- Coatrieux, C., Sanson, M., Negre-Salvayre, A., Parini, A., Hannun, Y., Itohara, S. et al. (1997) *Free Radic Biol Med.* **43**, 80
- Carlos, Fernández-Hernando., Masak,i F., Pascal, N. B., Yuko, F., et al. (2006) *J. Cell Biol.* **174**, 369-377.
- Castro, P., F., Diaz-Araya, G., Nettle, D., Corbalan, R., Perez, O., Nazzal, C. et al. (2002) *Am J Cardiol.* **89**, 236
- Ce`lio, X. C., Santos L. Y., Tanaka, J. W., Frencioco, R. M. L., et al. *Antioxid Redox Signal.* (2009) **11**, 2409-2427
- Chen, M., Mason, R. P., and Tulenko, T. N. (1995) *Biochim. Biophys. Acta* **1272**, 101–112
- Chen, P.,F., and Wu, K.K. (2000) *J Biol Chem.* **275** 13155–63
- Cheng, J and Neil, K. (2006) *Journal of Hepatology* **45**, 321-333.
- Chiang, C. Y., and Darensbourg, M. Y. (2006) *J. Biol. Inorg. Chem.* **11**, 359–370
- Clara, D. P., Elisabetta, M., Cristiana, P., Paola, B., and Emilio, C. (2006) *Arterioscler Thromb Vasc Biol.* **26**, 99-105
- Cohen, D., E., (1999) *Curr. Opin. Lipidol.* **10**, 295
- Colgan, S. M., Tang, D., Werstuck, G. H., and Austin, R. C. (2007) *Int. J. Biochem. Cell Biol.* **39**,1843-1851
- Compton, M., M. (1992) *Cancer Metastasis Rev.* **11**, 105
- Cooke, J., P., et al. (1994) *Arterioscler. Thromb.* **14**, 653
- Cruz, J., C., Sugii, C., et al. (2000) *J. Biol Chem.* **275**, 4013
- Davin, J., William, C. S., and David, F. (2005) *Am J Physiol Cell Physiol* **289**, C1024-C1033
- Davignon, J and Ganz, P. (2004) *Circulation* **109**, III27–III32
- Davies, J., P., et al. (2000) *J. Biol Chem.* **275**, 24367
- De´cio, L. E., Alessandra, K. C., and Miriam, C. (2007) *Endocrine Reviews* **29**, 42–61
- Dedio, J., Konig, P., Wohlfart, P., et al. (2001) *FASEB J* **15**, 79

- Defer, N., Azroyan, A., Pecker, F., Pavoine, C. (2007) *J Biol Chem.* **282**, 35564
- Diane, E., H., and Joseph, L. (2006) *Arterioscler. Thromb Vasc. Biol.* **26**, 1207
- Dietrich, C.L.A. Bagatolli, Z. N., Volovyk, N. L., et al. (2001) *Biophysical J.* **80**, 1417-1428
- Dimmeler, S., and Zeiher, A. M.(1997) *Nitric Oxide.* **1**, 275
- Diringer, H., Marggraf, W., D., Koch, M., A., Anderer, F. A. (1972) *Biochem. Biophys. Res. Commun.* **47** 1345–1352
- Doehner, W., Bunck, A., C., Rauchhaus, M., von Haehling, S., Brunkhorst, F., M., Cicoira, M. et al. (2007) *Eur Heart J.* **28**, 821
- Dolo, V., et al. (2000) *Biochim. Biophys. Acta* **1486**, 265
- Dudzinski, D., M., Igarashi, J., Greiff, D., M., et. al. (2006) *Annu Rev. Pharmacol Toxicol.* **116** 2075
- Dudzinski, D., M., and Michel, T. (2005) *Hemostasis and thrombosis: basic principles and clinical practice.* 5th ed. Philadelphia: Lippincott Williams & Wilkins; 653-66
- Erwin, P., A., Lin, A.,J., Golan, D.,E., Michel, T. (2005) *J Biol Chem.* **280**, 19888
- Espey, M. G., Miranda, K. M., Thomas, D. D., and Wink, D. A. (2001) *J. Biol. Chem.* **276**, 30085–30091
- Espey, M. G., Thomas, D. D., Miranda, K. M., and Wink, D. A. (2002) *Proc. Natl. Acad. Sci. U. S. A.* **99**, 11127–11132
- Fawcett, T., W., Martindale, J., L., Guyton, K., Z., Hai, T., Holbrook, N. J. (1999) *Biochem J.* **339**, 135
- Feng, B., Yao, P., M., Li, Y., et al. (2003) *Nat Cell Biol.* **5**,781
- Fidorra M, Duelund L, Leidy C, Simonsen AC, Bagatolli LA. (2006) *Biophys J.* **90**, 4437-51
- Fischkoff, S., and Vanderkooi, J. M. (1975) *J. Gen. Physiol.* **65**, 663–676
- Flanagan, J. J., Tweten, R. K., Johnson, A. E., et al. (2009) *Biochemistry* **48**, 3977-3987
- Fowler S. (1969) *Biochim Biophys Acta* **191**, 481–484

- Fujimoto, T., Nakade, S., Miyawaki, A., Mikoshiba, K., Ogawa, K. (1992) *J Cell Biol.* **119**, 1507–13
- Fulton, D., Gretton, J. P., McCabe, T. J., et. al (1999) *Nature* **399**, 597-601
- Fulton, D., Gratton, J-P., Sessa, W.C. (2001) *J Pharmacol Exp Ther.* **299**, 818
- Furchgott, R.,F., Zawadzki, J.V. (1980) *Nature* **288**, 373–6
- Futerman, A., H., Stieger, B., Hubbard, A., L., Pagano, R. E. (1990) *J. Biol. Chem.* **265** 8650–8657
- Garcia Arguinzonis, M. I., Galler, A. B., Walter, U., Reinhard, M., and Simm, A. (2002) *J. Biol. Chem.* **277**, 45604–45610
- Garcia-Cardena, G., Fan, R., Shah, V., Sorrentino., R., Cirino, G., Papapetropoulos, A., et al. (1998) *Nature* **392**, 821
- Gardner, R., G., Shearer, A., G., Hampton, R. Y. (2001) *Mol Cell Biol.* **21**, 4276
- Geppert, A., et al. (1998) *Arterioscler. Thromb. Vasc. Biol.* **18**, 1634
- Gilmore, A., P., (2005) *Cell Death Differ.* **12**, 1473
- Goetz, R.,M., Thatte, H.,S., Prabhakar, P., et. al. (1999) *Proc Natl Acad Sci U S A.* **96** 2788–93.
- Govers, R., Rabelink, T. J. (2001) *Am. J. Physiol Renal Physiol.* **280** F193-F206
- Gonzalez, E., Kou, R., Lin, A., J., Golan, D., E., Michel, T. (2002) *J Biol Chem.* **277**, 39554
- Grammatikos, G., Teichgraber, V., Carpinteiro, A., Trarbach, T., Weller, M., Hengge, U., R. et al. (2007) *Antioxid Redox Signal* **9**, 1449
- Gulbins, E. (2003) *Pharmacol Res.* **47**, 393
- Hammadi A., Billiard C., Fauchet A., M., Kolb J. P. (2008) *Nitric Oxide* **19**, 138-145
- Handy, D. E., and Loscalzo, J., (2006) *Arterioscler Thromb Vasc Biol.* **26**, 1207-1214
- Hao, M., Mukherjee, S., and Maxfield, F. R. (2001) *Proc. Natl. Acad. Sci.U. S. A.* **98**, 13072–13077

- Harding, H., P., Zhang, Y., Bertolotti, A., Zeng, H., Ron, D. (2000) *Mol Cell*. **5**, 897
- Harris, M., B., Ju, H., Venema, V., J., Liang, H., Zou, R., Michell, B., J., et al. (2001) *J Biol Chem*. **276**, 16587
- Harris, S., L., and Levine, A. J. (2005) *Oncogene*. **24**, 2899
- Hayakawa, H and Raij, L. (1999) *J. Hypertens*. **17**, 611-619
- Henderson, A., H., (1991) *Br. Heart J*. **65**, 116
- Higgins, M., E., Davies, J., P., et al. (1999) *Mol. Genet. Metab*. **68**, 1
- Hotze EM, Wilson-Kubalek J Biol Chem. 2001;**276**8261-8
- Huang, B., and Chen, C. *Free Rad. Biol. Med.* (2006) **41**, 557-561
- Hua, Cai and David, G. H. (2000) *Circ. Res*. **87**, 840-844
- Icking, A., Schilling, A., Wiesenthal, A., Opitz, N., Müller-Esterl, W. (2006) *FEBS Lett* **580**, 223
- Ignarro, L. J. (2000) *Nitric Oxide; Biology and Pathology*. London: Academic Press
- Issner, R., Nauser, T., Bugnon, P., Lye, P. G., and Koppenol, W. H. (1997) *Chem. Res. Toxicol*. **10**, 1285–1292
- Jia, S., J., Jin, S., Zhang, F., Yi, F., Dewey, W., L., Li, PL. (2008) *Am J Physiol Heart Circ Physiol*. **295**, H1743
- Jin, S., Yi, F., Zhang, F., Poklis, J., L., Li, P., L. (2008) *Arterioscler Thromb Vasc Biol* **28**, 2056
- Jin, Y., Robert, B. R., Ryutaro, K., Xi, C., Utpal, P. D., et al. (2000) *Molecular Cell*, **6**, 1355-1364
- Johnson, W., J., et al. (1991) *Biochim. Biophys. Acta* **1085**, 273
- Kailash, P., and Paul, L. (2003) *J. Cardiovasc. Pharmacol. Ther.* **8**, 61-69
- Kailash, P., Subrahmanyam, V. M., Jawahar, K. and Paul, L. (1997) *Int. J. Angiology* **6**, 13-17
- Kallen, K., J., Allan, D., Whatmore, J., Quinn, P. (1994) *Biochim. Biophys. Acta* **1191** 52–58

- Karakashian, A. A., Natalia, V. et al. (2004) *The FASEB J.* **18**, 968-970
- Keaney, J. Jr., and Vita, J. A. (1995) *Prog. Cardiovasc. Dis.* **38**, 129–154
- Keaney, J., F., Jr. et al. (2005) *Circulation* **112**, 2585
- Kehoe, M. A., Miller, L., Walker, J. A., and Boulnois, G. J. (1987) *Infect. Immun.* **55**, 3228-3232
- Keith, M., Geranmayegan, A., Sole, M., J., Kurian, R., Robinson, A., Omran, A., S. et al. (1998) *J Am Coll Cardiol.* **31**, 1352
- Kerr, J., F., Wyllie, A., H., et al. (1972) *Br. J. cancer* **26**, 239
- Khan, M. I., Pichna, B. A., Shi, Y., Bowes, A. J., and Werstuck, G. H. (2009) *Antioxid Redox Signal.* **11**, 2289-2298
- Kim, A. J., Shi, Y., Austin, R. C., and Werstuck, G. H. (2001) *J. Cell Sci.* **118**, 89-99
- Kimiko, M., Hiroko, K., and Sei, K. (2005) *FEBS Lett.* **579**, 393-397
- Kinya, K., Yoshimasa, I., Kiyohide, K., and Tatsuzo, F., (1976) *J. Biochem.* **79**, 739-748
- Koike, T., Ishida, G., Taniguchi, M., Higaki, K., Ayaki, Y., Saito, M., Sakakihara, Y., Iwamori, M., and Ohno, K. (1998) *Biochim. Biophys. Acta* **1406**, 327–335
- Kolmakova, A., Kwiterovich, P., Virgil, D., Alaupovic, P., Knight-Gibson, C., Martin, S., F. et al. (2004) *Arterioscler Thromb Vasc Biol.* **24**, 264
- Kou, R., Greif, D., Michel, T. (2002) *J Biol Chem.* **277**, 29669
- Kirstin, Zimmermann., Nils, Opitz., Ju¨rgen Dedio., Christoph, Renne., Werner, Mu¨ller-Esterl., and Stefanie, Oess. (2002) *Proc Natl Acad Sci. USA.*; **99**, 17167
- Kro¨ncke, K., D., Fehsel, K., Kolb-Bachofen, V. (1997) *Nitric Oxide.* **1**, 107
- Krown, K., A., Page, M., T., Nguyen, C., Zechner, D., Gutierrez, V., Comstock, K., L. et al. (1996) *J Clin Invest.* **98**, 2854
- Kyosuke, H., Hiderou, Y., Hideki, Y., Takashi, Y., and Kazutoshi, M. (1999) *Molecular Biology of the Cell* **10**, 3787–3799
- Landmesser, U., Dikalov, S., et al. (2003) *J. Clin. Invest.* **111**, 1201

- Lange, Y., Swaisgood, M. H., Ramos, B. V. and Steck, T. L.(1989) *J Biol Chem.* **264**, 3786–3793
- Lange, Y., Ye, J., et al. (2000) *J. Biol Chem.* **275**, 17468
- Laursen, J., B., Somers, M., et al. (2001) *Circulation* **103**, 1282
- Lee, A. H., Iwakoshi, N. N., and Glimeher, L. H. (2003) *Mol. Cell Biol.* **23**, 7448-7459
- Lee, J. N., and Ye, J. (2004) *J. Biol. Chem.* **279**, 45257-45265
- Lee, K., Tirasophon, W., Shen, X., Michalak, M., Prywes, R., Okada, T., et al. (2002) *Genes Dev.* **16**, 452
- Lee, J., Reich, R., Xu, F., and Sehgal, P. B. (2009) *Am J. Physiol. Lung Cell Mol. Physiol.* **297**, L715-728
- Leppimäki, P., Kronqvist, R., and Slotte, J. P. (1998) *Biochem. J.* **335**, 285-291
- Lerman, A., et al. (1991) *N. Engl. J. Med.* **325**, 997
- Lewis, R. S., and Deen, W. M. (1994) *Chem. Res. Toxicol.* **7**, 568–574
- Ley, K., et al. (2006) *Handb. Exp. Pharmacol.* **176(Pt. 2)**, 97-133
- Li, J., H., and Pober, J. S. (2005) *J. Immunol.* **175**, 1858
- Lima, E. S., Di Mascio, P., and Abdalla, D. S. (2003) *J. Lipid Res.* **44**, 1660–1666
- Lin, M., I., Fulton, D., Babbitt, R., Fleming, I., Busse, R., Pritchard, Jr, K., A., et al. (2003) *J Biol Chem.* **278**, 44719
- Linder, A. E., McCluskey, L. P., Cole, K. R., III, Lanning, K. M., and Webb, R. C. (2005) *J. Pharmacol. Exp. Ther.* **314**, 9–15
- Liscum, L., and Munn, N., J. (1999) *Biochim. Biophys. Acta* **1438**, 19
- Liscum, L., et. al. (2000) *Traffic* **1**, 218
- Liu, H., Nishitoh, H., Ichijo, H., Kyriakis, J. M. (2000) *Mol Cell Biol.* **20**, 2198
- Liza, M., Chico, Y., Fresnedo, O., and Ochoa, B. (2003) *Lipids* **38**, 53-63

- Logue, S., E., Martin, S. J. (2008) *Biochem. Soc. Trans.* **36**, 1
- Loidl, A., Sevcsik, E., Riesenhuber, G., Deigner, H., P., Hermetter, A. (2003) *J Biol Chem.* **278**, 3292
- Loscalzo, J., and Welch, G. (1995) *Prog Cardiovasc Dis.* **38**, 87–104
- Macdonald, J. L., and Pike, L. J. (2005) *J Lipid Res.* **46**, 1061
- Mallat, Z., Philip, I., Lebre, M., Chatel, D., Macclouf, J., Tedgui, A. (1998) *Circulation* **97**, 1536
- Marathe, S., Schissel, S., L., Yellin, M., J., Beatini, N., Mintzer, R., Williams, K., J. et al. (1998) *J Biol Chem.* **273**, 4081
- Marchesini, N., Osta, W., Bielawski, J., Luberto, C., Obeid L. M., and Hannun, Y. A. (2004) *J Biol Chem.* **279** 25101-25111
- Marciniak, S., J., and Ron, D. (2006) *Physiol Rev.* **94**, 1133
- Marciniak, S., J., Yun, C., Y., Oy adomari, S., et al. (2004) *Genes Dev.* **18**, 3066
- Martínez-Ruiz, A., Villanueva, L., González de Orduña, C., López-Ferrer, D., et al. (2005) *Proc Natl Acad Sci U S A.* **102**, 8525
- Mason, M. G., Nicholls, P., Wilson, M. T., and Cooper, C. E. (2006) *Proc. Natl. Acad. Sci. U. S. A.* **103**, 708–713
- Matsukawa, J., Matsuzawa, A., Takeda, K., Ichijo, H. (2004) *J Biochem (Tokyo).* **136**, 261
- McMurray, J., Chopra, M., Abdullah, I., Smith, W., E., Dargie, H., J. (1993) *Eur Heart J.* **14**, 1493
- Messmer, U., K., Bruñe, B. (1996) *Biochem J.* **319**, 299
- Mete, C., Elisabetta, M., Rebecca, J. R., Christian, J. S., Jr, and Peter, F. D. (2009) *Circ. Res.* **105**, 453
- Meusser, B., Hirsch, C., Jarosch, E., Sommer, T. (2005) *Nat Cell Biol.* 2005 **7**, 766
- Michell, J., B., Chen, Z., P., Tiganis, T., Stapleton, D., Katsis, F., Power, D., A., et al. (2001) *J Biol Chem.* **276**, 17625
- Michel, J. B., Feron, O., Sacks, D., and Michel, T. (1997) *J. Biol. Chem.* **272**, 15583- 15596

- Michel, J.,B., Feron, O., Sase, K., Prabhakar, P., Michel, T. (1997) *J. Biol Chem.* **272** 25907
- Miersch, S., Espey, M. G., Chaube, R., Akarca, A., Tweten, R., Ananvoranich, S., and Mutus, B. (2008) *J Biol Chem.* **283**, 18513-21
- Mizutani Y., Tamiya-Koizumi, K., Nakamura N., Kobayashi M., Hirabayashi, Y., Yoshida S. (2001) *Journal of Cell Science* **114** 3727-3736
- Mo, E., Amin, H., Bianco, I. H., and Garthwaite, J. (2004) *J. Biol. Chem.* **279**, 26149–26158
- Moncada, S., Erusalimsky, J., D., et al. (2002) *Nat. Rev. Mol. Cell Biol.* **3**, 214
- Moncada, S., Palmer, R.,M., Higgs, E.A. (1991) *Pharmacol Rev.* **43**,109–42
- Mukhopadhyay, S., Xu, F., and Sehgal, P. B. (2007) *Am J Physiol Heart Circ Physiol.* **292** H1373-H1389
- Murata, T., Sato, K., Hori, M., Ozaki, H., and Karaki, H. (2002) *J. Biol Chem.* **277**, 44085
- Nakagawa, T., and Yuan, J. (2000) *J Cell Biol.* **150**, 887
- Nakagawa. T., Zhu, H., Morishima, N., Li, E., Xu, J., Yankner, B., A., Yuan, J.(2000) *Nature.* **403**, 98
- Naoyuki, M., Yukio, H., Yoshika, T., and Yuichi, H. (2006) *J. Pharmacol. Exp. Ther.* **106**, 109785
- Nathan, C., Xie, Q. (1994) *J. Biol. Chem.* **269**, 13725–13728.
- Neufeld, E., B., et al. (1996) *J. Biol Chem.* **271**, 21604
- Neufeld, E., B., et al. (1999) *J. Biol Chem.* **274**, 9627
- Nicolini C, Baranski J, Schlummer S, Palomo J, Lumbierres-Burgues M, Kahms M, Kuhlmann J, Sanchez S, Gratton E, Waldmann H, Winter R. (2006) *J Am Chem Soc.* **128**, 192-201.
- Nishitoh, H., Matsuzawa, A., Tobiume, K., Saegusa, K., Takeda, K. et al. (2002) *Genes Dev.* **16**, 1345
- Nishikawa, T., Edelstein, D., et al. (2000) *Nature* **404**, 787
- Nohturfft, A., Yabe, D., et al. (2000) *Cell* **102**, 315

- Ohara, Y., Peterson, T. E., and Harrison, D. G. (1993) *J. Clin. Invest.* **91**, 2546–2551
- Ohno-Iwashita Y, Iwamoto M, Ando S, Mitsui K, Iwashita S. (1990) *Biochim Biophys Acta.* **1023**, 441
- Ohno-Iwashita Y, Iwamoto M, Mitsui K, Ando S, Nagai Y. (1988) *Eur J Biochem.* **176**, 95-101
- Ohno-Iwashita, Y., Shimada, Y., Waheed, A. A., Hayashi, M., Inomata, M., Nakamura, M., Maruya, M., and Iwashita, S. (2004) *Anaerobe* **10**, 125–134
- Okamura, K., Kimata, Y., Higashio, H., Tsuru, A., Kohno, K. (2000) *Biochem Biophys Res Commun.* **279**, 445
- Olivier, F., Chantal, D., Stephane, M., Jean-Pierre, D., et al. (1999) *J. Clin. Invest.* **103**, 897– 905
- Olofsson, S., O., et al. (1999) *Curr. Opin. Lipidol.* **10**, 341
- Oral, H., Dorn, G., W., II., Mann, D., L. (1997) *J. Biol Chem.* **272**, 4836
- Oude Efferink, R., P., J., et al. (1999) *Gastroenterol Clin. North Am.* **28**, 59
- Outinen, P. A., Sood, S. K., Pfeifer, S. I., Pamidi, S. et al. (1999) *Blood* **94**, 959-967
- Oyadomari, S., Araki, E., Mori, M. (2002) *Apoptosis* **7**, 335
- Oyadomari, S., and Mori, M. (2004) *Cell Death Differ.* **11**, 381
- Pál, P., Irina, G.O., Jon, G. M., and Csaba, S. (2005) *Curr. Med. Chem.* **12**, 267–275
- Parat, M-L., and Fox, P. L. (2001) *J Biol Chem.* **276**, 15776
- Peter, H. M., Shiva, S., and Gladwin, M. T. (2007) *Journal of Chromatography B* **851**, 93- 105
- Philippides, A., Husbands, P., and O'Shea, M. (2000) *J. Neurosci.* **20**, 1199–1207
- Preston Mason, R., Tulenko, T. N., and Jacob, R. F. (2003) *Biochim. Biophys. Acta* **1610**, 198–207
- Pritchard, K., A., Jr., Groszek, L. et al. (1995) *Circ. Res.* **77**, 510

- Pucadyil, T. J., and Chattopadhyay, A. (2006) *Chem. Phys. Lipids* **143**, 11–21
- Puri, V., et. al. (1999) *Nature cell Biol.* **1**, 386
- Qian, Zhang., Jarrod, E. C., Davin, J., John, D. C., William, C. S., and David, F., (2006) *Arterioscler Thromb Vasc Biol.* **26**, 959-961
- Radin, M., J., Holycross, B., J., Dumitrescu, C., Kelley, R., Altschuld, R., A. (2008) *Mol Cell Biochem.* **315**, 179
- Rao, R., V., Hermel, E., Castro-Obregon, S., Del Rio, G. et al. (2001) *J Biol Chem.* **276**, 33869
- Rhee, S., G., Bae, Y., S., et al. (2000) *Sci. STKE* **53**, pe1
- Ridgway, N. D. (2000) *Biochim. Biophys. Acta* **1484**, 129
- Ridgway, N., D., Dawson, P., A., et al. (1992) *J. Biol Chem.* **116**, 307
- Ridgway, N., D., Lagace, T., A., et al. (1998) *J. Biol Chem.* **273**, 31621
- Robert, M. Weisbrod, M. C., Griswold, Y. D., and Victoria, M. et al. (1997) *Arterioscler Thromb Vasc Biol.* **17**, 394-402
- Ross, R., (1990) *Nature* **362**, 801
- Rothberg, K., G., Heuser, J., E., Donzell, W., C., Ying, Y., S., Glenney, J., R., Anderson, R. G. (1992) *Cell* **68**, 673
- Rothblat, G., H., et al. (1999) *J. Lipid Res.* **40**, 781
- Rubanyi, G., M. (1993) *J. Cardiovasc Pharmacol.* **22**, S1
- Rukmini, R., Rawat, S. S., Biswas, S. C., and Chattopadhyay, A. (2001) *Biophys. J.* **81**, 2122–2134
- Ruqin, K., and Thomas, M. (2007) *Circulation* **116**, II_308
- Rust, S., et al. (1999) *Nature Genet.* **22**, 352
- Rutkute, K., Asmis R. H., and Mariana N. Nikolova-Karakashian (2007) *J Lipid Res.* **48**, 2443-2452
- Saltiel, A., R., Kahn, C., R., (2001) *Nature* **414**, 799

- Scheek, S., Brown, M. S., and Goldstein, J. L. (1997) *Proc Natl Acad Sci U S A*. **94**,11179
- Schilling, K., Opitz, N., Wiesenthal, A., Oess, S., Tikkanen, R., Müller-Esterl, W., and Icking, A., (2006) *Mol Biol Cell*. **17**, 3870-80
- Schissel, S., L., Jiang, X., Tweedie-Hardman, J., Jeong, T., Camejo, E., H., Najib, J. et al. (1998) *J Biol Chem*. **273**, 2738
- Schroder, M., and Kaufman, R. J. (2005) *Annu Rev Biochem*. **74**, 739
- Sessa, W. C. *J. Cell Sci.* (2004) **117** 2427-2429
- Shank, K. J., Su, P., Brglez, I., Boss, W. F., et al. (2001) *Plant Physiol* **126**, 267-277
- Shatursky O, Heuck AP, Shepard LA, Rossjohn J, Parker MW, Johnson AE, Tweten RK. (1999) *Cell*. 29; **99** 293
- Shaul, P. W. (2002) *Annu Rev Physiol* **64** 749–74
- Shimizu, T., Okabe, A., Minami, J., and Hayashi, H. (1991) *Infect. Immun.* **59**, 137-142
- Simons, K., and Ikonen, E. (1997) *Nature* **387**, 569–572
- Smith, A. R. and Hagen, T. M. (2003) *Biochem Soc Trans.* **31**,1447-1459
- Slotte, J. P., Bierman, E. L. (1988) *Biochem J*. **250**, 653-658
- Soltani C.,E. et al. (2007) *Proc Natl Acad Sci U S A*. **104**, 20226
- Subczynski, W. K., Lomnicka, M., and Hyde, J. S. (1996) *Free Radic. Res.* **24**, 343–349
- Sugahara, M., Sekino-Suzuki, N., Ohno-Iwashita, Y., and Miki, K. (1996) *J. Crystal Growth* **168**, 288-291
- Suzuki, H., Eguchi, K. et al. (2006) *Endocrinology* **147**, 5914-5920
- Tabas, I. (1999) *Chem Phys Lipids* **102**, 123–130
- Tabas, I., Williams, K., J., Boren, J. et al. (2007) *Circulation* **116**,1832
- Takahashi, S., and Mendelsohn, M. E. (2003) *J Biol Chem*. **278**, 30821
- Tani, M., and Hannun Y. A. (2007) *J Biol Chem*. **282**, 10047-10056

- Tani, M., and Hannun Y. A. (2007) *FEBS Lett.* **581**, 1323–1328
- Tani, M., Ito, M., Igarashi, Y. (2007) *Cell Signal* **19**, 229
- Tomiuk, S., Zumbarsen, M., and Stoffel, W. (2000) *J. Biol Chem.* **275**, 5510
- Toporsian, M., Gros, R., Kabir, M., G., et. al. (2005) *Circ Res.* **96**, 684
- Trigatti, B., et al. (2000) *Curr. Opin. Lipidol* **11**, 123
- Tweten, R. K. (1988) *Infect. Immun.* **56**, 3235-3240
- Ubeda, M., Habener, J. F. (2000) *Nucleic Acids Res.* **28**, 4987
- Ullman, M., D., and Radin, N. S. (1974) *J. Biol. Chem.* **249**, 1506– 1512
- Underwood, K., W., Jacobs, N., L., et al. (1998) *J. Biol Chem.* **273**, 4266
- Vainio, S., Bykov, I., Hermansson, M., Jokitalo, E. et al. (2005) *Biochem. J.* **391**, 465–472
- Vanhaesebroeck, B., Leeyers, S., J., Panayotou, G., Waterfield, M. D. (1997) *Trends Biochem Sci.* **22**, 267
- Veatch SL, Keller SL. (2003) *Biophys J.* **84**, 725-6.
- Veldman, R. J., Maestre, N., Aduib, O. M., Medin, J. A., Salvayre, R., and Levade, T. (2001) *Biochem J.* **355**, 859–868
- Venema, V., J., Marrero, M., B., Venema, R. C. (1996) *Biochem Biophys Res Commun.* **226**, 703
- Vergnani, L., Hatik, S. et al. (2000) *Circularion* **101**, 1261
- Wagner, D.,A., Young, V.,R., Tannenbaum, S.,R., Schultz, D.,S., Deen, W.M. *IARC Sci Publ* 1984
- Waheed, A A., Shimada, Y., Heijnan, H. F. G., Nakamura, M., et al. (2001) *Proc Natl Acad Sci* **98**, 4926-4931
- Walton, K. A., Gugiu, B. G., Thomas, M., Basseri, R. J., et al. (2006) *J Lipid Res.* **47**, 1967-1974
- Wang, X., Z., Harding, H., P., Zhang, Y. et al. (1998) *EMBO J.* **17**, 5708
- Wang, X., Z., Ron, D. (1996) *Science.* **272**, 1347

- Warnholtz, A., Nickenig, G., et al. (1999) *Circulation* **99**, 2027
- Wei, Q., Xia, Y. (2005) *J Biol Chem.* **280**, 18081
- Wei, Q., Xia, Y. (2006) *J Biol Chem.* **281**, 21652
- Werstuck, G. H., Lentz, S. R., Dayal, S., Hossain, G. S., Sood, S. K., et al. (2001) *J. Clin. Invest.* **107**, 1263-1273
- White, C., R., Brock, T., A., et al. (1994) *Proc Natl Acad Sci U S A.* **91**, 1044
- Wood, J., and Garthwaite, J. (1994) *Neuropharmacology* **33**, 1235–1244
- Xu, K., Y., Huso, D., L., Dawson, T., M., Bredt, D. S. et al. (1999) *Proc Natl Acad Sci U S A.* **96**, 657
- Xu, L., Eu, J., P., Meissner, G., Stamler, J. S. (1998) *Science* **279**, 234
- Xu, W., Liu. L. (1998) *Cell Research* **8**, 251-258
- Xu, W., Liu, L., Charles, I., G., Moncada, S. (2004) *Nat Cell Biol.* **6**, 1129
- Yanhong, Z., Agnes, K., Katarzyna, A. B., and Neil, Hogg (2005) *Free Rad Biol & Med.* **38**, 874– 881
- Yasuko, I., Ming-Hung, T., Timothy, J. M., Jean-Philippe, G., David, F., et al. (2002) *Am J Physiol Heart Circ Physiol.* **282**, H2084-H2090
- Ye, J., Rawson, R., B., Komuro, R., Chen, X., Dave, U., P., Prywes., R., Brown, M., S., Goldstein J. L. (2000) *Mol Cell.* **6**, 1355
- Yoneda, T., Imaizumi, K., Oono, K., Yui, D., et al. (2001) *J Biol Chem.* **276**, 13935
- Yoshida. H., Matsui, T., Hosokawa, N., Kaufman, R., J., Nagata, K., Mori, K. (2003) *Dev Cell.* **4**, 265
- Yoshida, H., Matsui, T., Yamamoto, A., Okada, T., Mori, K. (2001) *Cell.* **107**, 881
- Zabel, U., Kleinschnitz, C., Oh, P., Nedvetsky, P., Smolenski, A., Muller, H., Kronich, P., Kugler, P., Walter, U., Schnitzer, J. E., and Schmidt, H. H. (2002) *Nat. Cell Biol.* **4**, 307–311
- Zeidan, Y., H., Wu, B., X., Jenkins, R., W., Obeid, L., M., Hannun, Y., A. (2008) *FASEB J* **22**, 183

Zhang, A., Y., Yi, F., Jin, S., Xia, M., Chen, Q., Z., Gulbins, E. et al. (2007) *Antioxid Redox Signal* **9**, 817

Zhang, Q., Church, J. R., Jagnandan, D., et al. (2006) *Arterioscler Thromb Vasc Biol.* **26**, 959-961

Zheng, T., Li, W., Wang, J., Altura, B. T., and Altura, B. M. (2000) *Eur J Pharmacol.* **391**, 127-35

Zinszner, H., Kuroda, M., Wang, X., Batchvarova, N., Lightfoot, R., T., et al. (1998) *Genes Dev.* **12**, 982

Zhou, Q., Band, M. R., Hernandez, A., Liu, Z. L., and Kummerow F. A., (2004) *Life Sciences* **75**, 1567-1577

Zulli, A., Widdop, R. E., Hare, D. L., Buxton, B. F., and Black. M. J. (2003) *Arterioscler Thromb Vasc Biol.* **23**, 1358-1363

VITA AUCTORIS

NAME: RUCHI CHAUBE

PLACE OF BIRTH: SAGAR, MADHYA PRADESH, INDIA

YEAR OF BIRTH: 1978

EDUCATION: Sagar University, Sagar (MP), India
1996-1999 B.Sc.

Sagar University, Sagar (MP), India
1999-2001 M.Sc.